

The cannabinoid receptor 2: from mouse to human

Dissertation

zur

Erlangung des Doktorgrades (Dr. rer. nat.)

der

Mathematisch-Naturwissenschaftlichen Fakultät

der

Rheinischen Friedrich-Wilhelms-Universität Bonn

vorgelegt von

Benjamin Gennequin

aus

Tourcoing, Frankreich

Bonn, January 2015

Angefertigt mit Genehmigung der Mathematisch-Naturwissenschaftlichen Fakultät der
Rheinischen Friedrich-Wilhelms-Universität Bonn

1. Gutachter: Prof. Dr. Andreas Zimmer

2. Gutachter: Prof. Dr. Jörg Höfeld

Tag der Promotion: 30.04.2015

Erscheinungsjahr: 2015

Experience is what you get when you didn't get what you wanted

Randy Pausch

Our greatest glory is not in never falling, but in rising every time we fall.

Confucius

ABBREVIATIONS

°C: Celsius degrees

2-AG: 2-arachidonylglycerol

AC: Adenylate cyclase

AEA: N-arachidonoyl ethanolamide

AMPC: Cyclic adenosine monophosphate

ampR: Ampicillin resistance gene

Arg (R): Arginine

B2M: Beta-2-microglobulin

BAC: Bacterial artificial chromosome

BCP: Beta-Caryophyllene

bGHPA: Bovine growth hormone polyadenylation signal

BMMs: Bone marrow-derived macrophages

bp: Base pair

Cas: CRISPR-associated protein

CB1: Cannabinoid receptor 1

CB2: Cannabinoid receptor 2

CBh: Hybrid form of the cytomegalovirus (CMV) and the chicken β -actin (CBA)

CD: Cluster of differentiation

cDNA: Complementary deoxyribonucleic acid

cmR: Chloramphenicol resistance gene

CMV: Cytomegalovirus

CNR2: Human CB2 gene locus

Cnr2: Mouse CB2 gene locus

CNS: Central nervous system

CRISPR: Clustered regularly interspaced short palindromic repeats

crRNAs: CRISPR-RNAs

DAPI: 4',6'-diamidino-2-phenylindole

DIG: Digoxigenin

DMEM: Dulbecco's modified eagle medium

DMSO: Dimethylsulfoxide

DNA: Deoxyribonucleic acid

dNTPs: Deoxynucleotide triphosphates

DSB: Double-strand break

DSBs: Double-strand breaks

DTT: Dithiothreitol

eCBs: Endocannabinoids

ECS: Endocannabinoid system
EDTA: Ethylenediaminetetraacetic acid
eGFP: Enhanced green fluorescent protein
EMN: Neutral sphingomyelinase enzyme
ERK: Extracellular signal-regulated kinase
ES: Embryonic Stem (cell)
FACS: Fluorescence-activated cell sorting
FAK: Focal adhesion kinase
FAN: Factor associated with neutral sphingomyelinase activation
FBS: Fetal bovine serum
FITC: Fluorescein isothiocyanate
FLPe: Flippase enzyme
Fmol: Femtomol
FRT: Flippase recognition target site
g: G-force
gb2: E. Coli prokaryotic promoter
G_{i0}: Gi alpha subunit is a heterotrimeric G protein subunit that inhibits the production of cAMP from ATP.
Gln (Q): Glutamine
GPCR: G protein-coupled receptor
gRNA: Guide RNA
HBSS: Hank's balanced salt solution
hCB2: Human CB2 receptor
HCl: Hydrochloric acid
HCV: Hepatitis C virus
HDR: Homology-directed repair
HR: Homologous recombination
HEK: Human embryonic Kidney
IFN γ : Interferon gamma
IL: Interleukin
IRES2: Internal ribosome entry site version 2
IU: Infectious unit
JNK: c-Jun N-terminal kinase
kanR: Kanamycin resistance gene
kb: Kilo-base pair
LIC: Ligation-independent cloning
LIF: Leukemia inhibitory factor

LPS: Lipopolysaccharide
LTR: Long terminal repeat
M: Marker
M1: Pro-inflammatory phenotype
M2: Anti-inflammatory phenotype
MAPK: Mitogen-activated protein kinases
mbar: Millibar
mCB2: Mouse CB2 receptor
M-CSF: Macrophage colony-stimulating factor
MEFs: Mouse embryonic fibroblasts
MFI: Mean fluorescence intensity
MgCl₂: Magnesium Chloride
MHCII: Major histocompatibility complex class II molecules
Min: Minutes
ml: Millilitre
mM: Millimolar
MMR: Mannose receptor
mRNA: Messenger RNA
NaCl: Sodium chloride
NaOH: Sodium hydroxide
Neo: Neomycin
neoR: Neomycin resistance gene
ng: Nanogram
NHEJ: Non-homologous end joining
NLS: Nuclear localization sequence
nm: Nanometer
nM: Nanomolar
nmol: Nanomol
ORF: Open reading frame
Ori: origin of replication sequence
pA: polyadenylation signal
PAM: Protospacer-adjacent motif
PBS: Phosphate buffered saline
PCR: Polymerase chain reaction
PFA: Paraformaldehyde
PGK: Eukaryotic promoter
PI3K: Phosphoinositide 3-kinase

PKA: Protein kinase A
PKB: Protein kinase B
pmol: Picomol
RNA: Ribonucleic acid
rpm: Revolution per minute
RT: Reverse transcriptase
RT-PCR: Reverse transcription polymerase chain reaction
RVD: Repeat variable di-residue
s: Second
SDS: Sodium dodecyl sulfate
sgRNA: Single guide RNA
SNPs: Single-nucleotide polymorphisms
SSC: Saline-sodium citrate buffer
T4 PNK: T4 polynucleotide kinase
TALENs: Transcription activator-like effector nucleases
TE buffer: Tris-EDTA buffer
THC: Tetrahydrocannabinol
TNF α : Tumor necrosis factor alpha
tracrRNA: Trans-activating crRNAs
TU: Transducible units
UV: Ultraviolet
v/v: Volume/volume
w/v: Weight/volume
WPRE: Woodchuck hepatitis virus posttranscriptional regulatory element
WT: Wild type
 μ g: Microgram
 μ l: Microliter
 μ M: Micromolar
 Ψ : Viral vector packaging signal

SUMMARY

The endocannabinoid system (ECS) regulates numerous cellular and physiological processes. Nowadays, the system comprises two G protein-coupled receptors named CB1 and CB2 receptor, and the endogenous ligands anandamide (N-arachidonylethanolamide: AEA) and 2-arachidonylglycerol (2-AG). The CB1 receptor is mainly expressed in the central nervous system, whereas the CB2 receptor is mainly expressed by peripheral cells including immune and bone cells. Unlike the CB1 receptor, CB2 receptor activation does not induce psychoactive negative effects. Together with its expression pattern, the CB2 receptor thus offers a great potential for the treatment of different immune related diseases. The CB2 receptor became a target of choice for the development of new drugs.

A genetic variation within the human gene coding for the CB2 receptor was discovered ten years ago. This genetic variation results in the amino acid exchange from glutamine to arginine at protein position 63 (Q63R), which is localized in the first intracellular loop of the G protein. As a consequence, the signaling activity of the receptor is generally reduced. To address the functional differences between these human variants of the CB2 receptor *in vivo*, humanized targeting vectors were generated and subsequently used for the generation of chimeric mice by injecting targeted ES cells into blastocysts. Due to the lack of germ-line transmission, new engineering technologies (CRISPR/Cas9 system and TALENs) were designed and tested for their ability to target the *Cnr2* locus. The study presented here revealed that applying the CRISPR/Cas9 technology tremendously improved the homologous recombination efficiency in ES cells. In order to assess the functional differences between the human CB2 receptor variants *in vitro*, recombinant viral vectors were developed using the innate ability of lentiviruses to deliver genetic material into non-dividing cells. Due the low transduction efficiencies measured in bone marrow-derived macrophages (BMMs) for all viral vectors generated, lentiviruses were not further used during the study.

Since its discovery, CB2 receptor activation has been shown to inhibit activation, cell motility and secretion of inflammatory mediators in different kinds of immune cells. In this study, the anti-inflammatory role played by murine CB2 receptor activation was analysed in BMMs. Different pro- and anti-inflammatory activation states of BMMs were induced and characterized. Under pro-inflammatory conditions, CB2 activation had no effect on pro-inflammatory cytokine (TNF α) release. Gene expression analysis revealed that genes encoding cannabinoid receptors are differentially regulated upon stimulation with different combination of pro-inflammatory substances. Finally, CB2 receptor activation with different agonists did not modulate the phagocytic activity of zymosan particles by BMMs. Hence, the data presented here could not clearly confirm an anti-inflammatory role of murine CB2 receptor in BMMs.

CONTENTS

1 INTRODUCTION	6
1.1 Discovery of the endocannabinoid system	6
1.2 ECS: the global view.....	7
1.3 The cannabinoid receptor 2: from mice to human.....	9
1.3.1 The cannabinoid receptor 2.....	9
1.3.2 Genetic variations within the human cannabinoid receptor 2 gene	9
1.4 Aim of the study: functional testing of the CB2 receptor	12
1.4.1 Generation of Humanized CB2 mice with conventional and new DNA engineering strategies	13
1.4.1.1 ES cells based strategies.....	13
1.4.1.2 New engineering technologies	14
1.4.2 Generation of hCB2 recombinant viral vectors	15
1.4.3 Immune cells characterization	16
2 MATERIAL	18
2.1 Equipment	18
2.2 Chemical and reagents.....	19
2.2.1 Kits	19
2.2.1.1 Molecular biology kits	19
2.2.1.2 pRed/ET kits.....	19
2.2.1.3 Elisa kit.....	20
2.2.1.4 TaqMan® Gene Expression Assays from Life Technologies	20
2.2.2 Selection cassettes	20
2.2.3 Molecular weight standards.....	20
2.2.4 Desoxyribonucleotides (dNTPs)	20
2.2.5 Enzymes and antibodies	21
2.2.5.1 Enzymes.....	21
2.2.5.2 Antibodies.....	21
2.2.6 Antibiotics.....	22
2.2.7 CB2 receptor agonists	22

2.2.8	Oligonucleotides.....	23
2.2.8.1	Oligonucleotides	23
2.2.8.2	Long oligonucleotides.....	23
2.2.9	Solutions	23
2.2.9.1	Cultivation of bacteria	23
2.2.9.2	DNA isolation.....	24
2.2.9.3	Southern blot.....	24
2.2.9.4	Agarose gel electrophoresis.....	26
2.2.9.5	Cell culture media.....	26
2.2.9.6	Cell culture stimulants	29
2.2.9.7	Cell transfection reagents	29
2.2.9.8	Elisa solutions	29
2.2.9.9	FACS solutions	30
2.3	BAC, plasmids	30
2.3.1	BAC.....	30
2.3.2	Original plasmids.....	31
2.3.3	Cloned plasmids.....	31
2.4	Cells	33
2.4.1	Bacteria.....	33
2.4.2	Embryonic Stem cells	33
2.4.3	Cells	33
2.5	Software.....	33
3	METHODS	35
3.1	Molecular biology methods	35
3.1.1	DNA	35
3.1.1.1	DNA preparation from <i>E.coli</i>	35
3.1.1.2	Purification of DNA fragments.....	35
3.1.1.3	DNA preparation from living cells	36
3.1.1.4	Measurement of DNA concentration	36
3.1.1.5	Digestion of DNA.....	36
3.1.1.6	DNA ligation.....	37
3.1.1.7	Amplification of DNA fragments by polymerase chain reaction	37
3.1.1.8	PCR reaction for Southern blot probes	37
3.1.1.9	DNA sequencing.....	39
3.1.1.10	RNA preparation	39

3.1.1.11	Measurement of RNA concentration	39
3.1.1.12	Reverse transcriptase polymerase chain reaction (RT-PCR)	39
3.1.1.13	Real-time reverse transcription-PCR (real-time RT-PCR)/ TaqMan gene expression analysis	40
3.1.2	Southern blot	41
3.1.3	Cloning of targeting vectors by Red/ET recombination	42
3.1.4	Cloning of TALEN plasmids	44
3.1.5	Cloning of CRISPR/Cas9 plasmids	45
3.1.6	Cloning of vector constructs	47
3.2	Embryonic Stem (ES) cells	48
3.2.1	Cultivation of mouse embryonic fibroblasts (MEFs)	48
3.2.2	Cultivation of mouse embryonic stem cells	48
3.2.3	Deep-freezing and re-cultivation of ES cells	48
3.2.4	Electroporation and selection of ES cell clones	49
3.2.5	RESGRO culture of positive ES cell clones	50
3.3	Experiments requiring NIH3T3 cells	50
3.3.1	Cultivation of NIH3T3 cells	50
3.3.2	Transfection of NIH3T3 cells	50
3.3.3	SURVEYOR assay	51
3.4	Mouse bone marrow-derived macrophages (BMMs) experiments	52
3.4.1	Isolation and differentiation of myeloid stem cells into macrophages	52
3.4.2	Transduction of bone marrow-derived macrophages with recombinant lentiviral vectors	53
3.4.3	Preparation of bone marrow-derived macrophages for fluorescence-activated cell sorting (FACS)	53
3.4.3.1	Extracellular labelling for transduction analysis	53
3.4.3.2	Intracellular labelling for transduction analysis using CB2 polyclonal C-terminal antibody	54
3.4.3.3	Extracellular labelling for polarization analysis	54
3.4.4	Analysis of cytokine release by enzyme-linked immunosorbent assay (ELISA)	55
3.4.5	Analysis of cannabinoid receptors expression by real time PCR (TaqMan)	55
3.4.6	Phagocytosis assay	55
3.4.6.1	Phagocytosis assay	55
3.4.6.2	Analysis of phagocytic activity by Fluorescence-activated cell sorting (FACS)	55
3.4.6.3	Analysis of phagocytic activity by microscopy	56

4 RESULTS.....	57
4.1 Humanizing the Cnr2 locus.....	57
4.1.1 Generation of hCB2 targeting constructs.....	57
4.1.1.1 Subcloning.....	57
4.1.1.2 Verification of the subcloning step.....	59
4.1.1.3 Replacement of the murine ORF.....	59
4.1.1.4 Cloning of Human ORF subclones.....	62
4.1.1.5 Insertion of the FRT-PGK-gb2-neo-FRT cassette for selection.....	63
4.1.1.6 Verification of targeting constructs.....	65
4.1.2 Screening strategies for targeted mutagenesis of the Cnr2 gene locus.....	66
4.1.2.1 PCR.....	66
4.1.2.2 Southern Blot.....	69
4.1.3 Cloning of new genetic engineering technologies to humanized the Cnr2 locus	71
4.1.3.1 TALEN pair design and generation.....	71
4.1.3.2 Design and Generation of CRISPR/Cas plasmid.....	74
4.1.3.3 Surveyor assay.....	76
4.1.4 Efficiency comparison to humanized the Cnr2 locus.....	79
4.1.4.1 Generation of chimeric mice to produce humanized CB2 mice.....	79
4.1.4.2 Testing the CRIPR/Cas system to enhance the humanization of the Cnr2 locus.....	81
4.2 Generation of human CB2 recombinant lentiviral vectors.....	83
4.2.1 rrl-CMV-hCB2 vector construct generation.....	83
4.2.2 rrl-CMV-hCB2-IRES2-eGFP vector constructs generation.....	85
4.2.3 Mouse bone marrow-derived macrophages expressing the human CB2 receptors variants.....	88
4.2.3.1 Specificity control of CB2 polyclonal N-Terminal antibody.....	88
4.2.3.2 Specificity control of CB2 polyclonal C-Terminal antibody.....	90
4.2.3.3 Measurement of transduction efficiency independent of CB2 antibody use.....	91
4.3 Functional analysis of CB2 receptor activation in mouse bone marrow derived-macrophages.....	93
4.3.1 Activation state analysis of mouse bone marrow-derived-macrophages.....	93
4.3.1.1 Markers expression analysis.....	93
4.3.1.2 Effect of CB2 agonists on pro-inflammatory cytokine release.....	94
4.3.1.3 Cannabinoid receptors real time expression.....	95
4.3.2 Analysis of zymosan phagocytosis by BMMS.....	96
4.3.2.1 Zymosan phagocytosis by BMMS upon CB2 agonists stimulation measured by FACS.....	96

4.3.2.2 Zymosan phagocytosis by BMMS upon CB2 agonists stimulation measured by fluorescence microscopy.....	101
5 DISCUSSION	103
5.1 Humanizing the mouse CB2 locus	103
5.2 Functional analysis	108
5.2.1 Recombinant lentiviral vectors expressing the human CB2 variants	108
5.2.2 Functional analysis of CB2 receptor activation in mouse bone marrow derived-macrophages	110
5.2.2.1 Bone marrow macrophages phenotypes	110
5.2.2.2 Zymosan phagocytosis	111
6 BIBLIOGRAPHY	113
7 APPENDIX	121
7.1 Supplemental material.....	121
7.2 Declaration	125
7.3 Curriculum Vitae	126
8 ACKNOWLEDGMENTS	127

1 INTRODUCTION

1.1 Discovery of the endocannabinoid system

“Cannabis is a generic term used to denote the several psychoactive preparations of the plant *Cannabis sativa*. It is by far the most widely cultivated, trafficked and abused illicit drug.” (WHO, 2013). Nowadays cannabis is mainly used for recreational purposes due to its psychotropic effects. But in ancient history, a lot of evidences show that this drug was presumably used for medical or divinatory purposes. The last concrete example is the recent discovery of a 2700-year-old grave near Turpan, in North China, containing a shaman and a large cache of cannabis (789 grams). Scientists supposed that the cannabis was used for pharmaceutical, psychoactive or divinatory purposes (Russo et al., 2008). Moreover evidences for cannabis use can be traced back for more than 4000 years (Murray et al., 2007).

Cannabis interest rose among scientists who clearly wanted to identify and elucidate the drug and its effects. Like for the discovery of the opioid system, which started by the chemical synthesis of heroin by morphine diacetylation in the late 1800s, research on cannabinoid system started, in 1965 (Mechoulam and Gaoni, 1965), with the isolation and synthesis of the active constituent of Hashish: Δ^1 -tetrahydrocannabinol (THC) by Raphael Mechoulam and colleague. Twenty years later, the molecular target of this substance was identified in the rat brain (Devane et al., 1988) and cloned (Matsuda et al., 1990). This first cannabinoid receptor was named the cannabinoid receptor 1 (CB1). This step initiated the research era of the so-called endocannabinoid system (ECS). Few years later a second target was identified. While CB1 was found to be extremely abundant in the brain, and was immediately suggested to be responsible for THC psychoactivity, the second target was discovered in rat spleen and was consecutively cloned (Munro et al., 1993). This receptor was named the cannabinoid receptor 2 (CB2). The molecular characterization of THC binding sites opened the way for the identification of endogenous lipid mediators or ligands. The term cannabinoid compound encompasses three categories of compounds. Those derived from the *Cannabis sativa* plant (phytocannabinoids), synthetically derived compounds (synthetic cannabinoids), as well as endogenous compounds, which were shown to bind to CB1 and CB2 receptors (endocannabinoids). The two major endocannabinoids (eCBs) anandamide (N-arachidonylethanolamide: AEA) (Devane et al., 1992) and 2-arachidonylglycerol (2-AG) (Mechoulam et al., 1995; Sugiura et al., 1995) are the most extensively studied. The system comprising the two receptors and the endogenous ligands was then referred to as the endocannabinoid system (ECS). Investigations of this system

became really interesting with the emergence and use of transgenic animals lacking the CB1 (Zimmer et al., 1999) and the CB2 receptor (Buckley et al., 2000). Nowadays, many transgenic animal models related to the ECS exist: from receptors to enzymes involved in the synthesis or degradation of the endogenous ligands.

However, researches on the ECS did not fully elucidate the mechanisms, targets and signaling pathways. And it is well accepted that the endocannabinoid system does not involve only two receptors and two ligands. During the last past years, G coupled protein receptors (GPCR) were identified and were thought to be new members of the cannabinoid receptor family, like GPR55 and GPR18. As GPR55 being a real cannabinoid receptor is still under debate (Gasperi et al., 2013), GPR18 is considered as a really good candidate to be the third cannabinoid receptor but further investigations are still required (Console-Bram et al., 2014).

1.2 ECS: the global view

To better understand the ECS system, it is necessary to dissect the effects occurring via the CB1 and the CB2 receptors. Unlike the CB1 receptor which is expressed at high levels in the central nervous system (CNS), the CB2 receptor is found predominantly in the periphery and more precisely in cells of hematopoietic and mesenchymal cell lineages. The differential expression pattern of these receptors leads to different physiological effects. In the CNS, endocannabinoids act as powerful regulators of synaptic function. Defined as a retrograde signaling system, endocannabinoids are synthesized at the postsynaptic site and released in the synaptic cleft. They bind at the CB1 receptor expressed at the presynaptic site, to suppress transmitter release in a transient or long-lasting manner, at both excitatory and inhibitory synapses (Alger, 2012; Katona and Freund, 2012). As CB1 activation by THC or other synthetic cannabinoid is inducing psychoactive effects, many scientists started to concentrate their efforts to study the CB2 receptor whose activation does not induce such negative effects.

As described in figure 1, CB1 and CB2 receptors, are $G_{i/o}$ coupled GPCR. Binding of ligands (eCBs or other agonists) to these receptors activates several cellular signaling pathways and leads to the inhibition of adenylyl cyclase and stimulation via ceramide production of several mitogen-activated protein (MAP) kinases (extracellular-signal-regulated kinase: ERK, c-Jun N-terminal kinase: JNK, p38 and p42/44). It also results in the activation of the PI3 kinase (phosphatidylinositol-3-kinase), protein kinase B-Akt pathway, and gene transcription. Moreover, both receptors modulate high voltage-activated calcium channels or inwardly rectifying potassium channels (Atwood and Mackie, 2010; Bifulco et al., 2008;

Fernandez-Lopez et al., 2013). Unlike the ability of the CB1 receptor activation to inhibit synaptic transmission in the CNS, the CB2 receptor activation in immune cells has been shown to inhibit activation, cell motility and secretion of inflammatory mediators (Basu and Dittel, 2011; Tanasescu and Constantinescu, 2010). This receptor became a target of choice for the development of new pharmacological compounds to treat immune related diseases. However, during drug discovery process an important point rose while trying to target specifically the CB2 receptor. In fact different pharmacological responses to identical drugs were reported in different species (Bingham et al., 2007; Mukherjee et al., 2004; Yao et al., 2006) thus leading to difficulties during the development of drugs targeting specifically the human CB2 receptor.

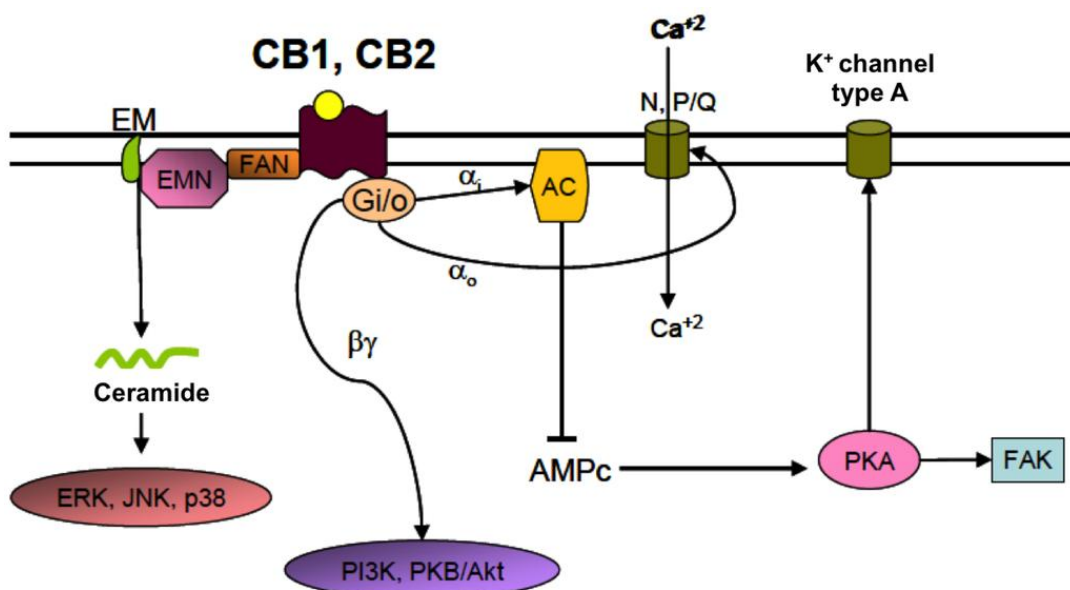


Figure 1: Main signaling pathways activated by cannabinoid receptors.

AC: adenylyl cyclase; EMN: neutral sphingomyelinase enzyme; EM: sphingomyelin; FAN: factor associated with neutral sphingomyelinase activation; N, P/Q: voltage-dependent calcium channels type N, P/Q; PKA: protein kinase A; PKB/Akt: protein kinase B; ERK: extracellular signal-regulated kinase; JNK: c-Jun *N*-terminal kinase; FAK: focal adhesion kinase; PI3K: phosphoinositide-3 kinase. David Fernández-López¹, Ignacio Lizasoain², Maria Ángeles Moro² and José Martínez-Orgado³. Cannabinoids: Well-Suited Candidates for the Treatment of Perinatal Brain Injury review *Brain Sci.* 2013, 3(3), 1043-1059; doi:10.3390/brainsci3031043,

Physiological consequences of ECS modulation has been extensively studied since the discovery of the system and the growing use of transgenic mouse models. The system was shown to play a role in many physiologic processes and diseases, as few examples: neurotransmission, aging, inflammation/migration, neuropathic and inflammatory pain, metabolic syndromes, osteoporosis, drug addiction and liver diseases (Baldassarre et al.,

2013; Bilkei-Gorzo, 2012; Castillo et al., 2012; Guindon and Hohmann, 2009; Idris, 2010; Oliere et al., 2013; Rom and Persidsky, 2013; Silvestri and Di Marzo, 2013).

1.3 The cannabinoid receptor 2: from mice to human

1.3.1 The cannabinoid receptor 2

The cannabinoid receptor 2 was discovered by a polymerase chain reaction (PCR)-based strategy designed to isolate G-protein-coupled receptors (GPCR) in differentiated myeloid cells and based on its similarity in amino-acid sequence to the CB1 receptor (Munro et al., 1993). The human CB1 and CB2 receptors share approximately 44 % amino acid similarity. As the CB1 amino acid sequence is really highly conserved across human and rodent species, the CB2 receptor is a bit less, but still well conserved, across human and murine species. The human CNR2 gene and its mouse ortholog Cnr2, are located on chromosomes 1p36 and 4QD3, respectively. As for the CB1 receptor, the CB2 receptor is composed of the non-coding exons 1a and 1b, and a single coding exon 2. The coding exon 2 open reading frame (ORF) contains 1083 base pairs (bp) for the human gene and 1044 bp for the mouse one, resulting in a 360 amino acid long human CB2 receptor protein and a 347 amino acid long mouse one. An open reading frame alignment of the human CB2 (hCB2) and the mouse CB2 (mCB2) nucleic acid sequences revealed 82 % homology. An alignment of the hCB2 and mCB2 peptide sequences revealed 83 % homology. The main differences observed between the mouse and the human peptide sequences are located at the N and C terminal regions of the protein and in the extra and intra cellular loops whereas the most conserved regions are the transmembrane domains of the protein.

1.3.2 Genetic variations within the human cannabinoid receptor 2 gene

Among mammalian species, individuals are identical over most of their genomes. Thus, only a relatively small number of genetic differences have resulted in the striking variation seen among individuals within the same species, mainly due to single base changes also defined as single nucleotide polymorphisms or SNPs. SNPs can be found in intronic regions (within introns), and in 5' or 3' untranslated regions of genes. Studying the role played by those SNPs located in non coding exon is challenging. Moreover SNPs are also located in coding exons of genes. When the nucleotide substitution does not change the amino acid, it is called a synonymous SNPs whereas nucleotide substitution that result in a change to the amino acid is defined as a nonsynonymous SNPs. The cannabinoid receptor 2 and its single coding exon was extensively studied for the presence of nonsynonymous SNPs within the ORF and their roles and consequences. In 2005, Doctor Karsak and colleagues discovered three interesting nonsynonymous SNPs within the CNR2 gene that were associated with human

osteoporosis (Karsak et al., 2005) and few years later with hand bone strength phenotypes (Karsak et al., 2009). One of the discovered SNPs was referenced under the name rs2229579 and the genetic variation was the result of the amino acid exchange from histidine to tyrosine at protein position 316 (H316Y), which is localized at the C-terminal part of the protein. The two others nonsynonymous SNPs discovered were located on adjacent nucleotides, named rs2502992–rs2501432 and resulting in the amino acid exchange from glutamine to arginine at protein position 63 (Q63R), which is localized in the first intracellular loop of the G coupled protein.

In 2010, Carrasquer and colleagues tested the CB2 receptor variant containing the amino acid arginine at the position 63 (hCB2Arg63) for the functional significance of this mutation. Using site-directed mutagenesis and HEK293 cells transfected with the CB2 variants, they showed in ligand-induced cyclic AMP accumulation assays that cannabinoid agonists like WIN55212-2 and 2-AG had reduced efficacy in cells expressing the hCB2Arg63 as compared with the wild type receptor hCB2Gln63. This was the first demonstration of a reduced signaling of the polymorphic variant as compared to the wild type receptor. Moreover these findings strengthen the idea that the CB2 polymorphic receptor may contribute to the etiology of certain diseases (Carrasquer et al., 2010). The hCB2Arg63 variant was further investigated in different human case/control samples and for different diseases in which the CB2 receptor was supposed to play a role as depicted in figure 2.

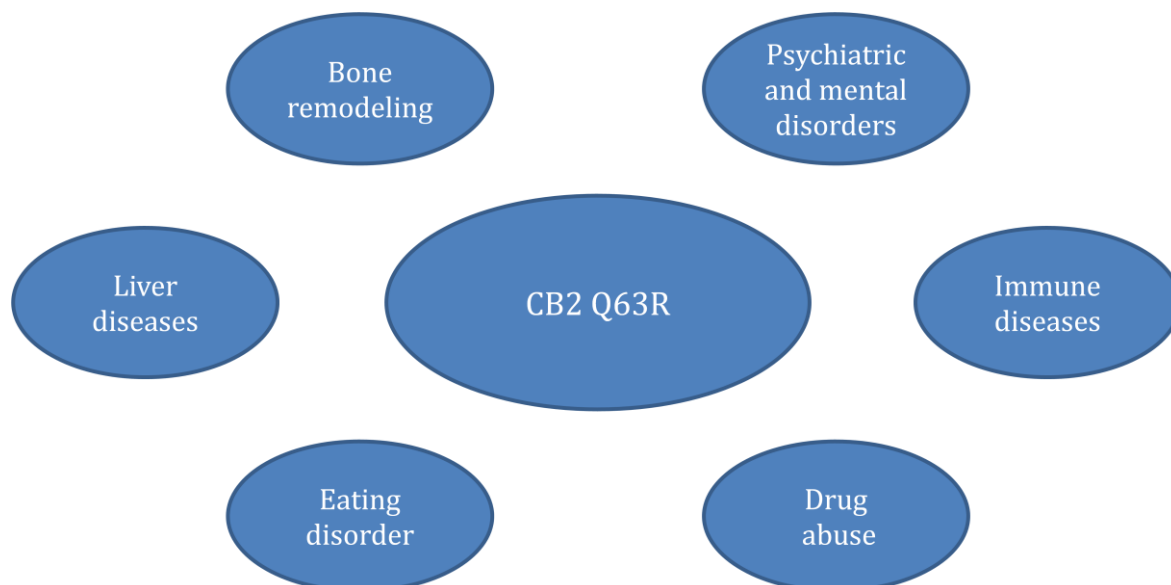


Figure 2: Involvement of human CB2 variant in different diseases.

Not much is known about the cannabinoid receptor 2 distribution pattern due to a lack of specific antibodies (Baek et al., 2013). Due to the therapeutic advantage of targeting the CB2 receptor without interfering with the CB1, many scientists have spent efforts and energy to identify expression of the CB2 receptor in the central nervous system and particularly in neurons without clear evidence (Atwood and Mackie, 2010). However, different groups of scientists investigated the genetic associations between CNR2 gene polymorphisms and disease altering the central nervous system like for example schizophrenia. A genetic association was found between the CNR2 gene polymorphisms Q63R and schizophrenia in a Japanese and a Han Chinese independent case/control populations (Ishiguro et al., 2010b; Tong et al., 2013). The two teams of scientists found that the hCB2Arg63 variant was significantly increased among schizophrenic patients compared with control subjects. And their results indicate an increased risk of schizophrenia for people with low CB2 receptor function. Associations between the R63Q polymorphisms of the CNR2 gene and eating disorders (Ishiguro et al., 2010a), alcoholism (Ishiguro et al., 2007) and depression (Onaivi et al., 2008) were found in Japanese case/control populations.

Today, it is clear that the CB2 receptor plays an important role in the peripheral system especially in pain (Anand et al., 2009) and immune system (Cabral and Griffin-Thomas, 2009) regulations. Some scientific groups focussed their efforts to show a genetic association between the CNR2 gene polymorphisms Q63R and immune diseases. In 2005, Sipe and colleagues showed a genetic association between the Q63R dinucleotide polymorphism and endocannabinoid-induced inhibition of T lymphocyte proliferation (Sipe et al., 2005). Again, T lymphocyte expressing the hCB2Arg63 variant showed a lower function of the CB2 receptor resulting in a twofold reduction of endocannabinoid-induced inhibition of proliferation compared with cells expressing the hCB2Gln variant. An interesting point from this study is that the authors found significant results using N-arachidonylglycine which is an agonist for the CB2 receptor, but also for the GPR18 receptor, as it was recently showed by McHugh et al., (McHugh et al., 2014; McHugh et al., 2012). Moreover the reduced endocannabinoid inhibitory response was only "nearly significant" using 2-AG agonist and these effects were only partially blocked using a specific CB2 receptor antagonist. Altogether these results indicate the major role played by the CB2 receptor and the genetic variant in autoimmune disease but also the necessity to identify the precise role of the CB2 receptor and the GPR18 receptor in immune cells.

Following this discovery, genetic associations between the Q63R dinucleotide polymorphism in the CNR2 gene and autoimmune disorders were investigated. An association was found by two different groups in two different case/control populations

(Egyptian and Italian) between the hCB2Arg63 variant and the immune thrombocytopenia, which is an autoimmune disorder resulting in significant defects in immune self-tolerance (Mahmoud Gouda and Mohamed Kamel, 2013; Rossi et al., 2011b). An Italian group showed also that the hCB2Arg63 variant increases the risk of celiac disease which is an autoimmune disorder of the small intestine. They raised the point that genotyping the CNR2 gene for this dinucleotide polymorphism could be a novel molecular biomarker and maybe interesting for future therapeutic intervention (Rossi et al., 2012b).

Finally, as no specific CB2 antibody exist, it is difficult to claim where the CB2 receptor is expressed. Real time expression of the CB2 gene performed since the discovery of the receptor showed the presence of CB2 mRNA in the liver and the spleen with the highest, or more precisely, with "detectable" levels. Some genetic associations between the CNR2 gene polymorphisms Q63R and liver diseases were found, principally in Italian case/control populations. The same group found in obese Italian children with fatty liver, or steatosis, that the hCB2Arg63 variant is associated with liver damage progression due to a defect in the modulation of hepatic inflammation state (Rossi et al., 2012a; Rossi et al., 2011a). Another Italian group showed that the hCB2Gln variant is associated with more severe inflammation and hepatocellular necrosis in patients with HCV infection (Coppola et al., 2014). These results corroborate the idea of a hepatoprotective role for the CB2 receptor, and the two CB2 genetic variants could play an hepatoprotective role depending on the liver disease.

Altogether, these findings are in concordance with the demonstration of a reduced signaling of the hCB2Arg63 variant and its implication in different diseases, or process, making the CB2 receptor a target of choice for the development of new drugs. To perform a deeper investigation of the two human variants, it is more than necessary to assess the functional differences *in vivo* by the generation of humanized mice harboring both CB2 receptor variants and *in vitro* by the development of different techniques in order to express and characterized the human CB2 receptor variants. The next part will be dedicated to the introduction of the different technologies which were used during this work, in order to achieve the *in vivo* and *in vitro* characterization of the human CB2 variants.

1.4 Aim of the study: functional testing of the CB2 receptor

The present PhD work is divided into three aims which finally converged into one unique direction: clarifying the CB2 receptor function based on the generation of different tools. The first aim consists in the generation of CB2 receptor humanized mice using embryonic stem

(ES) cells or new engineering technologies. The second aim consists in developing recombinant viral vectors containing the human CB2 receptor variants using the innate ability of lentiviruses to deliver genetic material into a chosen infected cell type. Finally a third aim consists in the characterization of the CB2 receptor role in different functions played by immune cells such as macrophages.

1.4.1 Generation of Humanized CB2 mice with conventional and new DNA engineering strategies

The unique way to understand the functional consequences *in vivo* of the genetic variations present among the human CB2 receptor gene is to generate two mutant mouse models containing the two different variants of the human gene identified. In order to achieve this, genomic engineering techniques based on homologous recombination (HR) in ES cells using a targeting constructs and new engineering technologies were used.

1.4.1.1 ES cells based strategies

Nowadays, genomic engineering techniques based on HR in ES cells are widely used for the generation of mutant mouse models, which are essential tools for biomedical research to analyze gene functions in disease processes. In some instances these techniques have also been used to generate mice in which a human disease-associated gene variant replaced the cognate mouse gene. Such “humanized” mice can provide important information about the role of specific protein variants and they may be useful for drug development (Scheer et al., 2013).

The generation of transgenic mice started in the early 1980s with the direct microinjection of cloned DNA into the pronuclei of fertilized eggs resulting into transgenic mice in which the transgene is stably integrated into the genome. The main disadvantage of this technique is the random integration of the transgene, because neither the copy number nor the site of integration is controlled. These limitation was overcome in the late 1980s with the generation and use of ES cells to generate transgenic animals. ES cells were derived from preimplantation embryos and present the remarkable ability to colonize a host embryo, including its germ line (Evans and Kaufman, 1981; Martin, 1981). These cells, which can be cultured in large numbers, yields the possibility of selecting genetic modifications in culture and obtaining corresponding mice via the generation of germ line chimeras (Babinet, 2000). This is generally achieved by the use of targeting vectors. Despite their widespread use, the generation of transgenic animals via techniques based on ES cells is time consuming and extremely costly.

1.4.1.2 New engineering technologies

Novel DNA engineering technologies for the generation of mutant alleles have been developed during the last five years and are based on the introduction of double-strand breaks (DSBs) into a target gene locus by sequence specific nucleases (Gaj et al., 2013). For this purpose, either zinc-finger nucleases or transcription activator-like effector nucleases (TALENs) have been engineered to recognize and cleave specific DNA sequences (Zinc finger: (Hockemeyer et al., 2009), TALEN: (Cermak et al., 2011; Hockemeyer et al., 2011; Li et al., 2011)). The resulting DSBs in the targeted DNA sequence can be repaired by either of two mechanisms, nonhomologous end joining (NHEJ) or homology directed repair (HDR) (Porteus and Carroll, 2005; Urnov et al., 2005). NHEJ leads to small genetic modifications such as deletions or insertions (indels) that can cause disruption of genetic loci and lead to the generation of gene knockout animal. On the other hand the HDR allows either precise modification of a target sequence or precise introduction of a specific sequence into the targeted site. Thus when a small double-stranded or single stranded template of DNA is supplied consecutively to these DNA engineering tools, HR is stimulated by double strand breaks and lead to precise genetic engineering (Hockemeyer et al., 2011; Wang et al., 2013b).

Nevertheless, cloning of these nucleases still requires a considerable effort, which offsets their advantages to some extent. Recently, the very powerful and much simpler CRISPR/Cas9 system for the introduction of targeted DSBs has been developed (Li et al., 2013a; Menke, 2013). It is based on the discovery that many eu- and archaebacteria detect and destroy invading phages using ribonucleoprotein complexes composed of “clustered regularly interspaced short palindrome repeat” CRISPR-RNAs (crRNAs), *trans*-activating crRNAs (tracrRNA), and CRISPR-associated (Cas) proteins. In particular, Cas9 from *Streptococcus pyogenes* has been directed by single-guide or guide RNAs (sgRNA, gRNA), a fusion of crRNA and tracrRNA, to produce DSBs at specific genomic locations (Chylinski et al., 2013). Thus, the system can be adapted to target different genomic locations simply by modifying the sequence-specific motive in the sgRNA (Cong et al., 2013; Wang et al., 2013b). This system has been used to enhance the frequency of gene targeting by homologous repair in *C. elegans* (Chen et al., 2013; Dickinson et al., 2013), as well as protoplasts from *Arabidopsis thaliana* and *Nicotiana benthamiana* (Li et al., 2013b).

In this study a TALEN pair and a CRISPR/Cas9 system were developed and tested for their efficiency to produce DSBs within the coding exon of the *Cnr2*. Furthermore, the potential of the CRISPR/Cas9 system to enhance the efficiency of “humanizing” the mouse

Cnr2 gene in mouse embryonic stem cells was assessed, revealing the potential of this technology for the further generation of "humanized" transgenic animals.

1.4.2 Generation of hCB2 recombinant viral vectors

The basic concept of viral vectors is to harness the innate ability of viruses to deliver genetic material into the infected cell. Unfortunately, viruses deliver different genes whose products are hazardous to the host and lead to pathogenesis. The basic principle of turning these pathogens into delivery systems relies on the ability to separate the components needed for replication from those capable of causing disease (Verma and Weitzman, 2005). As represented in figure 3, the parental virus genome consists of genes involved in replication, production of the virion, genes responsible of the pathogenicity of the virus. This viral genome is flanked by *cis*-acting sequences that provide the viral origin of replication and the signal for encapsidation. Lentiviral delivery systems were created by separating this viral genome in two parts: one packaging construct consisting of the gene responsible for the replication and the production of structural proteins. The vector construct consists of the transgene construct containing a promoter, the gene of interest, and a posttranscriptional regulatory element. This vector construct is flanked by the *cis*-acting sequences. Both constructs are then transfected into packaging cells like 293T cells. These cells are derived from human embryonic kidney cells (HEK293 cells) and the "T" means that it express the Large T antigen which is important for increasing the replication of plasmids containing a SV40 origin. The lentiviral packaging and vector constructs contain this SV40 origin of replication.

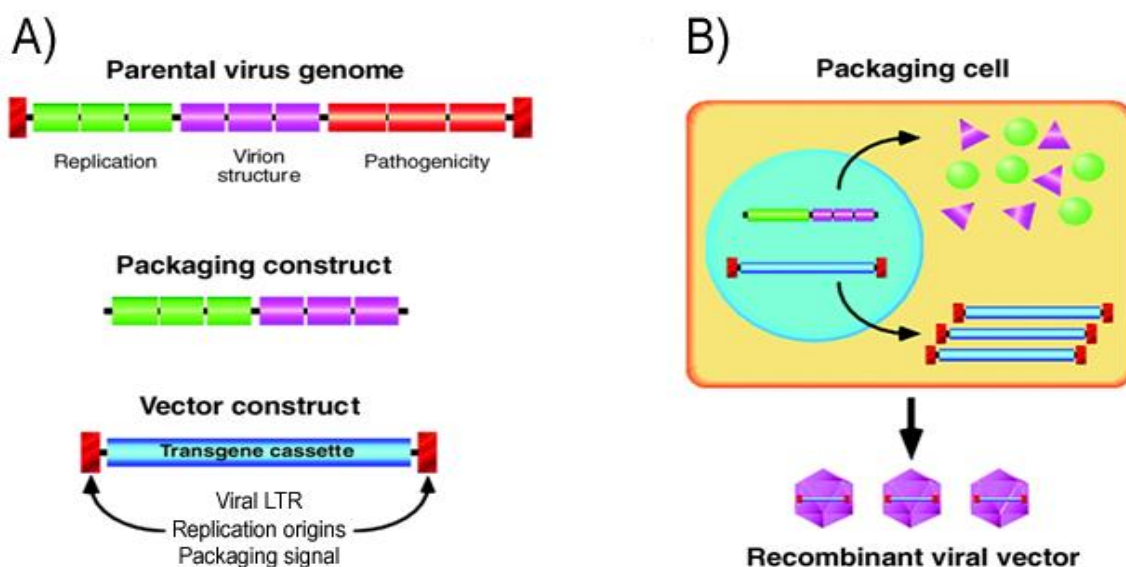


Figure 3: Principle of generating a viral vector.

A) Converting a virus into a recombinant viral vector. Schematic of a generic viral genome is shown with genes that are involved in replication, production of the virion, and pathogenicity of the virus. The *cis*-acting sequences represented by the red boxes flanking the parental virus genomes provide the viral origin of replication and the signal for encapsidation. The packaging construct contains only genes that encode functions required for replication and structural proteins. The vector construct contains the essential *cis*-acting sequences and the transgene cassette that contains the required transcriptional regulatory elements. LTR: long terminal repeat. B) The packaging and vector constructs are introduced into the packaging cell (293T cells) by transfection. Proteins required for replication and assembly of the virion are expressed from the packaging construct, and the replicated vector genomes are encapsidated into virus particles to generate the recombinant viral vector. Picture and legend modified from original: Inder M. Verma and Matthew D. Weitzman. Gene therapy: twenty-first century medicine. *Annu Rev Biochem.* 2005;74:711-38.

The lentiviruses are a subgroup of retroviruses that integrate into the genomes of non-dividing cells. Consequently, these viruses have the most potential for primary cells such as bone marrow-derived macrophages human CB2 genes delivery.

1.4.3 Immune cells characterization

BMMs are primary macrophage cells, derived from bone marrow cells *in vitro* in the presence of the growth factor: the macrophage colony-stimulating factor (M-CSF). Once differentiated, the mature BMMs are suitable for different types of experimental manipulations like transduction with recombinant lentiviral vectors even if these cells are not the easiest to transduce (Burke et al., 2002).

It also permits to study gene expression using flow cytometry. BMMs have the ability to be polarized. In response to the environment, macrophages undergo M1 “classically activated” pro-inflammatory or M2 “alternatively activated” anti-inflammatory activation states. These polarization states are defined by the inducing stimulus and by the ensuing patterns of gene expression, which determine the function. The cytokine interferon gamma (IFN γ) and the Toll like receptor activator lipopolysaccharide (LPS) polarize macrophages towards the M1 phenotype, which induces the release of a large amount of pro-inflammatory cytokines (tumour necrosis factor alpha: TNF α , interleukin 12 and 23: IL-12, IL-23) and expression of molecule like the cluster of differentiation 86 (CD86). M1 polarized macrophages drive antigen specific cells and are effective in killing microbes. But also they have the potential to cause toxicity and collateral tissue damage. Exposure of macrophages to the cytokine IL-4 induces the M2 phenotype, which initiates the expression of anti-inflammatory cytokines such as interleukin 10 (IL-10) and interleukin 1-RA (IL-1RA), but also cell surface markers like the mannose receptor (MMR). Alternatively activated M2 macrophage appears to be involved in

immunosuppression, wound healing and tissue repair (Mantovani et al., 2004). Moreover, BMMs such as macrophages have a unique ability to ingest microbes via phagocytosis (Murray and Wynn, 2011; Weischenfeldt and Porse, 2008). The ability of the CB2 receptor to modulate the anti-inflammatory functions of BMMs was assessed during this study.

2 MATERIAL

2.1 Equipment

Technical instrument	Identifier, Company
Analytical balance	BP 121 S, Sartorius
Cell culture incubator	Binder GmbH
Centrifuges	Biofuge fresco, Heraeus Instruments
	Biofuge pico, Heraeus Instruments
	Biofuge stratos, Heraeus Instruments
	Megafuge 1.0R, Heraeus Instruments
Digital gel documentation	ChemiDoc MP imaging systems, Bio-Rad Laboratories
Electroporation System	Gene pulser Xcell, Micropulser, Bio-Rad Laboratories
Electrophoresis chamber	Sub-Cell GT System, Bio-Rad Laboratories
Film processing machine	CP1000, AGFA
Flow cytometer	FACS Canto II, BD Biosciences
Hybridization oven	HB-1000 Hybridizer UVP
Laminar flow hood	Herasafe, Kendro
Liquid handling platform	Janus [®] , Perkin Elmer
Magnetic stirrer	MR 3001 K, Heidolph, Fisher
Microplate analyzer	MRX TC II, Dynex Technologies
Microscope	Eclipse TS 1000, Nikon
	Axiovert 40 CEL, Zeiss
	Axio Imager M2, Zeiss
PCR Cycler	iCycler, Bio-Rad Laboratories
pH meter	inoLab, WTW

Real-time PCR Cycler	7900HT Fast Real-time PCR System, Applied Biosystems
Spectrophotometer	NanoDrop 1000 Thermo scientific
Sterilizing oven	Varioklav 25T, H+P Labortechnik
UV crosslinker	UV Stratalinker 2400, Stratagene
UV lamp	Bio-Rad
Vacuum Blotter	Bio-Rad
Vortexer	Vortex-Genie 2, Scientific Industries

2.2 Chemical and reagents

2.2.1 Kits

2.2.1.1 Molecular biology kits

Kits	Company
QiaPrep MiniPrep Buffers P1-P3	Qiagen
GeneElute™ HP Plasmid MidiPrep Kit	Sigma
peqGOLD Plasmid Miniprep Kit	Peqlab
peqGOLD Gel Extraction Kit	Peqlab
PCR DIG Labeling Mix	Roche
Surveyor® mutation detection kit for standard gel electrophoresis	Transgenomic

2.2.1.2 pRed/ET kits

Kits	Company
BAC Subcloning Kit	Genebridges™
Quick & Easy Conditional Knockout Kit (FRT/FLPe)	Genebridges™

2.2.1.3 Elisa kit

Target	Species	Company
TNF α	Mouse Ready-SET-Go!	eBioscience

2.2.1.4 TaqMan[®] Gene Expression Assays from Life Technologies

Target mRNA	Assay ID
B2M	Mm00437762_m1
Cnr1	Mn00432621_S1
Cnr2	Mn00438286_m1
Gpr18	Mn01224541_m1

2.2.2 Selection cassettes

Selection cassette	Company
ColE1-amp minimal vector	Genebridges TM
FRT-PGK-gb2-neo-FRT	Genebridges TM

2.2.3 Molecular weight standards

Marker	Company
DNA Molecular weight marker II	Roche
100 bp DNA ladder	Invitrogen
1 kb DNA ladder	Invitrogen

2.2.4 Desoxyribonucleotides (dNTPs)

Marker	Company
PCR DIG Probe Synthesis Mix: dATP, dCTP, dGTP (2 mM each); 1.3 mM dTTP; 0.7 mM DIG-11-dUTP, alkali-labile; pH 7.0 10 mM dNTP Mix	Roche Invitrogen

2.2.5 Enzymes and antibodies

2.2.5.1 Enzymes

Enzyme	Company
Proteinase K	NEB
Superscript II Reverse Transcriptase	Invitrogen
Taq Polymerase	NEB
Phusion® High-Fidelity DNA Polymerase	NEB
T4 DNA ligase	Invitrogen
Antarctic Phosphatase	NEB
Quick ligase	NEB
T7 endonuclease I	NEB
T4 DNA polymerase	Enzymatics
T4 Polynucleotide Kinase (PNK)	NEB
<i>Mva</i> 1269I	Fermentas
<i>Pst</i> I FastDigest	Fermentas
<i>Kpn</i> I FastDigest	Fermentas
<i>Bbs</i> I FastDigest	Fermentas
Restriction endonucleases enzymes	NEB

2.2.5.2 Antibodies

Antigen	Species	Conjugation	Company
Anti-Digoxigenin-AP, Fab fragments	Sheep	AP (Revealed with DCP-Star)	Roche
Alexa Fluor® 488	Donkey	Alexa Fluor® 488	Invitrogen
CD11b	Rat	APC	eBioscience
CD11b	Rat	Biotin	BD Pharmingen
CD11b	Rat	eFluor® 450	eBioscience
CD11b	Rat	FITC	Biozol
CD11b	Rat	PE	eBioscience
CD40	Rat	Biotin	eBioscience
CD86	Rat	PE	BD Pharmingen
Cnr2 N-terminal	Rabbit	None	Abcam (3561)
Cnr2 N-terminal	Rabbit	None	Thermo Scientific (PA1-744)
Cnr2 C-terminal	Rabbit	None	Abcam (45942)
Fc-Block (CD16/CD32)	Rat	None	Biozol
MHCII	Rat	APC	eBioscience
MMR	Rat	Biotin	Biozol
Streptavidin	Streptomyces	PerCP-Cy5.5	BD Pharmingen

2.2.6 Antibiotics

Substance	Company	Working concentration
Ampicillin	Applichem	100 µg/ml
Chloramphenicol	Sigma Aldrich	15 µg/ml
Kanamycin	Applichem	50 µg/ml
Tetracycline	Applichem	10 µg/ml
G418	Sigma-Aldrich	170 ng/ml

2.2.7 CB2 receptor agonists

Substance	Company	Vehicule
2-AG	Tocris Bioscience	100 % EtOH
β -caryophyllene	Provided by Prof. Dr. Jürg Gertsch	Tocrisolve
JWH-133	Applichem	Tocrisolve

2.2.8 Oligonucleotides

All oligonucleotides sequences are provided in the supplemental material.

2.2.8.1 Oligonucleotides

Normal oligonucleotides were designed using Primer3 software. The optimal conditions chosen were: 20 bp for the size, a GC content of 50 % and a T_m of 58 °C. Oligonucleotides were ordered at Metabion GmbH. Desalted, scale of synthesis of 20 nmol, Desalted, lyophilised. When Primers arrived, they were dissolved at 100 pmol/ μ l as stock solution and diluted at 10 pmol/ μ l as working solution.

2.2.8.2 Long oligonucleotides

Long oligonucleotides were mainly used for cloning using the Red/ET technology. These oligos were designed with 50 bp used as homologous region followed by 25 bp for annealing and amplifying the desired DNA sequence. The oligos were ordered at Invitrogen. They were lyophilised, with a scale of synthesis of 200 nmol and PAGE purified. Oligonucleotides were dissolved at 100 pmol/ μ l as stock solution and diluted at 10 pmol/ μ l as working solution.

2.2.9 Solutions

All solutions were prepared with sterile deionized MilliQ water. If not stated otherwise, all chemicals and reagents used were purchased from Applichem, Invitrogen, Merck, Roth or Sigma-Aldrich.

2.2.9.1 Cultivation of bacteria

LB medium

H₂O

Tryptone 1 % (w/v)

Yeast extract 0.5 % (w/v)

NaCl 1 % (w/v)

Autoclaved at 121 °C, 20 min

LB agar

LB medium

Agarose 1.5 %

2.2.9.2 DNA isolation

Lysis buffer

Tris/HCl pH 8 100 mM

EDTA 5 mM

NaCl 200 mM

SDS 0.2 % (w/v)

TE buffer

Tris 10 mM

EDTA, pH 8 1 mM

Adjusted to pH 7.4

2.2.9.3 Southern blot

Depurination

HCl 250 mM

Denaturation

NaOH	500	mM
NaCl	1.5	M

Neutralization

Tris/HCl, pH 7	500	mM
NaCl	1.5	M

SSC (20X)

NaCl	3	M
Na-citrate dihydrate	300	mM
Adjusted to pH 7		

Maleic acid buffer

Maleic acid	100	mM
NaCl	150	mM
Adjusted to pH 7.5		

Blocking solution (10X)

Maleic acid buffer		
Blocking reagent (Roche)	10	% (w/v)
Autoclaved at 121 °C, 20 min		

Hybridization buffer

SSC (20X)	25	% (v/v)
SDS	0.2	% (w/v)
Blocking solution (10X)	10	% (v/v)
N-lauroylsarcosine	1	% (w/v)

Washing buffer

Maleic acid buffer

Tween 20	0.3	% (v/v)
----------	-----	---------

Detection buffer

Tris/HCl, pH 9.5	100	mM
------------------	-----	----

NaCl	50	mM
------	----	----

MgCl ₂	25	mM
-------------------	----	----

2.2.9.4 Agarose gel electrophoresis

6X loading dye

Glycerol	30	% (v/v)
----------	----	---------

Orange G	0.4	% (w/v)
----------	-----	---------

TAE buffer (1X)

Tris-acetate	40	mM
--------------	----	----

EDTA, pH 8	1	mM
------------	---	----

2.2.9.5 Cell culture media

If not stated otherwise, all the cell culture solutions and medi used were purchased from Gibco Life technologies.

MPI ES cell medium

DMEM, high glucose

FBS (ES cell approved)	20	% (v/v)
Sodium pyruvate	1	% (v/v)
Penicillin streptomycin mix	0.5	% (v/v)
Nonessential amino acids (100X)	1	% (v/v)
β -mercaptoethanol	70	nM
LIF (Merck Millipore)	500	U/ml

Bruce4 ES cell medium

DMEM, high glucose

FBS (ES cell approved)	12.5	% (v/v)
Sodium pyruvate	1	% (v/v)
Penicillin streptomycin mix	1	% (v/v)
Nonessential amino acids (100X)	1	% (v/v)
β -mercaptoethanol	0.1	mM
LIF (Merck Millipore)	1000	U/ml

RESGRO Culture Medium**Merk Millipore**

L-Glutamine (200 mM)	2	% (v/v)
----------------------	---	---------

Mouse embryonic fibroblast medium

DMEM, high glucose

FBS	10	% (v/v)
Sodium pyruvate	0.5	% (v/v)

Mitomycin solution

Mouse embryonic fibroblast medium

Mitomycin C (Sigma-Aldrich)	10	μ g/ml
-----------------------------	----	------------

Freezing medium 10% DMSO

DMEM, high glucose	40	% (v/v)
FBS (ES cell approved)	50	% (v/v)
DMSO	10	% (v/v)

Freezing medium 20 % DMSO

DMEM, high glucose	40	% (v/v)
FBS (ES cell approved)	40	% (v/v)
DMSO	20	% (v/v)

Mouse bone marrow-derived macrophages medium

RPMI 1640 (PAA)

Inactivated FBS	10	% (v/v)
Penicillin streptomycin mix	1	% (v/v)
β -mercaptoethanol	50	μ M
M-CSF (Self prepared)	15	% (v/v)
Or M-CSF (eBioscience)	20	ng/ml

The solution was sterile filtrated before use.

NIH3T3 medium

DMEM, high glucose

FBS	10	% (v/v)
Sodium pyruvate	1	% (v/v)
Penicillin streptomycin mix	1	% (v/v)

Formaldehyde 4 %

1X PBS

Paraformaldehyde	4	% (v/v)
------------------	---	---------

Slides mounting solution

Dapi-Fluoromount-G	SouthernBiotech
--------------------	-----------------

2.2.9.6 Cell culture stimulants

Stimulant	Species	Company	Concentration
Interleukin-4 (IL-4)	Mouse	eBioscience	100 U/ml
Interferon gamma (IFN γ)	Mouse	R & D Systems	20 ng/ml
Lipopolysaccharide (LPS)	<i>E. coli</i>	Invitrogen	100 ng/ml

Stimulant	Company
Zymosan A <i>S. cerevisiae</i> BioParticles®, Fluorescein Conjugate	Life Technologies
Zymosan A Bioparticles® Opsonizing Reagent	Life Technologies

2.2.9.7 Cell transfection reagents

Transfection reagents	Company
Lipofectamine 2000	Invitrogen
X-tremeGENE 9 DNA transfection reagent	Roche

2.2.9.8 Elisa solutions

Assay	Solutions Provided	Solutions Prepared	Standard Concentration
Mouse TNF α	Coating Solution	Wash Buffer	1 μ g/ml
Ready-SET-Go! eBioscience	5X Assay diluent Substrate Solution	(0.05 % TWEEN 20 in PBS 1X) Stop Solution (1 M H ₃ PO ₄)	
Mouse IL-1 β	Coating Solution	Wash Buffer	1 μ g/ml
Ready-SET-Go! eBioscience	5X Assay diluent Substrate Solution	(0.05 % TWEEN 20 in PBS 1X) Stop Solution (1 M H ₃ PO ₄)	

2.2.9.9 FACS solutions

FACS Buffer	
PBS 1X	
FBS	2 %

FACS reagents:	BD Cytofix/Cytoperm™ kit	BD Biosciences
BD Cytofix/Cytoperm solution		
BD Perm/Wash buffer 10X		Diluted in sterile deionized MilliQ water

2.3 BAC, plasmids

2.3.1 BAC

RPCIB731B063Q: Genomic clone renamed as mCB2 BAC containing the whole mouse *Cnr2* genomic region and cloned into the pBACe3.6 vector. The vector contains an origin of replication and a chloramphenicol antibiotic resistance gene. The genomic clone is hosted in DH10B *E. coli* and was purchased from ImaGenes.

2.3.2 Original plasmids

hCB2 GC without tag pcDNA3.1D V5-His-TOPO: This plasmid contains the human CB2 open reading frame with the bases GG at position 189, encoding for an arginine at position 63 in the human CB2 receptor protein. This plasmid was used to amplify the human CB2 open reading frame by PCR. Plasmid cloned and provided by Dr Karsak.

hCB2 AC without tag: pcDNA3.1D V5-His-TOPO: This plasmid contains the human CB2 open reading frame with the bases AA at position 189, encoding for a glutamine at position 63 in the human CB2 receptor protein. This plasmid was used to amplify the human CB2 open reading frame by PCR. Plasmid cloned and provided by Dr Karsak.

pLuc-1xIRES2EGFP-SV40pA: Plasmid provided by Dr. Bouabe from Max von Pettenkofer institute for Hygiene and Medical Microbiology (Bouabe et al., 2008). This plasmid was used to amplify the IRES2-eGFP fragment by PCR.

pRed/ET: This plasmid encode the genes of a protein pair of 5' - 3' exonucleases under an arabinose-inducible promoter. Upon expression, these proteins mediate the recombination between regions of homology. The plasmid was provided in Genebridges kits.

pX330-U6-Chimeric BB-CBh-hSpCas9: This plasmid was used to clone small annealed oligonucleotides in order to be used as CRISPR/Cas9 system for generating targeted double strand breaks. This plasmid was purchased from Addgene.

rrl-CMV-eGFP: Self inactivated vector construct provided by Dr. Zimmermann from Institute for Pharmacology and Toxicology. This vector contains an ampicillin resistance gene and was used to clone the human CB2 open reading frame linked or not to an IRES2-eGFP in order to generate lentiviral particles to transduce bone marrow derived-macrophages.

TAL-BBL1-ID14, TAL-BBL1-ID43, TAL-BBL1-ID23: Level 1 plasmids used during the ligation independent cloning of TALEN assembly. These plasmids were purchased from Addgene.

TAL-ID12-C, TAL-ID12-G: Level 2 plasmids used during the ligation independent cloning of TALEN assembly. These plasmids were purchased from Addgene.

2.3.3 Cloned plasmids

mCB2 ORF Subclone: Plasmid containing a 8619 bp fragment subcloned from the mCB2 BAC into a destination vector containing the *Cnr2* gene, an ampicillin resistance gene and an origin of replication sequence.

hCB2Arg63 Subclone: The mCB2 ORF subclone plasmid was used as the original plasmid and the murine CB2 ORF was replaced by the human CB2 ORF (arginine variant). The plasmid contains the CNR2 ORF (arginine), an ampicillin resistance gene and an origin of replication sequence.

hCB2Gln63 Subclone: The mCB2 ORF subclone plasmid was used as the original plasmid and the murine CB2 ORF was replaced by the human CB2 ORF (glutamine variant). The plasmid contains the CNR2 ORF (glutamine), an ampicillin resistance gene and an origin of replication sequence.

hCB2Arg63 targeting construct: The hCB2Arg63 subclone plasmid was used as the original plasmid. A FRT-PGK-gb2-neo-FRT cassette was inserted into it. The plasmid contains the CNR2 ORF (arginine variant), an ampicillin resistance gene, a kanamycin resistance gene and an origin of replication sequence.

hCB2Gln63 targeting construct: The hCB2Gln63 subclone plasmid was used as the original plasmid. A FRT-PGK-gb2-neo-FRT cassette was inserted into it. The plasmid contains the CNR2 ORF (glutamine variant), an ampicillin resistance gene, a kanamycin resistance gene and an origin of replication sequence.

mCB2-left-TALEN: Plasmid cloned from original level 2 plasmid (TAL-ID12-C) using the ligation independent cloning of TALEN assembly protocol. This plasmid contains an ampicillin resistance gene and was used in combination with the mCB2-right-TALEN to generate targeted DSBs within the Cnr2 ORF.

mCB2-right-TALEN: Plasmid cloned from original level 2 plasmid (TAL-ID12-G) using the ligation independent cloning of TALEN assembly protocol. This plasmid contains an ampicillin resistance gene and was used in combination with the mCB2-left-TALEN to generate targeted DSBs within the Cnr2 ORF.

px330-mCB2: Small annealed oligonucleotides containing a 20 bp homologous sequence to the Cnr2 ORF were cloned into the original pX330-U6-Chimeric_BB-CBh-hSpCas9 plasmid. The plasmid contains an ampicillin resistance gene.

rrl-CMV-hCB2-Arg63: Vector construct cloned from the original rrl-CMV-eGFP vector construct. The eGFP ORF was replaced by the CNR2 ORF (arginine variant). The vector construct contains an ampicillin resistance gene.

rrl-CMV-hCB2-Gln63: Vector construct cloned from the original rrl-CMV-eGFP vector construct. The eGFP ORF was replaced by the CNR2 ORF (glutamine variant). The vector construct contains an ampicillin resistance gene.

rrl-CMV-hCB2-Arg63-IRES2-eGFP: Vector construct cloned from the original rrl-CMV-hCB2-Arg63 vector construct. The IRES2-eGFP fragment was amplified from the original pLuc-1xIRES2EGFP-SV40pA plasmid and cloned adjacently to the CNR2 ORF (arginine variant). The vector construct contains an ampicillin resistance gene.

rrl-CMV-hCB2-Gln63-IRES2-eGFP: Vector construct cloned from the original rrl-CMV-hCB2-Gln63 vector construct. The IRES2-eGFP fragment was amplified from the original pLuc-1xIRES2EGFP-SV40pA plasmid and cloned adjacently to the CNR2 ORF (glutamine variant). The vector construct contains an ampicillin resistance gene.

2.4 Cells

2.4.1 Bacteria

DH10b: An *E.coli* strain harboring the unmodified BAC clones. The initial subcloning step was performed in this strain. Chemically competent DH10b bacterial cells were used for the ligation-independent cloning of TALENs. These bacteria were purchased from Invitrogen.

Stbl3: Chemically competent bacteria purchased from Invitrogen. These bacteria were used to clone the px330 CRISPR/Cas9 plasmids.

TOP10: Electrocompetent TOP10 was an *E.coli* strain used for the transformation of the different recombinant plasmids. These bacteria were purchased from Invitrogen.

2.4.2 Embryonic Stem cells

Bruce4 embryonic stem cells: An ES cell line derived from C57BL/6 mice (Kontgen et al. 1993). The cell line was kindly provided by Ralf Kühn, Max-Planck Institute for Biochemistry, Martinsried, Germany.

MPI2 embryonic stem cells: An ES cell line derived from 129/Sv mice. The cell line was generated at the Max Planck Institute Göttingen in the laboratories of Prof. P. Gruss (Voss et al. 1998).

2.4.3 Cells

Bone marrow-derived macrophages: These cells were prepared from 6 to 8 weeks old mice. A detailed description of the preparation is given in section 3.4.1.

NIH3T3 cells: Mouse embryonic fibroblast derived from Swiss mouse embryo tissue. This cell line was isolated and initiated in 1962 at the New York University School of Medicine Department of Pathology.

Primary mouse embryonic fibroblasts (MEF): These cells were used as feeder cells for the cultivation of ES cells. A detailed description of the preparation is given in section 3.2.1.

2.5 Software

Double Digest Finder: The software is provided by NEB and was used to find optimal buffer and temperature conditions for double restriction endonucleases digestion. (<https://www.neb.com/tools-and-resources/interactive-tools/double-digest-finder>).

Flowjow: The software is required to analyse data obtained with the flow cytometer FACS Canto II, BD Biosciences. (www.flowjo.com).

ImageJ: The software was used to analyse and count engulfed zymosan particles in the phagocytosis assay. (<http://rsbweb.nih.gov/ij/>).

LIC TALE gene Assembler Version 1.0: The software was used to pick the appropriate 2-mer fragments that are required to assemble an 18.5 RVD TALEN construct. (<http://www.hornunglab.de/Tassembly.html>).

Ligation Calculator: The software was used to calculate the amounts of vector and insert to perform DNA ligation. (http://www.insilico.uni-duesseldorf.de/Lig_Input.html)

NEBcutter V2.0: The software is provided by NEB and was used to find or validate restriction endonucleases sequences. (<http://tools.neb.com/NEBcutter2/index.php>).

Primer3: This software was used to design oligonucleotides for PCR reactions. (<http://bioinfo.ut.ee/primer3-0.4.0/>).

Prism 5: Software commonly used to analyse and graph data.

UCSC genome browser: The software was used to find sequences of gene of interest and validated the specificity of designed oligonucleotides. (<http://genome.ucsc.edu/>).

Vector NTI[®] software: The software was used to design, clone, and align DNA sequences *in silico*.

3 METHODS

This section is divided into four parts. The first part contains general molecular biology methods used to clone different plasmid vectors. The second and third parts deal with the cultivation and manipulation of the ES cells and NIH3T3 cells. And finally the fourth part contains methods to isolate, cultivate, transduce and characterize bone-marrow derived macrophages from mice.

All manufacturers' protocols mentioned are archived at the Institute of Molecular Psychiatry and are available upon request.

3.1 Molecular biology methods

Methods concerning the cultivation, transformation and long-term storage of *E. coli* were performed according to the protocols of Sambrook, Fritsch and Maniatis (Sambrook, Fritsch and Maniatis, 1989). Agarose gel electrophoresis and detection of DNA in agarose gels by ethidium bromide staining were conducted as described in Molecular Cloning by Sambrook and Russel (Sambrook and Russel, 2001).

3.1.1 DNA

3.1.1.1 DNA preparation from *E.coli*

3.1.1.1.1 Mini preparation

Two different methods were used to purify plasmid DNA from *E.coli*. The DNA preparation described in the technical protocol provided in the Quick & Easy Conditional Knockout Kit manual (Genebridges™) was the preferential method for analytical purposes (routine plasmid screenings like restriction analysis) whereas silica columns based miniprep kit was used to isolate pure plasmid DNA for further cloning steps or sequencing analysis. To isolate pure plasmid DNA using silica columns, peqGOLD Plasmid Miniprep kit I (Peqlab biotechnologies GmbH) was used following the manufacturer's instructions.

3.1.1.1.2 Midi preparation

For Midi preparation, the GeneElute™ HP Plasmid MidiPrep Kit (Sigma) was used following the manufacturer's instructions.

3.1.1.2 Purification of DNA fragments

3.1.1.2.1 From agarose gel and PCR reactions

In order to purify DNA fragments from agarose gels, DNA was loaded on an 0,8 % agarose gel. After fifteen minutes incubation of the gel in an ethidium bromide bath, the DNA fragment of interest was excised using a UV light lamp.

Before purifying DNA from PCR reactions, 5 μ l were loaded on an agarose gel to verify the PCR results. The rest of the PCR reaction was purified.

Purification of DNA fragments from agarose gels and PCR reactions was performed using peqGold Gel Extraction Kit (Peqlab biotechnologies GmbH) following the manufacturer's instructions.

3.1.1.2.2 Phenol-Chloroform extraction

DNA fragments used for ES cell electroporation were purified by a phenol-chloroform extraction. The sample volume was filled up to 500 μ l with Milli-Q water. The same volume (500 μ l) of phenol/chloroform/isoamylalcohol (25:24:1) was added to the tube. After mixing by inversion for 1 minute followed by centrifugation (16000 *g*, 10 min), the supernatant was carefully pipetted and transferred into a fresh tube. The supernatant was supplemented with 500 μ l of chloroform followed by another mixing and centrifugation step. The supernatant was pipetted into a new fresh tube. The DNA was precipitated by adding 3 M sodium acetate pH 7,2 (1:10) and 100 % ethanol (2.5:1). To improve the precipitation, tubes were placed one hour at -20°C. After centrifugation (16000 *g*, 20 min) and removal of the supernatant, the DNA pellet was washed twice with 70 % ethanol, air-dried and dissolved in TE buffer.

3.1.1.3 DNA preparation from living cells

Cultured ES cells or NIH3T3 cells were incubated minimum 2 hours in lysis buffer and proteinase K (1 mg/ml) at 55 °C. The DNA was precipitated by addition of one volume of isopropanol. After centrifugation (16000 *g*, 20 min) and removal of the supernatant, the DNA pellet was washed twice with 70 % ethanol, air-dried and dissolved in TE buffer.

3.1.1.4 Measurement of DNA concentration

DNA sample concentration was measured using a Nanodrop-1000 spectrophotometer. DNA absorbs ultraviolet light at a wavelength of 260 nm (A_{260}). The absorbance of 1 unit at A_{260} is equivalent to a DNA concentration of 50 μ g/ml. The purity of a DNA preparation is assessed by the ratio of absorbance at 260 and 280 nm. A pure DNA preparation exhibits an A_{260}/A_{280} ratio between 1,8 and 2.

3.1.1.5 Digestion of DNA

Sequence-specific cleavage of DNA was checked *in silico* using Vector NTI[®] software, NEBcutter V2.0 or Double Digest Finder in case of double restriction endonucleases digestion. Restriction digestion was performed according to manufacturers in recommended buffer

conditions. For analytical and cloning purposes, 1 to 5 µg of DNA were digested at the recommended enzyme temperature for minimum one hour in a water bath. To digest higher DNA amount (linearization of targeting constructs before ES cells electroporation, 60 µg) or for genomic DNA (Southern blot), DNA were digested during 8 hours or longer at the recommended temperature in a PCR cycler.

3.1.1.6 DNA ligation

Before DNA ligation, blunt end vectors were dephosphorylated using antarctic phosphatase during 15 minutes at 37 °C. The enzyme was then heat inactivated for 5 minutes at 70 °C as recommended by NEB. The ligation was performed by mixing 30 fmol of the vector and 90 fmol of the insert (insert: vector molar ratio of 3:1) into T4 DNA ligase reaction buffer supplemented with 1 unit of T4 DNA ligase enzyme. Ligation was incubated overnight at 16 °C. 5 to 20 µl of the ligation were used to transform 50 µl electrocompetent TOP10 bacteria.

3.1.1.7 Amplification of DNA fragments by polymerase chain reaction

For sequence specific amplification of DNA fragments, PCR was applied. For analytical purposes, PCR reactions were performed with Taq polymerase whereas for cloning purposes Phusion[®] High-Fidelity DNA polymerase was used. To increase specificity a hot start was applied when using the Taq polymerase enzyme. Each PCR reaction was specifically adapted to the annealing temperature requirements of the oligonucleotides and the length of the expected PCR product. Established PCR conditions and a list of oligonucleotides used are provided in the appendix.

3.1.1.8 PCR reaction for Southern blot probes

The Southern blot probes were labelled by digoxigenin-coupled nucleotides.

3' neo integration Southern blot probe for the identification of positive ES cell clones:

PCR setup (50 μ l)

MilliQ water	36	μ l
10X PCR-buffer	5	μ l
Forward primer (Fwd 3' CB2 probe, 10 μ M)	1	μ l
Reverse primer (Rev 3' CB2 probe, 10 μ M)	1	μ l
DIG labelled dNTPs	5	μ l
Taq polymerase	1	μ l
mCB2 BAC DNA (500 ng/ μ l)	1	μ l

5' Human CB2 Southern blot probe for the identification of positive ES cell clones:

PCR setup (50 μ l)

MilliQ water	36	μ l
10X PCR-buffer	5	μ l
Forward primer (Fwd 5' hCB2 probe, 10 μ M)	1	μ l
Reverse primer (Rev 5' hCB2 probe, 10 μ M)	1	μ l
DIG labelled dNTPs	5	μ l
Taq polymerase	1	μ l
mCB2 BAC DNA (500 ng/ μ l)	1	μ l

Cycling parameters

1 x	Initial denaturation	95 °C	2 min
25 x	Denaturation	95 °C	15 s
	Annealing	63 °C	15 s
	Elongation	68 °C	45 s
1 x	Final elongation	68 °C	5 min
	Cooling	4 °C	∞

3.1.1.9 DNA sequencing

Sample to be sequenced were send to Macrogen Company. Plasmid DNA was diluted to a concentration of 100 ng/μl and PCR to 50 ng/μl in a volume of 20 μl. Primers were sent at a concentration of 10 pmol/μl in 20μl (based on 5 samples).

3.1.1.10 RNA preparation

RNA was isolated from bone marrow derived-macrophages for subsequent quantitative gene expression analysis. Cells (1×10^6 cells per sample) were collected in TRIzol® and homogenized by pipetting up and down. 1-bromo-3-chloropropane (BCP) (1:5) was added and the samples were mixed well by sustained vortexing for 30 seconds. After 3 minutes incubation at room temperature and centrifugation (14000 g, 10 min, 4 °C), the upper phase containing RNA was transferred into a fresh tube. The RNA was then precipitated with isopropanol (1:1) and washed two times with ethanol (75 %). The air-dried RNA pellet cell-isolation was eluted in 20 μl RNase-free water and stored at -80 °C.

3.1.1.11 Measurement of RNA concentration

The concentration of the isolated RNA was measured using Nanodrop-1000 spectrophotometer. RNA has an absorption maximum at a wavelength of 260 nm (A_{260}). The absorbance of 1 unit at 260 nm is equivalent to a RNA concentration of 40 μg/ml. The purity of the RNA preparation is estimated by the ratio of absorbance at 260 and 280 nm. Pure RNA has an A_{260}/A_{280} ratio of 2.0.

3.1.1.12 Reverse transcriptase polymerase chain reaction (RT-PCR)

Isolated RNA from bone marrow derived-macrophages was transcribed into cDNA by reverse transcription. Concentration of each sample was normalized with milliQ water to 770 ng in a

polymerase used for the amplification, the fluorescent signal can be detected. The intensity of the fluorescence increases proportionally to the number of the probe cleavage cycles. For relative quantification, the expression of the gene of interest is normalized with the expression of a housekeeping gene, which is constitutively expressed. Here the beta-2-microglobulin (B2M) housekeeping gene was chosen due to its stable expression in our cell model (Stephens et al., 2011).

PCR setup for TaqMan gene expression analysis

cDNA (11 ng/μl)	4	μl
Taqman assay	0.5	μl
Taqman assay master mix	5	μl
MilliQ water	0.5	μl

Cycling parameters

1 x	95 °C	10 s
-----	-------	------

40 x	95 °C	15 s
------	-------	------

	60 °C	60 s
--	-------	------

3.1.2 Southern blot

Identification of homologous recombined ES cell clones was performed by Southern blot. The technique relies on the design of a digoxigenin-labelled DNA probe and the establishment of a restriction digestion strategy in order to specifically detect DNA fragments. Genomic DNA prepared from ES cells was digested overnight with the appropriate restriction endonuclease(s). After separation on a 0,8 % agarose gel by electrophoresis, and a 15 minutes incubation in an ethidium bromide bath, a picture was taken to verify that the DNA was correctly digested. The gel was subsequently submitted to a 250 mM HCl solution for 10 minutes in order to depurinate the DNA, followed by an incubation in a denaturation and neutralisation solution for 30 minutes, respectively. The DNA contained in the gel was blotted on a nylon membrane at 5 mbar for 1.5 hours in 10X SSC. In order to fix the DNA on the membrane, UV cross-linking was performed. In order to avoid unspecific binding of the digoxigenin-labelled probe, the membrane was pre-incubated 1 hour at 68 °C in a hybridization oven with denatured salmon sperm DNA. The incubation with the probe was performed overnight on the same conditions.

The next day, the membrane was washed first two times 10 minutes at room temperature with 2X SSC / 1 % SDS on an agitating shaker followed by three times 10 minutes in an oven at 68 °C, containing a shaking plate, with 0.2X SSC/ 0.1 % SDS. The membrane was then equilibrated in maleic acid buffer pH 7.5 for a short time and then incubated with the blocking solution for 1 hour at room temperature. After being shortly centrifuged, the anti-digoxigenin antibody (1:20000) was added into the blocking solution and incubated for 45 minutes. Thereafter the membrane was washed three times 10 minutes with washing buffer before being equilibrated into the detection buffer solution for a short time. The membrane was then submitted to CDP-Star (Roche, 1:100 in detection buffer) for 5 minutes with slow circular movement in order to avoid stagnation of the solution. The membrane was placed in a developing cassette and a hyperfilm (Amersham, Pharmacia) was placed on the membrane for about one hour. The film was finally revealed in a film-processing machine.

3.1.3 Cloning of targeting vectors by Red/ET recombination

Targeting vectors were cloned using the Red®/ET® recombination technology from GeneBridges and conventional cloning strategy based on restriction digestion/ligation.

Concerning the Red®/ET® recombination technology, this method permits the precise engineering of DNA molecules of any size such as bacterial artificial chromosome (BACs) by HR *in vivo* in *E. coli*. HR is driven by a plasmid that encodes for a phage-derived protein pair that consists of a DNA annealing protein and a 5'→3' exonuclease. The second component required for the HR to occur is a DNA fragment with homology arms, which are stretches of DNA shared by the two molecules that recombine. To amplify this DNA fragment, touchdown PCR and specific oligonucleotides purchased from Invitrogen were used.

PCR setup (50 µl)

MilliQ water	36	µl
5X Phusion HF buffer	10	µl
Forward primer (75 bp long, 10 µM)	1	µl
Reverse primer (75 bp long, 10 µM)	1	µl
dNTPs 10 mM	1	µl
Phusion polymerase	1	µl
Plasmid DNA	1	µl

Cycling parameters

1 x	Initial denaturation	98 °C	1 min
5 x	Denaturation	98 °C	1 min
	Annealing	62 °C	1 min
	Decreasing 1 °C every cycle		
	Elongation	72 °C	2:30 min
30 x	Denaturation	98 °C	1 min
	Annealing	57 °C	1 min
	Elongation	72 °C	2:30 min
1 x	Final elongation	72 °C	10 min
	Cooling	4 °C	∞

The oligonucleotides were 75 bp long, 25 bp for the annealing and amplification of the fragment and 50 bp as homology regions. The homology regions can be freely chosen at any position on a target molecule.

Two kits were used to clone the targeting vectors. First the BAC subcloning kit was used. Subcloning means moving the gene of interest from a parent vector, in our case the mCB2 BAC containing the mouse CB2 coding exon, into a destination vector in order to simplify the handling of the vector. Therefore a 9 kb fragment containing the mouse CB2 coding exon, a left arm of 5 kb and a right arm of 1.8 kb for the HR in ES cells, was subcloned into a plasmid vector. The PCR fragment used for HR was provided in kit. It consists of a minimal vector containing an ampicillin resistance gene and a ColE1 origin of replication. Bacteria carrying the BAC were transformed with the pRedET plasmid. Expression, by this plasmid, of genes mediating HR was induced by stimulating bacteria with 10 % L-arabinose. Then the minimal vector amplified with stretches homologous to the fragment of the BAC was electroporated into the bacteria and after the HR occurred, clones carrying the subcloned fragment were identified by selection for ampicillin resistance.

The mouse coding exon was replaced by human coding exons by conventional cloning strategy (digestion/ligation) using *Bam*HI and *Aat*II restriction sites. The mouse DNA sequences surrounding the mouse coding exon 2 containing the two restriction sites were

added to the human by two consecutive PCRs using 75 bp primers and the conditions described previously.

The second kit used was the Quick & Easy Conditional Knockout Kit (FRT/FLPe). It allowed the insertion of a cassette containing kanamycin and neomycin resistance genes flanked by FRT sites. Kanamycin resistance gene was expressed under a prokaryotic promoter (gb2) for selection in *E. coli* whereas neomycin resistance gene was expressed under an eukaryotic promoter (PGK) for the selection of homologous recombined ES cells. This cassette was inserted on the 3' arms, 933bp after the coding exons.

Targeting constructs were linearized with *EcoRV* restriction enzyme before being electroporated into ES cells.

3.1.4 Cloning of TALEN plasmids

Transcription activator-like effector nucleases (TALEN) plasmids were cloned using ligation-independent cloning (LIC) TALE assembly protocols (Schmid-Burgk et al., 2013). The TALEN were design and generated using the LIC TALE gene Assembler Version 1.0.

The ligation independent cloning is based on the 3' exonuclease activity of T4 polymerase in the presence of specific dNTPs (dATP or dTTP) to generate long, well define single stranded DNA overhangs called ID. By mixing different fragments with different complementary IDs, the ligation takes place with really high specificity between the complementary overhangs. A library containing 64 fragments composed of two consecutive TAL effector repeat units (2-mer) was used as minimal cloning unit. The assembly was performed into a 2 hierarchical assembly steps. In a first step, three 2-mer fragments were assembled into a 6-mer fragment inside a kanamycin resistant level 1 backbone. And in a second step, three 6-mer fragments were assembled into a 18-mer fragment inside an ampicillin resistant level 2 backbone. The level 2 backbone containing the 18-mer fragment is an expression-ready backbone with the last repeat unit and a C-terminal half nuclease domain of the *FokI* enzyme, giving rise to an 18.5 repeat variable di-residue (RVD) TALEN construct. The target specificity of the sequence is 5'-T(N)19-3'.

Fragments and backbone vectors were digested for 1 hour with the appropriate restriction enzymes at 37 °C. Backbone vectors were gel purified using peqGOLD Gel Extraction Kit. Fragments and backbone vectors were incubated with the appropriate stop dNTP (dATP or dTTP) and T4 DNA polymerase in order to generate the right IDs. This reaction was done at 27 °C for 5 minutes followed by 20 minutes at 75 °C. These reactions were diluted 20-fold using NEB buffer 2 before proceeding. Appropriate fragments and backbone vectors were mixed and incubated at 55 °C for 30 minutes and then at 25 °C for 3

hours. 2 μ l of the assembly reaction was used to transform ice-cold chemically competent DH10b E. coli. Ampicillin Resistant clones were picked and mini preparations using peqGOLD Plasmid Miniprep kit I were performed. Plasmids were checked by restriction digestion using *Xho*I *Xba*I restriction enzymes and the right ones were send for sequencing at Macrogen.

3.1.5 Cloning of CRISPR/Cas9 plasmids

CRISPR plasmids were cloned using Zhang et al protocol published in 2013. Oligonucleotides were design using UCSC genome browser and purchased from Metabion. They were designed with a 4 bp overhangs compatible with *Bbs*I digested overhangs. 1 μ g backbone vector was digested with *Bbs*I restriction enzyme for 30 minutes at 37 °C. The right fragment was gel purified using peqGOLD Gel Extraction Kit. Before proceeding with ligation, oligos were phosphorylated and annealed by mixing the two oligos with T4 PNK.

Annealing and phosphorylation mix of oligos

Fwd CB2 sgRNA	1	μ l
Rev CB2 sgRNA	1	μ l
10X T4 ligation Buffer (NEB)	1	μ l
MilliQ water	6.5	μ l
T4 PNK (NEB)	0.5	μ l

Cycling parameters

1 x	37 °C	30 min
1 x	95 °C	5 min
14 x	95 °C	Ramping down to 25 °C at 5 °C/min

Ligation was set up as described below and incubated at room temperature for 10 minutes.

Ligation reaction

<i>Bbs</i> I digested pX330	0.66	μl
Phosphorylated and annealed oligo duplex previously diluted 200-fold	1	μl
2X Quick ligation Buffer (NEB)	5	μl
MilliQ water	3.34	μl
Quick ligase (NEB)	1	μl

The complete ligation reaction was transformed into *Stb*I3 Chemically competent bacteria. Plasmids were checked by PCR using the Human U6 seq F_Insert as forward primer and the reverse oligo used for the annealing step: Rev CB2 sgRNA.

PCR setup (50 μl)

MilliQ water	36	μl
5X Phusion HF buffer	10	μl
Forward primer (Human U6 seq F_Insert, 10 μM)	1	μl
Reverse primer (Rev CB2 sgRNA, 10 μM)	1	μl
dNTPs 10 mM	1	μl
Phusion polymerase	1	μl
Plasmid DNA	1	μl

Cycling parameters

1 x	Initial denaturation	98 °C	30 sec
35 x	Denaturation	98 °C	10 s
	Annealing	63 °C	30 s
	Elongation	72 °C	15 s
1 x	Final elongation	72 °C	10 min
	Cooling	4 °C	∞

Correctly-recombined plasmids were sent for sequencing to Macrogen.

3.1.6 Cloning of vector constructs

Self inactivated vector constructs were cloned using recommendations of Dr. Zimmermann from the Institute for Pharmacology and Toxicology. Once the vector constructs were ready, they were provided back to the Institute for Pharmacology and Toxicology in order to generate the viral particles (S2 safety conditions). The vectors constructs were transfected with packaging constructs into HEK 293 packaging cells in which proteins required for replication and assembly of the virions are expressed from the packaging construct, and the replicated vector genomes are encapsidated into virus particles to generate the recombinant lentiviral vectors which were used to transduced bone marrow-derived macrophages from mice.

The original self inactivated vector construct rrl-CMV-eGFP provided by Dr. Zimmermann, was digested with *Bam*HI and *Sa*II restriction enzymes at 37 °C for 1 hour followed by gel purification. The human CB2 coding exons were amplified by PCR using primers containing *Bam*HI restriction site on the 5' side of the forward primer and a *Sa*II restriction site on the 5' side of the reverse primer. After verifying amplification of right fragments on an agarose gel, PCR products were column purified and double digested with *Bam*HI and *Sa*II. Ligation was performed by mixing 30 fmol of vector, 90 fmol of insert (ratio vector: insert; 1:3) and T4 DNA ligase overnight at 14 °C. The next day, the ligation reaction was electroporated into electrocompetent Top10 cells. Colonies were picked and cultivated overnight in miniculture. DNA minipreps were performed. The right recombined clones called rrl-CMV-hCB2(Arg/Gln), were identified with double digestion using *Bam*HI and *Sa*II restriction enzymes and sent for sequencing at Macrogen.

The rrl-CMV-hCB2-IRES2-eGFP vector constructs were generated using *Sa*II linearized previously generated rrl-CMV-hCB2 (Arg/Gln). The IRES2-eGFP fragment was amplified from pLuc-1xIRES2EGFP-SV40pA plasmid, by PCR, using primers containing *Sa*II restriction sites. After *Sa*II restriction digestion of the inserts, the ligation was performed overnight at 14 °C with T4 DNA ligase. The ligation reactions were electroporated into electrocompetent Top10 cells. Colonies were picked and cultivated overnight in miniculture. DNA minipreps were performed. The right recombined clones called rrl-CMV-hCB2(Arg/Gln)-IRES2-eGFP, were identified with double digestion using *Bam*HI and *Sa*II restriction enzymes and sent for sequencing at Macrogen.

3.2 Embryonic Stem (ES) cells

3.2.1 Cultivation of mouse embryonic fibroblasts (MEFs)

Mitotically inactivated mouse embryonic fibroblasts (MEFs) have been used as feeder cell layers for the maintenance of embryonic stem cells in an undifferentiated state. MEFs were prepared by Anne Zimmer and Caroline Hamsch (Institute of Molecular Psychiatry). During ES cell culture experiments; homologously recombined clones are selected by addition of geneticin (G418) antibiotic in the ES cell culture medium (Bruce4 medium or MPI medium). MEFs have to be resistant to G418. For this purpose, pregnant mice carrying a neomycin resistance gene were scarified. Embryos at stage E13.5 were extracted from uterine horns and placed in ice-cold PBS. After removal of embryonic internal organs from the abdominal cavity using dissecting forceps, the rest of the embryos were transferred into a clean dish to be cut into small pieces. Tissues, up to 12 embryos, were incubated in 50 ml 0.25 % trypsin/EDTA for 20 minutes at 37 °C and 5 % CO₂. Every third minutes the tube was gently inverted. Cells were then centrifuged (950 g, 2 min, 4 °C). The pellet was re-suspended in mouse embryonic fibroblast medium and plated on a 15 cm cell culture dish. At 80 - 90 % confluence, cells were split in a ratio of 1:4 in order to expand the culture. After this step, cells were deep-frozen for further use.

MEFs were inactivated by adding a mitomycin C solution (10 µg / ml) for 4 hours. After this incubation time, the cells were washed three times with HBSS and supplemented with mouse embryonic fibroblast medium.

3.2.2 Cultivation of mouse embryonic stem cells

ES cells were grown in appropriate cell culture medium on a layer of mitotically inactivated MEFs at 37 °C and 5 % CO₂. ES cell culture medium was changed every day. At a confluence of 70 - 80 %, ES cells were passaged in a ratio of 1:5 to 1:10 in order to avoid contact between the ES cells. For passaging, cells were washed once with Hank's buffered salt solution (HBSS) and incubated with 0.25 % trypsin/EDTA for 3 minutes at 37 °C and 5 % CO₂. The same amount of ES cell medium was added to inactivate the trypsin. After pipetting up and down three times cells were transferred into a Falcon tube and centrifuged (950 g, 2 min, 4 °C). The pellet was re-suspended by pipetting up and down three times with ES cell medium and distributed on cell culture dishes containing fresh mitotically inactivated MEFs.

3.2.3 Deep-freezing and re-cultivation of ES cells

For long-term storage, ES cells and MEFs were trypsinized and pelleted by centrifugation (950 g, 2 min, 4 °C). Pellet was re-suspended in freezing medium (10 % DMSO) by pipetting up and down three times and transferred into cryopreservation vials. Tubes were then placed at

20 minutes at 4 °C then 1 hour at -20 °C and finally 3 days at -80 °C. After this the tube were transferred in a liquid nitrogen tank.

When cells were needed, tubes were quickly defrosted at 37 °C, re-suspended in ES cell medium and pelleted by centrifugation (950 g, 2 min, 4 °C). Cells were re-suspended in fresh ES cell medium by pipetting up and down three times and dispensed on new cell culture dishes.

3.2.4 Electroporation and selection of ES cell clones

Before proceeding to the electroporation, ES cells were expanded on a layer of mitotically inactivated MEFs in 15 cm cell culture dishes until a confluence of 70 %. Two hours before electroporation, the ES cell medium was changed by fresh one. Cells were harvested by trypsinization, centrifuged (950 g, 2 min, 4 °C) and washed twice with ice-cold HBSS. The tube containing the cells was kept on ice while counting using a hemocytometer. Cells were centrifuged and re-suspended with ice-cold HBSS at a concentration of 1.25×10^7 cells/ml. 0.8 ml (1×10^7 cells) and transferred into an ice-cold electroporation cuvette which already contained 20 µl of the linearized plasmid DNA (1 µg/µl). Electroporation was performed at 250 V, 500 µF. Afterwards the cuvette was placed on ice for 10 minutes. The mixture was then dispensed on a 15 cm cell culture dish supplied with fresh mitotically inactivated MEFs.

Homologously recombined clones were selected by adding geneticin (G418) at a concentration of 170 µg/ml into the ES cell medium (selection medium). The selection started 24 hours after the electroporation and lasted for 7 to 9 days. Selection medium was changed daily. Just before picking surviving clones, the medium was replaced with HBSS. Each clone picked under a microscope with a 20 µl pipette was transferred into a well of a 96-well plate. The wells were filled with 100 µl 0.25 % trypsin/EDTA and the plate was incubated 3 minutes at 37 °C and 5 % CO₂. 100 µl was added into the wells to inactivate the trypsin and the cells were pipetted up and down five times in order to obtain a single cell suspension. ES cells of one colony were then dispensed into a well of a 24-well plate containing fresh mitotically inactivated MEFs. Cells were expanded for 3 days and medium was changed daily. After this period, clones were trypsinized with 200 µl 0.25 % trypsin/EDTA and incubated 3 minutes at 37 °C and 5 % CO₂. After five times pipetting up and down, 700 µl of the cell suspension was transferred into a new 24-well plate. 700 µl of freezing medium (20 % DMSO) was added to each well and the plate was gently shaken before proceeding to the deep-freezing, as described previously. The rest of the cell suspension (300 µl) in the original well was completed with 700 µl of ES cell medium and cultivated for further DNA preparation.

3.2.5 RESGRO culture of positive ES cell clones

RESGRO culture medium has the capacity to rescue established ES cell lines that have started drifting or have lost germ line transmission capability. Differentiation, which is present in the ES cells but not visible with traditional medium, will become recognizable when using RESGRO culture medium.

First, 10 ml of L-Glutamine Solution (200 mM) were added to 500 ml of RESGRO culture medium. ES cells were cultivated on mitotically inactivated MEFs with RESGRO culture medium for 2 passages. Afterwards cells were trypsinized with 0.25 % trypsin/EDTA and incubated 3 minutes at 37 °C and 5 % CO₂. After centrifugation (950 g, 2 min, 4 °C), cells were resuspended with RESGRO culture medium and replated 1:3 – 1:5 on the same size plate without MEFs. After 2 days, a clear difference was observed between 3-dimensional (undifferentiated) and flat growing (differentiated) colonies. By tapping the plate, the undifferentiated colonies detached. The supernatant containing the undifferentiated cells was collected and centrifuged. Medium was removed and cells were re-suspended in 0.5 ml 0.25 % trypsin/EDTA by pipetting up and down. The tube was placed in a water bath at 37 °C for 1.5 minutes. Cells were pipetted up and down 10 times and 9.5 ml RESGRO culture medium was added. The tube was centrifuged and the medium removed. Cells were re-suspended in RESGRO culture medium and replated 1:3 – 1:6 on mitotically inactivated MEFs. When cells were confluent, they were deep-frozen until proceeding to blastocyst injection.

3.3 Experiments requiring NIH3T3 cells

3.3.1 Cultivation of NIH3T3 cells

NIH3T3 cells were grown in plastic T75 flasks with NIH3T3 medium at 37 °C and 5 % CO₂. Cells were passaged at 70 -80 % confluency. They were trypsinized with 0.25 % trypsin/EDTA, incubated 3 minutes at 37 °C and 5 % CO₂ and centrifuged (950 g, 5 min, 4 °C). The medium was removed and the cells were re-suspended in NIH3T3 medium and replated at a ratio of 1:3. NIH3T3 cells were defrosted 2 weeks before transfection.

3.3.2 Transfection of NIH3T3 cells

NIH3T3 cells were transfected with X-tremeGENE 9 DNA transfection reagent. 18 – 24 hours before transfection, cells were plated in a 96-well plate at a density of 1.5×10^4 cells/well in 100 µl medium. After overnight incubation, the medium in every well was changed and X-tremeGENE 9 DNA transfection reagent was warmed at room temperature and vortex gently. 200 µl of DMEM medium was pipetted into a sterile tube in which 6 µl of X-tremeGENE 9 DNA transfection reagent were added. After gently mixing, 2 µg of DNA (3:1 ratio of reagent to DNA) was added to the mixture and the tube was again gently mixed. The tube was incubated

at room temperature for 30 minutes to allowed complex formation. Different amounts of complexes (50 ng, 100 ng and 200 ng) were distributed drop-wise to different areas of the wells. Cells were incubated for 48 -72 hours before DNA was collected for further assay.

3.3.3 SURVEYOR assay

The TALEN or CRIPSR/Cas9 targeted regions were amplified from the genomic DNA by PCR using specific primers surrounding targeted regions.

PCR setup (50 μ l)

MilliQ water	33.5	μ l
5X Phusion HF buffer	10	μ l
Forward primer (10 μ M)	1	μ l
Reverse primer (10 μ M)	1	μ l
dNTPs 10 mM	1	μ l
Phusion polymerase	1	μ l
DNA	2.5	μ l

Cycling parameters

1 x	Initial denaturation	98 °C	30 sec
35 x	Denaturation	98 °C	10 s
	Annealing	63 °C	30 s
	Elongation	72 °C	20 s
1 x	Final elongation	72 °C	10 min
	Cooling	4 °C	∞

The PCR amplicons were denatured by heating and re-annealed in order to form heteroduplex DNA.

Cycling parameters

1 x	95 °C	10 min
70 x	95 °C	1.40 min
		Ramping down to 25 °C at 1 °C/min
1 x	4 °C	∞

SURVEYOR Enhancer S (1 µl) and SURVEYOR Nuclease S (2 µl) were added to the PCR reaction mixture. Tubes were gently mixed and incubated at 42 °C for 60 minutes. The reaction was stopped by adding Stop solution (5.3 µl), gently mixed and subjected to electrophoresis in a 2 % agarose gel and visualized by staining with ethidium bromide.

3.4 Mouse bone marrow-derived macrophages (BMMs) experiments**3.4.1 Isolation and differentiation of myeloid stem cells into macrophages**

Myeloid stem cells were isolated from bone marrow of 6-8 weeks old mice. Mice were sacrificed by cervical dislocation. The abdomen and hind legs were sterilized with 70 % ethanol. An incision in the midline of the abdomen was performed. The bones (femur + tibia) were removed and transferred into a 10 cm cell culture dish containing ice-cold PBS. All muscle tissues were removed with scissors and forceps with caution to not cut the ends of the bones. Under the hood and in sterile conditions, both ends of the femur were cut with sterilized scissors. Bone marrow was flushed with ice-cold PBS using a 10 ml syringe and a 13 mm needle into a cell culture dish. The same procedure was performed with the tibia. Bone marrow was collected from both legs bones. Bone marrow was pipetted up and down several times with a Pasteur pipette until obtaining a single cells suspension. The cells were passed through a cell strainer into a sterile 50 ml conical tube. After adding ice-cold PBS to 50 ml, bone marrow cells were kept on ice and counted using a hemocytometer. Cells were centrifuged (950 g, 10 min, 4 °C) and resuspended in freshly filtrated mouse bone marrow derived-macrophages medium. Cells were plated in 10 cm Petri dishes at a density of 1.5×10^6 cells in 10 ml medium and cultured at 37 °C, 5 % CO₂. After 3 days in culture, 5 ml fresh medium was added to the plates. Bone marrow-derived macrophages were detached using a cell scraper and plated in 24 well plates at day 6. Analyses were performed on day 7.

3.4.2 Transduction of bone marrow-derived macrophages with recombinant lentiviral vectors

Recombinant lentiviral vector derived from vector constructs were produced by Dr. Katrin Zimmermann in the Institute of Pharmacology and Toxicology, Bonn. Before transducing BMMs with the recombinant lentiviral vectors, the titer was determined using a non-functional titration method based on the measurement of reverse transcriptase (RT) activity using a colorimetric assay (ELISA). Measuring the activity of reverse transcriptase present in the virions is a valuable technique to estimate the titer but does not represent the functional titer. The functional titer, which is defined as the number of functional vector particles required to infect a cell present in a volume can be determined in different ways. A reliable method to calculate the functional titer consists of transducing live cells following limiting dilution of vector and subsequent evaluation of reporter protein activity (eGFP), or protein of interest measurement by flow cytometry. This method is best because it only accounts for functional particles. The formula used is: $((\text{Number of cells at starting time}) \times (\text{percent infection})) / \text{volume virus solution added expressed in ml}$. It is reported in Transducible Units per millilitre, TU/ml.

Macrophages were seeded at a ratio of 1×10^5 cells per well in 24 well plates at day 6 and incubated at 37 °C, 5 % CO₂. The cells were transduced the next day, in the institute of Pharmacology and Toxicology (S2 laboratory). The mouse bone marrow-derived macrophages medium was removed and replaced with 300µl fresh one wherein the lentiviral vector particles were diluted. On day 8, medium was removed, cells were washed three times with PBS, and 1ml of fresh medium was added to each well. Cells were used for FACS analysis on day 10.

3.4.3 Preparation of bone marrow-derived macrophages for fluorescence-activated cell sorting (FACS)

3.4.3.1 Extracellular labelling for transduction analysis

After transduction cells were collected using a cell scraper into 1,5 ml Eppendorf tubes. After centrifugation (4500 rpm, 5 min, 4 °C), the pellet was resuspended by pipetting up and down three times with FACS buffer. Cells were centrifuged, and after discarding the buffer, resuspended in 45 µl FACS buffer containing CD16/32 (FC-Block) antibody diluted 1:300. This step is necessary to block unspecific binding of other used antibodies. Tubes were placed on ice in the dark for 15 minutes. 1 ml of FACS buffer was added to the cells followed by centrifugation and buffer discarding. Cells were resuspended with CD11b fluorochrome-conjugated antibody 1:200 and primary CB2 polyclonal N-terminal antibodies 1:50 diluted into FACS buffer. When lentiviruses vectors expressing eGFP were used to transduce BMMs, only CD11b fluorochrome-conjugated antibody was used. Tubes were incubated on ice in the dark

for 15 minutes. When secondary antibodies were required, a last step was performed with antibodies diluted 1:200. FACS buffer was added and the cells centrifuged again. After discarding the buffer cells were resuspended in 500 μ l FACS buffer filtered through a cell strainer (nylon mesh) to eliminate clumps and debris, and kept on ice before being analysed by FACS. All measurements were performed in triplicates.

3.4.3.2 Intracellular labelling for transduction analysis using CB2 polyclonal C-terminal antibody

Cells were collected and labelled for extracellular proteins as described previously. After the last washing step and discarding of the buffer, cells were resuspended in 45 μ l BD Cytotfix/Cytoperm solution and incubated for 20 minutes on ice in the dark. After incubation time, 1 ml of 1X BD Perm/Wash buffer was added to the cells that were then centrifuged (6000 *rpm*, 3 min, 4 °C). Buffer was discarded and the same procedure as for extracellular labelling was performed again for intracellular labelling. Differences were that antibodies were diluted in 1X BD Perm/Wash buffer at 1:100 for CD16/32, 1:50 for C-terminal CB2 antibody and 1:100 for the secondary antibody. All centrifugation steps were performed at 6000 *rpm*, 3 min, 4 °C instead of 4500 *rpm*, 5 min, 4 °C.

3.4.3.3 Extracellular labelling for polarization analysis

Macrophages were seeded at a ratio of 2×10^5 cells per well in 24 well plates at day 6 and incubated at 37 °C, 5 % CO₂. Cells were stimulated overnight with interferon-gamma (IFN- γ), lipopolysaccharide (LPS) and IFN- γ , or interleukin 4 (IL4). They were collected the next day using a cell scraper into 1,5 ml Eppendorf tubes. After centrifugation (4500 *rpm*, 5 min, 4 °C), the pellet was resuspended by pipetting up and down three times with FACS buffer. Cells were centrifuged, and after discarding the buffer, resuspended in 45 μ l FACS buffer containing CD16/32 (FC-Block) antibody diluted 1:300. This step is necessary to block unspecific binding of other used antibodies. Tubes were placed on ice in the dark for 15 minutes. 1 ml of FACS buffer was added to the cells followed by centrifugation and buffer discarding. Cells were resuspended with fluorochrome-conjugated antibodies for cluster of differentiation 86 (CD86), major histocompatibility complex II (MHCII) and mannose receptor (MMR) 1:200 diluted into FACS buffer. Tubes were incubated on ice in the dark for 15 minutes. FACS buffer was added and the cells centrifuged again. After discarding the buffer cells were resuspended in 500 μ l FACS buffer filtered through a cell strainer (nylon mesh) to eliminate clumps and debris, and kept on ice before being analysed by FACS. All measurements were performed in triplicates.

3.4.4 Analysis of cytokine release by enzyme-linked immunosorbent assay (ELISA)

BMMs were seeded at a ratio of 2×10^5 cells per well in 24 well plates at day 6 and incubated at 37 °C, 5 % CO₂. Macrophages were stimulated overnight with IFN- γ , LPS/IFN- γ and cannabinoid receptor 2 agonists: beta-caryophyllene and JWH-133. On Day 7, cell culture mediums were collected into 1,5 ml Eppendorf tubes. Tubes were deep-frozen into liquid nitrogen and placed at -80 °C for further analysis. ELISA kit for TNF α was performed according to the manufacturer's instructions.

3.4.5 Analysis of cannabinoid receptors expression by real time PCR (TaqMan)

BMMs were seeded at a ratio of 1×10^6 cells per well in 6 cm plates at day 6 and incubated at 37 °C, 5 % CO₂. On Day 7, RNA was isolated as described in section 3.1.1.10. After RT-PCR described in section 3.1.1.12, 4 μ l of cDNA (11 ng/ μ l) were used for the assay. cDNA and master mixes were pipetted using the liquid handling platform Janus from Perkin Elmer. All measurements were performed in triplicates.

3.4.6 Phagocytosis assay

3.4.6.1 Phagocytosis assay

BMMS were seeded at a ratio of 2×10^5 cells per well in 24 well plates at day 6 and incubated at 37 °C, 5 % CO₂. At day 7, Zymosan A *S. cerevisiae* BioParticles® Fluorescein Conjugate were reconstituted according to the manufacturer's instructions. 2 hours before phagocytosis assay, zymosan particles were diluted in tissue culture grade PBS. The particles were gently swirled into suspension and then, vigorously vortex (3 x 15 sec at the highest setting). The concentration was determined by counting the particles with a hemocytometer and adjusted to 4×10^5 particles/ μ l. The tube was protected from light and kept at 4 °C before starting the assay. Particles were vortex shortly before being used.

Particles (1×10^6) were pipetted directly into the BMMs medium. In order to allowed phagocytosis to occur, plates were incubated at 37 °C, 5 % CO₂. A plate was kept at 4 °C to measure passive phagocytosis and was used as a control. All experiments were performed in triplicates.

3.4.6.2 Analysis of phagocytic activity by Fluorescence-activated cell sorting (FACS)

After phagocytosis occurred, the medium was removed and cells were washed three times with ice-cold tissue culture grade PBS and finally resuspended in FACS buffer. The cells were collected using a cell scraper into 1,5 ml Eppendorf tubes. Cells were centrifuged (4500 rpm, 5 min, 4 °C), and after discarding the buffer, resuspended in 45 μ l FACS buffer containing

CD16/32 (FC-Block) antibody diluted 1:300. Tubes were placed on ice in the dark for 15 minutes. 1 ml of FACS buffer was added to the cells followed by centrifugation and buffer discarding. Cells were resuspended with CD11b Pacific Blue-conjugated antibody 1:200 diluted into FACS buffer. Tubes were incubated on ice in the dark for 15 minutes. FACS buffer was added and the cells centrifuged again. After discarding the buffer cells were resuspended into 500 μ l FACS buffer filtered through a cell strainer (nylon mesh) to eliminate clumps and debris, and kept on ice before being analysed by FACS. All measurements were performed in triplicates.

3.4.6.3 Analysis of phagocytic activity by microscopy

Macrophages were seeded at a ratio of 2×10^5 cells on cover slips in 24 well plates at day 6 and incubated at 37 °C, 5 % CO₂. The phagocytosis assay was performed exactly as for the FACS analysis. After phagocytosis occurred, the cover slips were washed twice, and roughly with tissue culture grade PBS. The cover slips were fixed in 4 % formaldehyde solution for 20 minutes at room temperature. They were washed again twice with PBS and mounted on slides with Dapi-Fluoromount-G. Preparations were air dried for 5 minutes before being examined under fluorescence microscope (Axio Imager M2). Experiments were performed in triplicates (3 cover slips per treatment condition) and six pictures per coverslip were taken from different regions. Engulfed particles were analysed and counted from the pictures using ImageJ software.

4 RESULTS

The results part is divided into three parts. In a first part, the results obtained for the humanization of the mouse CB2 locus are presented. In a second part, the results made in the generation of human CB2 recombinant lentiviral vectors are described. Finally a functional analysis of the CB2 receptor activation in mouse bone marrow derived-macrophages was performed and presented in the last part.

4.1 Humanizing the *Cnr2* locus

4.1.1 Generation of hCB2 targeting constructs

For the present thesis, the strategy to generate humanized CB2 mice aimed to exchange the mouse ORF located in exon 2 by the human counter parts. Humanized CB2 targeting vectors were cloned using the same cloning strategy performed in three steps. First a subcloning step was completed followed by the replacement of the murine ORF by the human ones and finally insertion of a cassette for selection in bacteria and ES cells. Each cloning step was verified by specific restriction pattern analysis.

4.1.1.1 Subcloning

The subcloning step was performed using the Genebridges™ Subcloning kit. The *E.coli* mCB2 BAC host previously transformed with the Red/ET expression plasmid (Wang and Zhang, 2005) was next transformed with the linear ColE1-amp minimal vector flanked by homology arms to achieve HR in bacteria. The linear minimal vector was generated by PCR using 75 bp oligonucleotides primers called forward and reverse mCB2 subcloning (figure 4A). These long oligonucleotides consist of 25 bp sequences necessary for the annealing and amplification of the pColE1-amp cassette and 50 bp homology arms required for HR. The 50 bp homology arms surrounding a fragment of 8619 bp were chosen in order to subclone the desired fragment from the mCB2 BAC into the mCB2 ORF subclone. After HR had occurred, clones carrying the subcloned fragment were identified by selection for ampicillin resistance that was conferred via expression of the ampicillin resistance gene (*ampR*) incorporated in the minimal vector (figure 5).

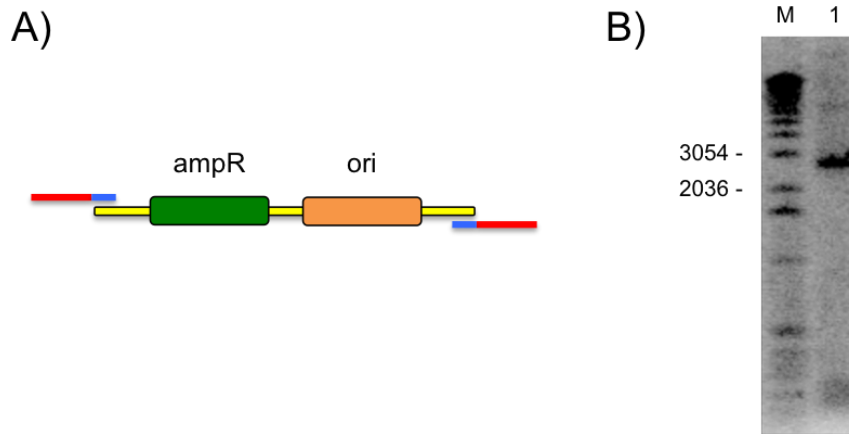


Figure 4: PCR amplification of the minimal vector.

A) PCR strategy to amplify the minimal vector cassette. Red lines represent the 50 bp homology regions chosen for homologous recombination to occur in bacteria. Blue lines represent the 25 bp sequence required for the amplification of the pColE1-amp cassette B) Representative picture of the pColE1-amp PCR product of 2735 bp checked on an 1 % agarose gel stained with ethidium bromide (lane 1). M: 1 kb marker. ampR: ampicillin resistance gene, ori: origin of replication sequence.

As shown in figure 4B, the fragment was successfully amplified and further used for subcloning a DNA fragment of 8625 bp from the mCB2 BAC by *in vivo* HR using the Red/ET technology.

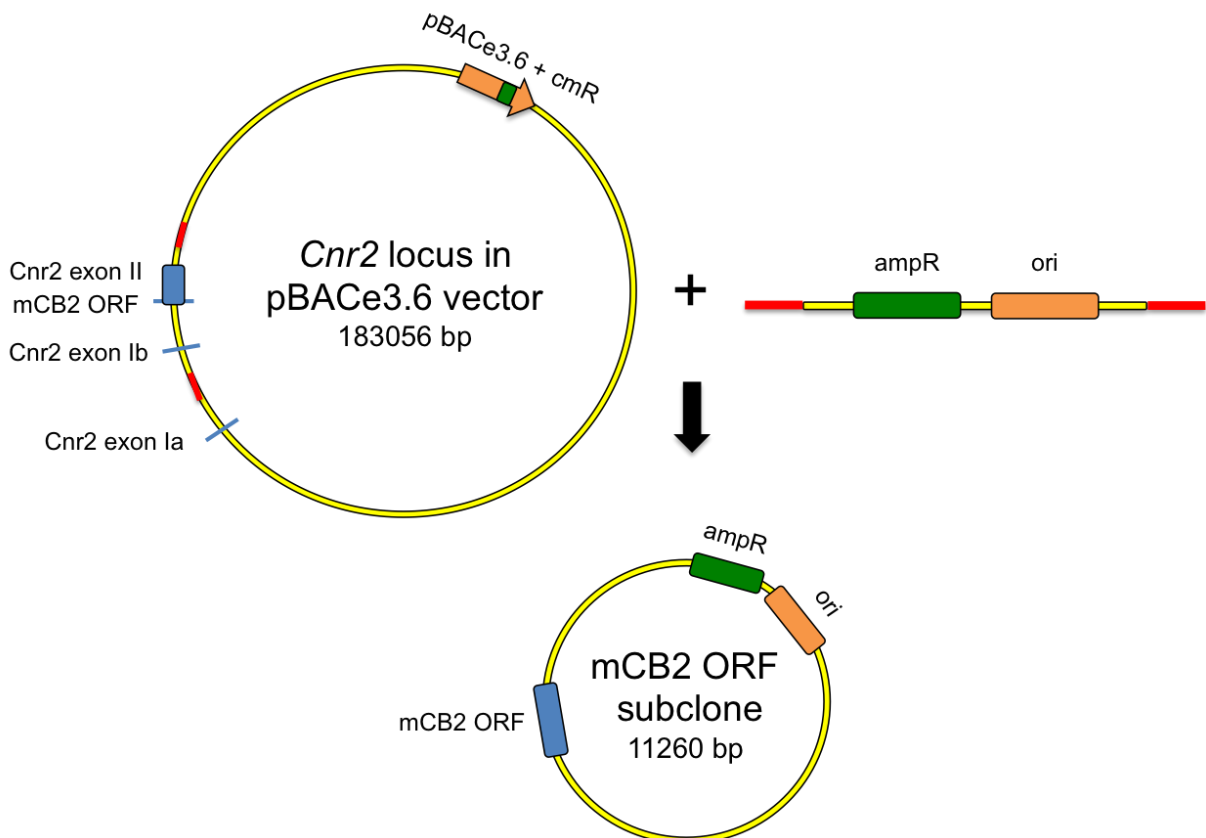


Figure 5: Subcloning of the 8625 bp DNA fragment from the mCB2 BAC

Schematic representation of the subcloning step using the Red/ET technology. The host bacteria harbouring the mCB2 BAC was electroporated with the linear minimal vector fragment containing homology arms (red lines). This resulted in the generation of the mCB2 ORF subclone via homologous recombination. ampR: ampicillin resistance gene, pBACe3.6: vector containing an origin of replication and a cmR: chloramphenicol antibiotic resistance gene, ori: origin of replication sequence, ORF: Open reading frame.

4.1.1.2 Verification of the subcloning step

Ampicillin resistant clones were picked and verified by *MfeI* restriction analysis. *MfeI* restriction sites were introduced into the oligonucleotides sequences used for the amplification of the pColE1-amp cassette (figure 6A). As shown in figure 6B, a mCB2 ORF subclone was identified by a two bands pattern of 8619 bp and 2641 bp, which corresponds to the expected band size after *MfeI* restriction.

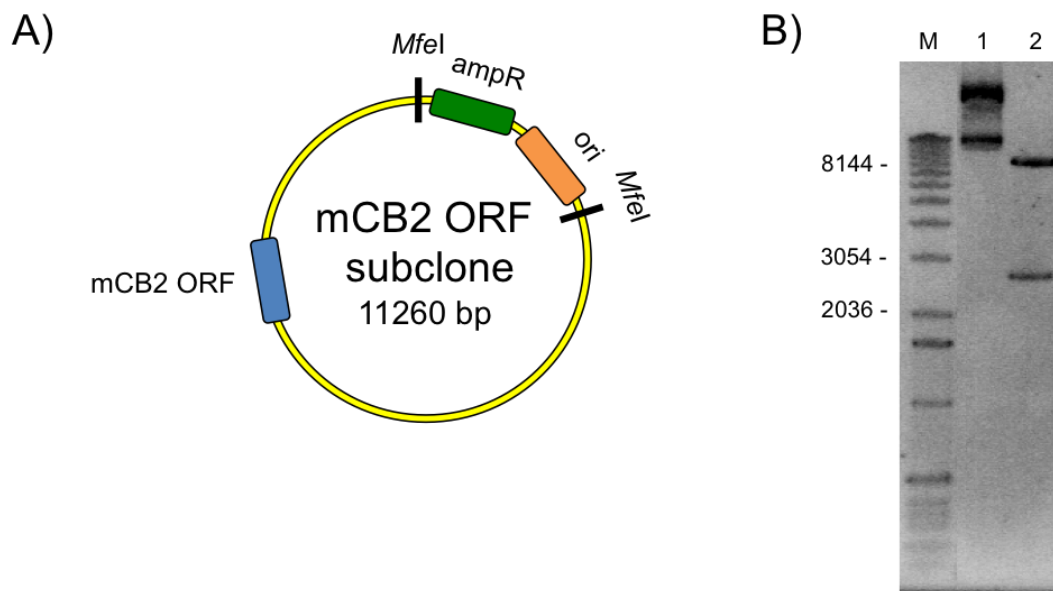


Figure 6: Subcloning step checked by *MfeI* restriction analysis

A) Schematic localisation of *MfeI* restriction sites in the mCB2 ORF subclone. ampR: ampicillin resistance gene, ori: origin of replication sequence, ORF: Open reading frame. B) Representative picture of the restriction digest checked on a 1 % agarose gel stained with ethidium bromide. M: 1 kb marker; lane1: undigested plasmid DNA from an ampicillin resistant clone; lane 2: Digestion of the mCB2 ORF subclone by *MfeI* resulted in the generation of the expected fragments of 8619 bp and 2641 bp.

4.1.1.3 Replacement of the murine ORF

The replacement of the murine to the human ORFs was performed using a conventional cloning strategy with digestion and ligation steps. The vector was obtained by digesting the mCB2 ORF subclone obtained previously with *AatII* and *BamHI* restriction enzymes (figure

7A) which results in the production of a two bands pattern of 10119 bp and 1141 bp. The upper band of 10119 bp (figure 7B) representing the vector was extracted from the gel and purified for subsequent ligation.

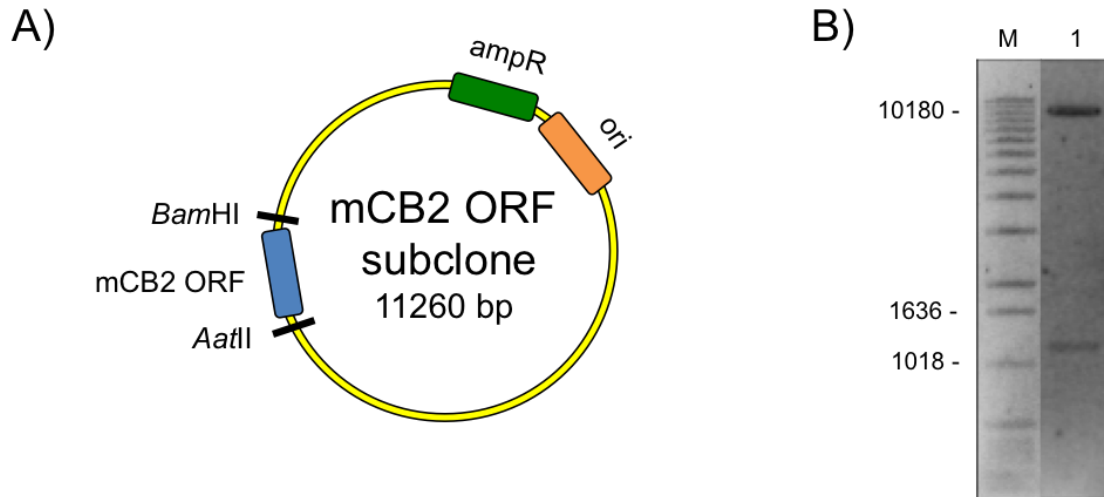


Figure 7: Double digestion of the mCB2 ORF subclone with the enzymes *AatII* and *BamHI*

A) Schematic localisation of *AatII* and *BamHI* restriction sites in the mCB2 ORF subclone. ampR: ampicillin resistance gene, ori: origin of replication sequence, ORF: Open reading frame. B) The 0.8 % agarose gel was stained with ethidium bromide. M: 1 kb marker; lane 1: mCB2 ORF subclone digested with *AatII* and *BamHI* resulted in two bands of 10119 bp and 1141 bp. The upper band was extracted from the gel further proceed with the ligation step.

In order to sustain the 5' and 3' untranslated regions flanking the 1044 bp sequence of the mouse CB2 ORF, the human CB2 ORFs with a length of 1083 bp were amplified by two successive PCRs. In a first PCR step, primers (Fwd and Rev hCB2 flanked HA first) were used to add 50 bp mouse DNA stretches to the human ORFs to introduce the *BamHI* restriction site on the 3' end. This led to the generation of 1183 bp PCR fragments (figure 8).

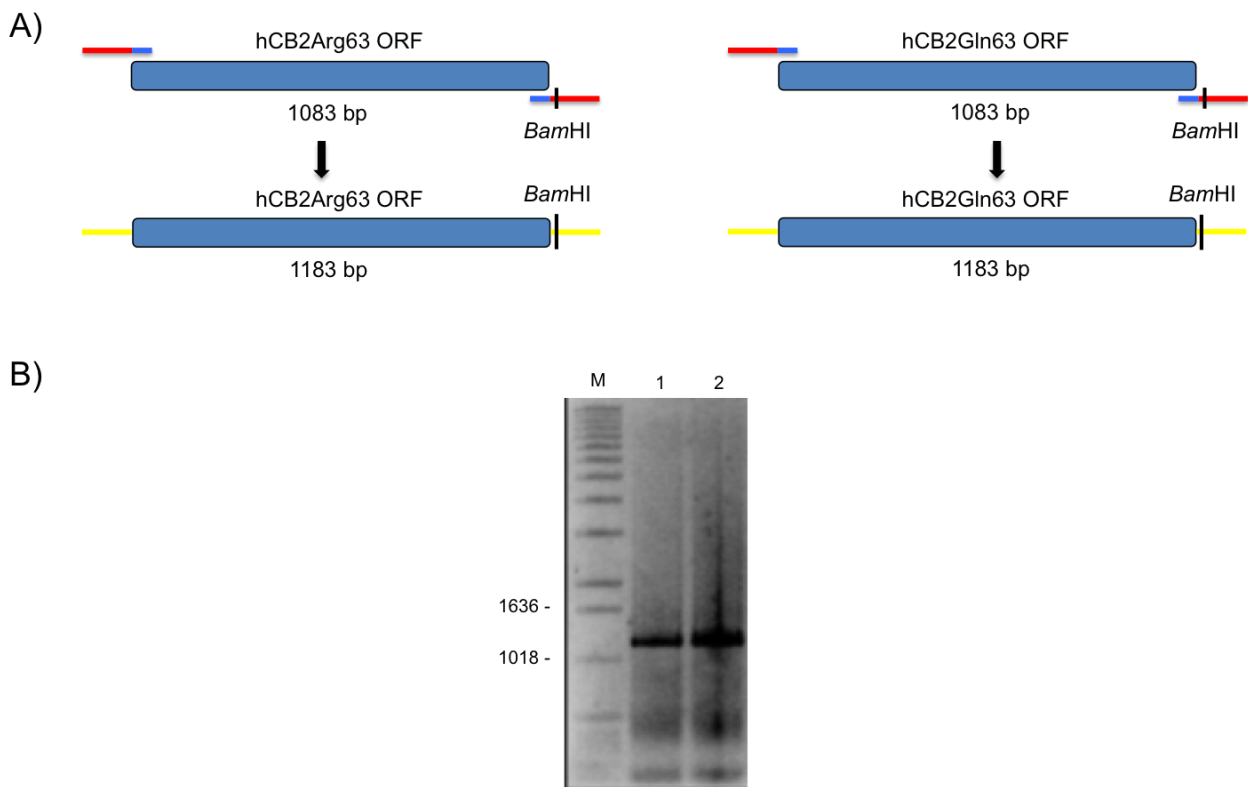


Figure 8: First PCR amplification of the hCB2 ORFs

A) Schematic representation of the first PCR performed to generate the human ORFs inserts. In this first PCR 75 bp primers were used (depicted with red and blue lines). The blue lines represent the 25 bp used to anneal and amplify the human ORFs. The red lines represent the 50 bp sequences that were homologous to the sequences adjacent to the murine ORF. B) First PCR reaction checked on an 1 % agarose gel stained with ethidium bromide. M: 1 kb marker; lane 1: hCB2Arg63 ORF + 50 bp on both sides; lane 2: hCB2Gln63 ORF + 50 bp on both sides. PCR product size for both ORFs: 1183 bp. The *Bam*HI restriction site is integrated at the 3' end of the human ORFs.

In a second PCR step, primers (Fwd and Rev hCB2 flanked HA second) were used to add 50 bp mouse DNA stretches to the previously amplified fragments to integrate an *Aat*II restriction site on the 5' end (figure 9). This amplification resulted in fragments of 1283 bp. The CNR2 ORFs PCR products generated after the two successive PCRs were digested with *Aat*II and *Bam*HI before proceeding with ligations.

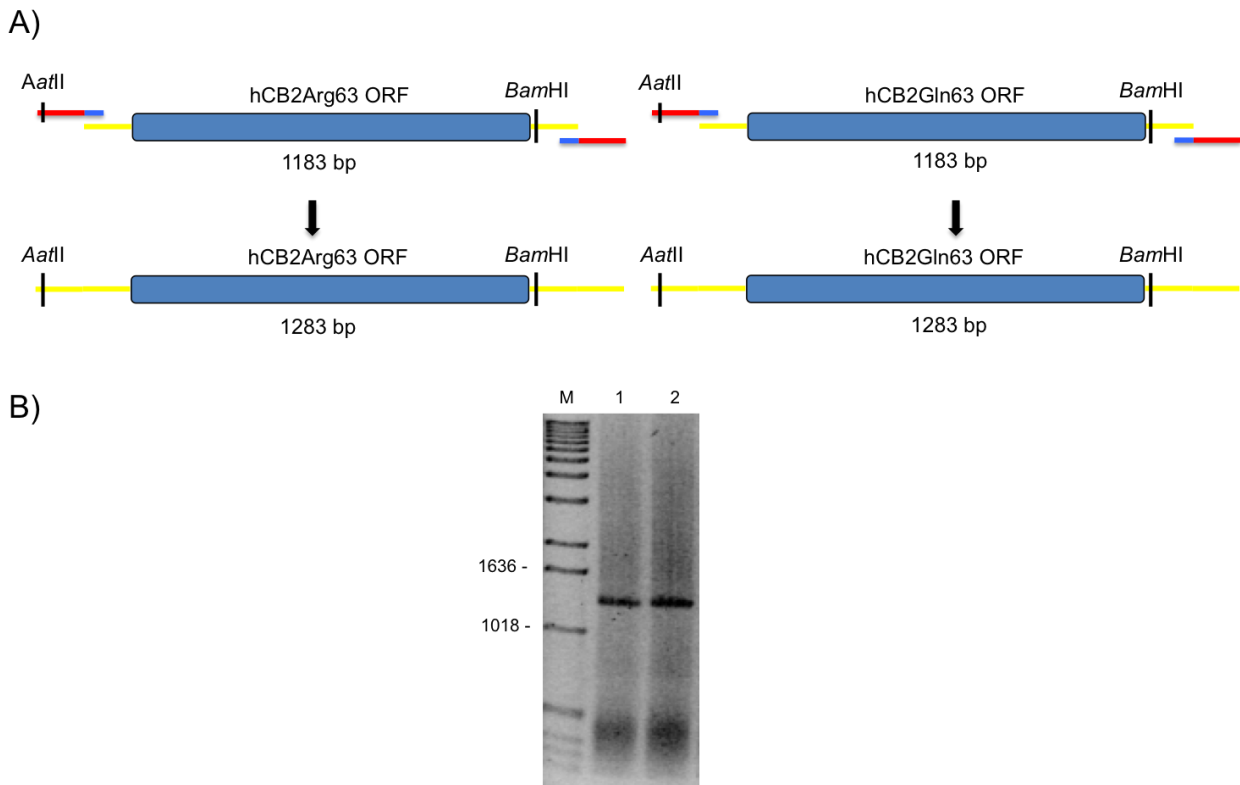


Figure 9: Second PCR amplification of the hCB2 ORFs

A) Schematic representation of the second PCR performed to generate the human ORFs inserts. The two ORFs of the human variants were amplified using 75 bp primers (depicted with red and blue lines). The blue lines represent the 25 bp used to anneal and amplify the 1183 bp fragments. The red parts represent the 50 bp that was homologous to the sequences adjacent to the previously added 50 bp DNA sequences. B) Second PCR reaction checked on an 1 % agarose gel stained with ethidium bromide. M: 1 kb marker; lane 1: hCB2Arg63 ORF + 100 bp on both sides; lane 2: hCB2Gln63 ORF + 100 bp on both sides. PCR product size for both ORFs+100 bp DNA sequences on both sides: 1283 bp. The *AatII* restriction site is integrated on the 5' end of the amplified fragments. The PCR fragments were digested with *AatII* and *BamHI* before proceeding with ligations.

As a result of the two PCRs, 100 base pairs were added that were homologous to the sequences flanking the mCB2 ORF. Ligations were performed by combining gel-purified vector and human ORF previously digested with *AatII* and *BamHI*.

4.1.1.4 Cloning of Human ORF subclones

After ligations of digested mCB2 ORF subclone and human ORFs flanked with mouse DNA stretches, the DNA was electroporated into TOP10 electrocompetent bacteria. DNA from Ampicillin resistant clones was prepared and checked by enzymatic restriction digestions using two enzymes: *SpeI* and *MfeI*. The *SpeI* restriction site is only present in the human CB2, but not in the murine ORF (figure 10A). Thus, correctly ligated clones exhibit three fragments with a size of 5450 bp, 3208 bp and 2641 bp after digestion. As seen in figure 10B and 10C, several recombined clones were identified for both CB2 variants.

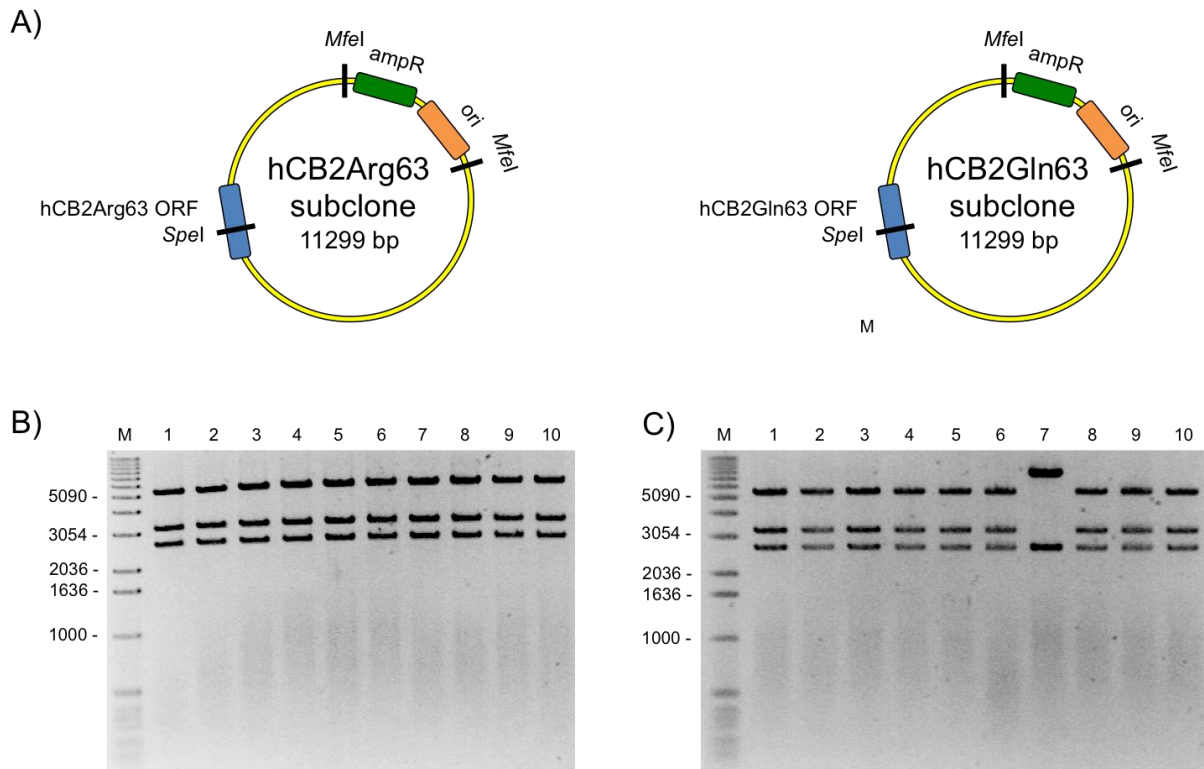


Figure 10: Verification of ligations

A) Schematic localisation of the restriction sites for both hCB2 variants. ampR: ampicillin resistance gene, ori: origin of replication sequence, ORF: Open reading frame. B) The 1 % agarose gel was stained with ethidium bromide. M: 1 kb marker; lane 1-10: hCB2Arg63 subclones digested with *MfeI* and *SpeI* and correctly recombined as indicated by the presence of the three fragments of 5450 bp, 3208 bp and 2641 bp. C) The 1 % agarose gel was stained with ethidium bromide. M: 1 kb marker; lane 1-6,8-10: hCB2Gln63 subclones digested with *MfeI* and *SpeI* and correctly recombined as indicated by the presence of the three fragments of 5450 bp, 3208 bp and 2641 bp, lane 7: incorrectly ligated clone.

4.1.1.5 Insertion of the FRT-PGK-gb2-neo-FRT cassette for selection

The last step of the targeting constructs generation was the insertion of a selection cassette. This cassette encodes the neomycin/kanamycin resistance gene, which combines a prokaryotic promoter (gb2) for expression of kanamycin resistance in recombined E.coli clones with an eukaryotic promoter (PGK) for expression of neomycin resistance gene in recombined ES cells. The selection cassette was flanked by FRT sites for further excision by the Flp-recombinase. The insertion site of the cassette was chosen 933bp downstream to the CNR2 ORFs. The cassette was generated via PCR using respective primers (Fwd and Rev FRT-neo-FRT) through which the homology arms were added. The resulting fragment of 1737 bp was used for Red/ET HR (Figure 11).

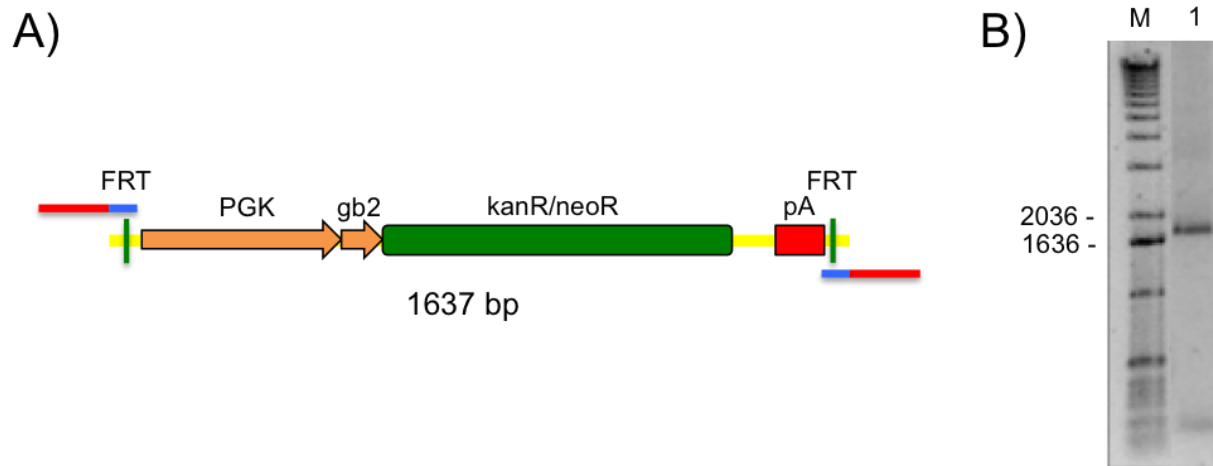


Figure 11: FRT-PGK-gb2-neo-FRT fragment generation

A) The FRT-PGK-gb2-neo-FRT fragment was generated by PCR using 75 bp primers (red and blue lines). The blue line represents the 25 bp used to anneal and amplify the FRT-PGK-gb2-neo-FRT cassette. The red line represents the homology arms (50 bp) necessary for homologous recombination. B) M: 1 kb marker; lane 1: the PCR product size (1737 bp) was checked on an 1 % agarose gel stained with ethidium bromide. FRT: flippase recognition target site, PGK: phosphoglycerate kinase eukaryotic promoter, gb2: *E. coli* prokaryotic promoter, kanR: Kanamycin resistance gene, neoR: neomycin resistance gene, pA: polyadenylation signal.

The *E. coli* hCB2Arg63 and *E. coli* hCB2Gln63 subclones, previously electroporated with the Red/ET expression plasmid, were next electroporated with the linear FRT-PGK-gb2-neo-FRT cassette flanked with homology arms (figure 12).

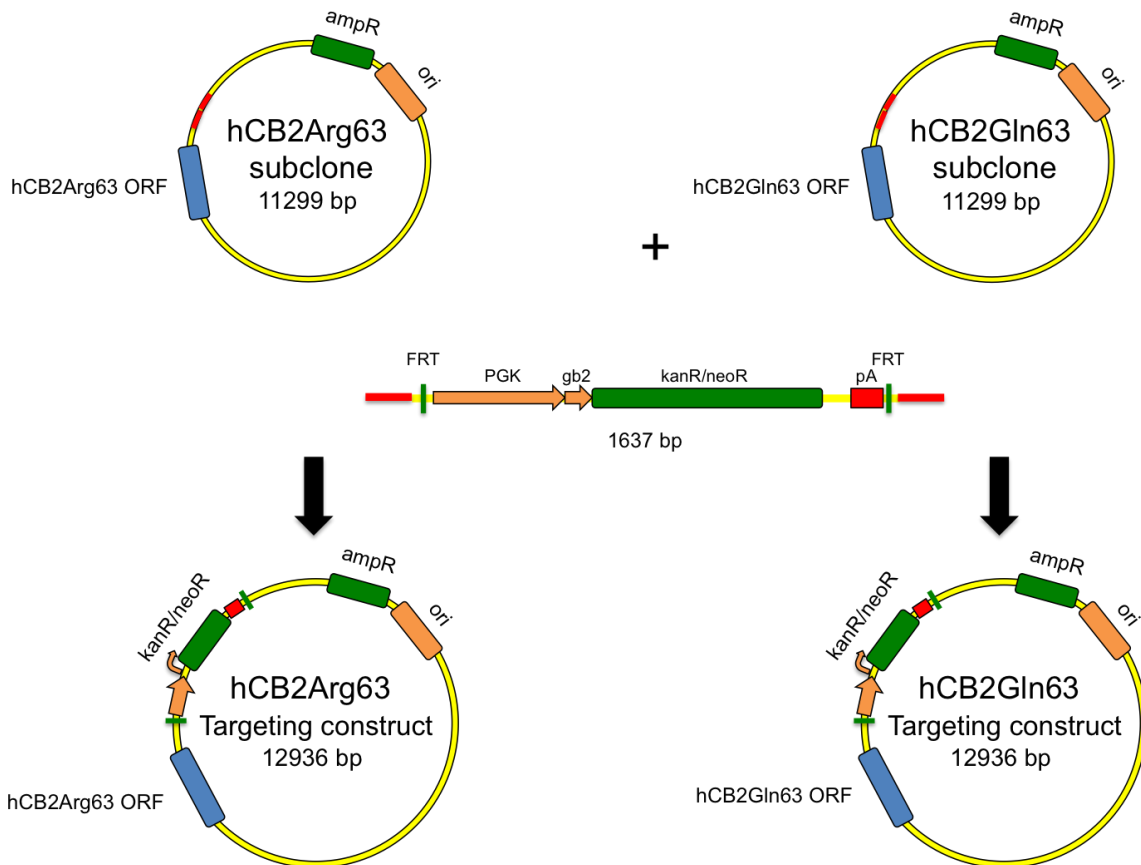


Figure 12: Recombination of FRT-PGK-gb2-neo-FRT cassette for selection in bacteria and ES cells

Schematic representation of the homologous recombination using the Red/ET technology. Recombination of the hCB2 subclones with the linear FRT-PGK-gb2-neo-FRT cassette result in the generation of final targeting constructs. Red lines represent the homology region chosen for the insertion of the cassette into the hCB2 subclones. ampR: ampicillin resistance gene, kanR: kanamycin resistance gene, neoR: neomycin resistant gene, ori: origin of replication sequence, ORF: Open reading frame.

After HR had occurred, clones carrying the recombined fragment were identified by selection for ampicillin and kanamycin resistance.

4.1.1.6 Verification of targeting constructs

Kanamycin and ampicillin resistant clones were analysed by double restriction digestions using *MfeI* and *SpeI* enzymes (figure 13A). The targeting constructs contained two *MfeI* restriction sites and two *SpeI* restriction sites. Therefore, enzymatic digestion was supposed to result in the generation of 4 DNA fragments (5450 bp, 3080 bp, 2641 bp and 1765 bp). As shown in figure 13B, these fragments were detectable after digestion of the constructs.

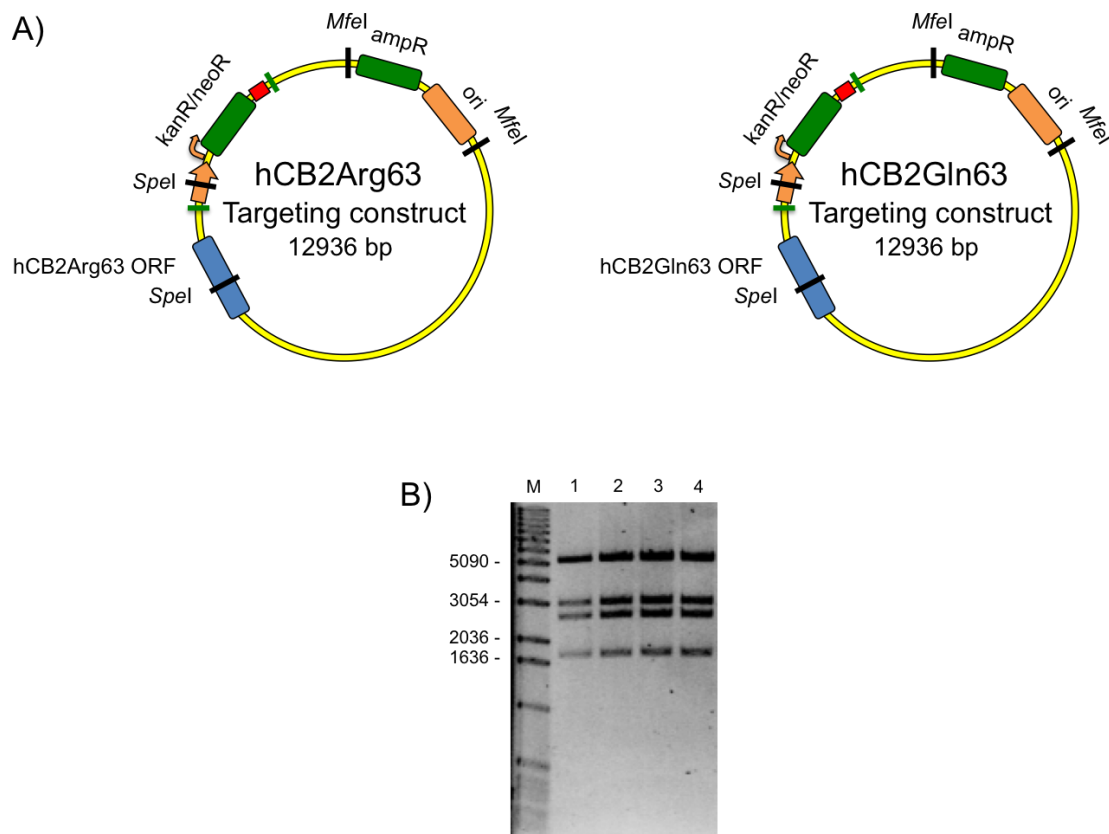


Figure 13: Targeting construct checked by *MfeI* and *SpeI* restriction analysis

A) Schematic localisation of the restriction sites *MfeI* and *SpeI* used for checking the targeting constructs. B) Restriction digestion checked on an 1 % agarose gel stained with ethidium bromide. M: 1 kb marker; lane 1,2: hCB2Arg63 targeting construct double digested with *MfeI SpeI*; lane 3,4: hCB2Gln63 targeting construct double digested with *MfeI SpeI*. All clones were correctly recombined as indicated by the presence of four fragments of 5450 bp, 3080 bp, 2641 bp and 1765 bp. ampR: ampicillin resistance gene, kanR: kanamycin resistance gene, neoR: neomycin resistant gene, ori: origin of replication sequence, ORF: Open reading frame.

The human CB2 ORFs inserts were verified by sequence analysis (Macrogen Corporation).

4.1.2 Screening strategies for targeted mutagenesis of the *Cnr2* gene locus

After linearization with *EcoRV*, the targeting constructs were electroporated into ES cells. Positive ES cell clones were selected via G418 resistance (conferred by the neoR gene) and screened for HR by PCR and Southern blot. For both techniques, two strategies were developed to verify the correct integration of the flanked neo cassette and the human ORFs.

4.1.2.1 PCR

The first PCR strategy was used to check if the neo gene was present at the correct location and a second one to confirm the presence of the human CB2 ORF.

4.1.2.1.1 PCR strategy for validation of neo gene integration

To exclude ectopic recombination, primers called Fwd and Rev ES cell check, were designed to bind at the 3' end of the flanked neo cassette and within the 3' genomic region, which was not included in the targeting construct (figure 14A). The PCR product resulting from the targeted gene locus comprised a fragment of 1953 bp whereas amplification of the non-targeted locus exhibits no band (figure 14B).

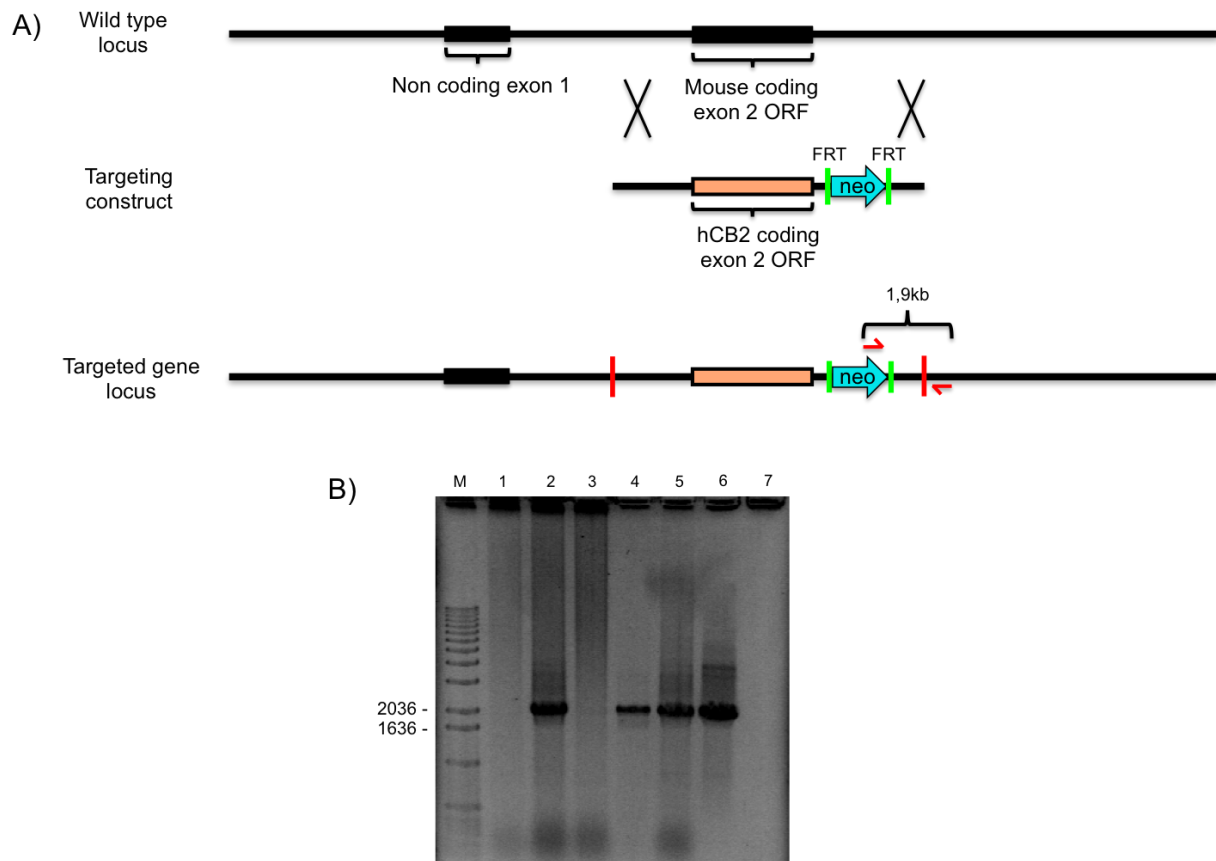


Figure 14: PCR strategy to check the FRT-neo-FRT integration in ES cells

A) PCR strategy. The red arrows represent the primers used. The wild type allele (top) led to no PCR product, whereas after homologous recombination of the targeting construct (centre), the presence of the neo cassette in the targeted gene locus (bottom) generated a fragment of 1.9 kb. ORF: open reading frame, neo: neo resistance gene, FRT: flippase recognition target site. B) 1 % agarose gel stained with ethidium bromide. M: 1 kb marker; lane 1,3: negative Bruce4 ES cell clones, lane 2,4,5: positive Bruce4 ES cell clones; lane 6: homologously recombined ES cell clone previously identified used as positive control; lane 7: water control.

4.1.2.1.2 PCR strategy for validation of the human ORF integration

The human ORF integration PCR was used to confirm the presence of the human ORFs in ES cells. In a first time and as depicted in figure 15A, fragments of 1212 bp for the mouse ORF or 1251 bp for the human ORF were amplified by PCR using primers flanking the ORFs (Fwd and Rev seq hCB2). Then amplicons were digested with *SpeI*. Due to the fact that the restriction site is only present in the human ORF, the restriction pattern revealed a single band

of 1212 bp for the mouse ORF and a double band of 605 bp and 646 bp when the human ORF is present (figure 15B).

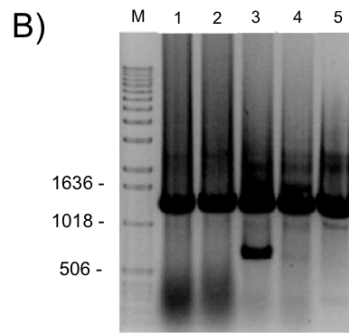
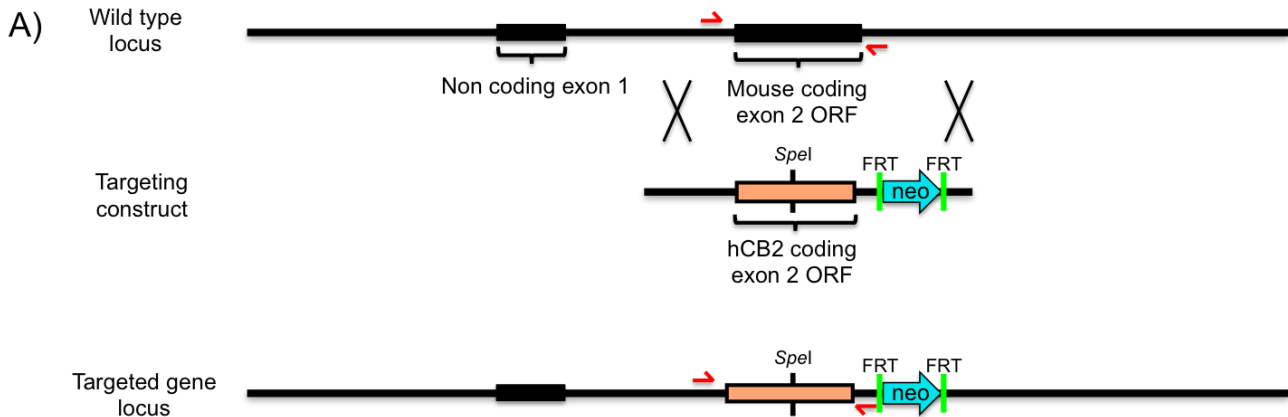


Figure 15: PCR strategy to check the human ORF integration in ES cells

A) Verification of targeted ES cell clones using PCR followed by *SpeI* restriction digestion. The red arrows represent the primers used. The wild type allele (top) led to a PCR product of 1212 bp, whereas after homologous recombination of the targeting construct (centre), the presence of the human ORF in the targeted gene locus (bottom) generated a fragment of 1251 bp. ORF: open reading frame, neo: neo resistance gene, FRT: flippase recognition target site. The *SpeI* restriction site is only present in the human CB2 ORF. Thus the amplification of the murine ORF followed by *SpeI* restriction digestion result in a fragment of 1212 bp, while the presence of the human ORF is indicated by two fragments of 605 bp and 646 bp. B) 1 % agarose gel stained with ethidium bromide. M: 1 kb marker; lane 1,2,4: ES cell clone negative for the human ORF integration; lane 3: ES cell clone positive for the human ORF integration; lane 5: WT ES cell DNA used as negative control.

When the human ORF is integrated, only one band is visible. In fact the double bands of 605 and 646 bp cannot be separated using a 1 % agarose gel. A gel with a higher percentage of agarose could have been used to separate these two bands, but the main purpose of this PCR was to rapidly identified clones which possibly contained the human ORFs. In fact the positive clones containing the human ORFs were further verified using the southern blot strategy described in section 4.1.2.2.2.

4.1.2.2 Southern Blot

Southern blot strategies were designed and used to confirm the positive clones that were identified by PCR. The sequence-specific probes were located within genomic regions at the 3' and 5' end, respectively (figure 16 and 17 part A). These regions were not included in the targeting constructs to exclude the detection of false positives due to ectopic recombination

4.1.2.2.1 Targeted mutagenesis of the *Cnr2* gene locus on the 3' side

As shown in figure 16B, digestion of selected ES cell clones with *Pst*I resulted in a 8.5 kb fragment for the mouse wild type locus. Upon HR at the 3' end, digestion with *Pst*I led to a smaller fragment of 3.9 kb due to the additional restriction site present in the neo cassette. After confirmation of HR at the 3' end the ES cell clones were further checked for HR at the 5' end.

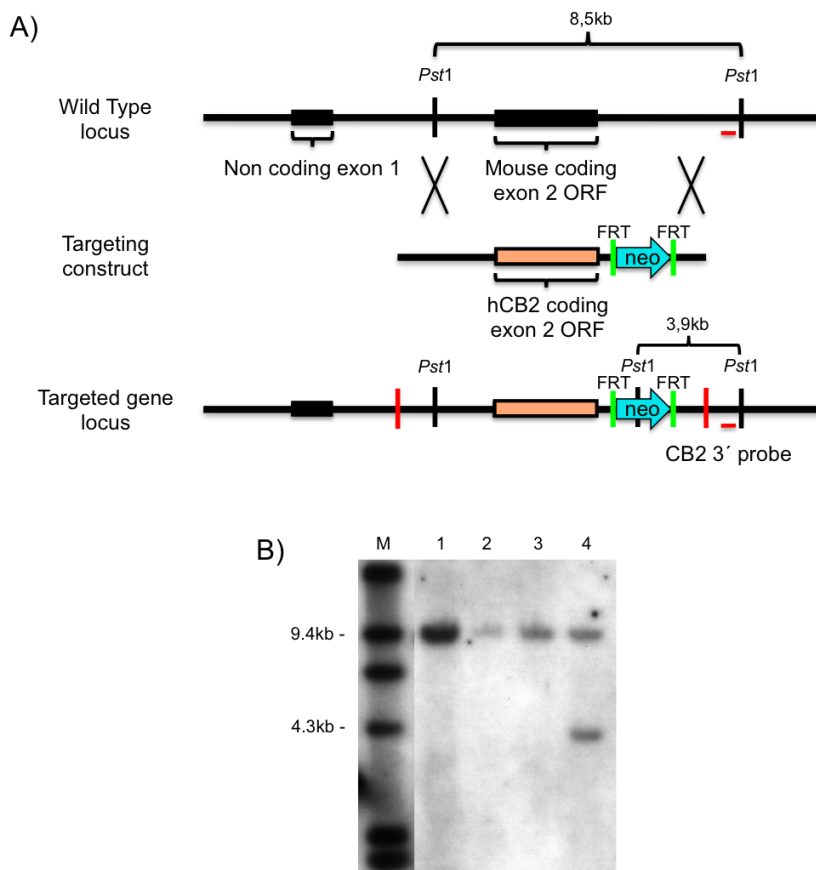


Figure 16: Southern blot strategy to analyse 3' homologous integration

A) Schematic representation of the 3' Southern blot strategy. The *Cnr2* wild type gene locus is illustrated in the upper scheme. The targeting construct (centre) consisted of the human CB2 ORF (orange) and a FRT (green vertical lines) flanked neo cassette (green arrow). Homologous recombination resulted in the targeted gene locus (bottom). Homologous recombination was verified by *Pst*I digestion and subsequent Southern blot using the probe shown in red. The red vertical lines indicate the limits of the targeting construct integration. B) Southern Blot analysis of the 3' homologous

integration revealed correct targeting in the hCB2-Arg 31 ES clones (lane 4) whereas three other ES cell clones (lane 1-3) showed no targeted integration. M: DNA molecular weight marker II (Roche).

4.1.2.2.2 Targeted mutagenesis of the *Cnr2* gene locus on the 5' side

As shown in figure 17B, double digestion of selected ES cell clones with *PacI* and *SpeI* resulted in a large fragment of 22 kb for the mouse wild type locus. Upon HR at the 5' end, digestion at a *SpeI* restriction site present in human ORFs, led to a smaller fragment of 8.9 kb.

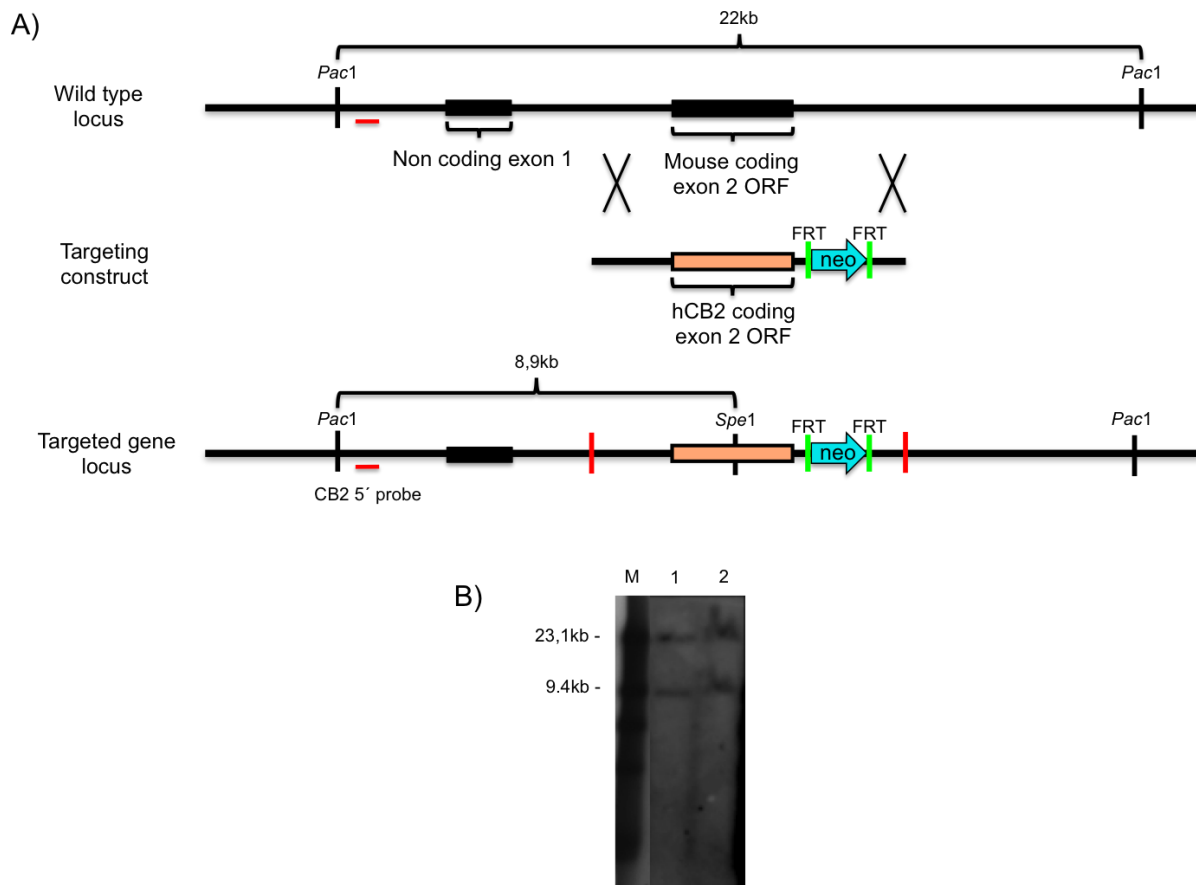


Figure 17: Southern blot strategy to analyse 5' homologous integration

A) Schematic representation of the 3' Southern blot strategy. Murine CB2 wild type gene locus is illustrated in the upper scheme. The targeting construct (centre) consisted of the human CB2 ORF (orange) and a FRT (green vertical lines) flanked neo cassette (green arrow). Homologous recombination resulted in the targeted gene locus (bottom). Homologous recombination was verified by *PacI* and *SpeI* digestion and subsequent Southern blot using the probe shown in red. The red vertical lines indicate the limits of the targeting construct integration. B) Analysis of 5' homologous integration revealed correct targeting in the hCB2-Arg31 ES cell clone (lane 1) and in the hCB2-Gln7 ES cell clone (lane 2). M: DNA molecular weight marker II.

ES cell clones that exhibited HR for both the 3' and 5' ends were further used for blastocyst injections.

4.1.3 Cloning of new genetic engineering technologies to humanized the *Cnr2* locus

Three new genetic engineering technologies emerged during the last 5 years: zinc finger, transcription activator-like effector nucleases (TALENs) and clustered regularly interspaced short palindromic repeats (CRISPR) coupled to a Cas9 enzyme (CRISPR/Cas9 system). All these nucleases share the ability to induce site-specific DSBs within the DNA. The aim was to design a guide RNA (gRNA) to target the Cas9 enzyme and a TALEN pair to produce DSBs within the *Cnr2* ORF, but not in the *CNR2* ORF, present in the targeting constructs previously generated. Therefore, first the sequences of the *CNR2*-ORF of coding exon 2 from both species were aligned (figure 18 and 21).

4.1.3.1 TALEN pair design and generation

4.1.3.1.1 TALEN design

TALENs are a combination of transcription activator-like (TAL) effectors with the non-specific DNA cleavage domain from the end of the *FokI* nuclease. TALENs bind and cleave DNA in pairs as the *FokI* domain functions as a dimer. Therefore TALEN binding sites and the number of bases between the two individual (left and right) TALENs, also called spacer region, appear to be important parameters for achieving high levels of activity (Schmid-Burgk et al., 2013). Therefore, a TALEN pair was designed respecting both, the mismatches criteria between mouse and human *CNR2*-ORF sequences and the size of the spacer region (figure 18).

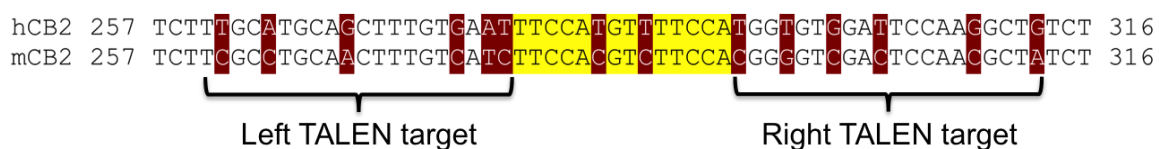


Figure 18: Design of a TALEN pair to target the mouse *CB2* ORF

Sequence alignment of the human and mouse *CNR2*-ORF revealed several mismatches, which are highlighted by the dark red background colour. Yellow background letters represent the spacer region of 14 bp. The left and right TALEN targets represent the binding sites of the left-mCB2-TALEN and the right-mCB2-TALEN.

After *in silico* design of a desired *Cnr2* targeting TALEN pair, the cloning was performed using a high-fidelity ligation-independent cloning technique.

4.1.3.1.2 Two steps generation of TALENs plasmids

The laboratory of Professor Dr. Veit Hornung from the Institute for Clinical Chemistry and Clinical Pharmacology developed a high-fidelity ligation-independent cloning (LIC) technique that enables generation of TALE genes requiring only the combinatorial mixing of fluids in

order to clone a desired TALEN pair. They generated a LIC-ready TALE repeat unit library of 2-mer fragments that can be assembled in 2 hierarchical assembly steps. The software LIC TALE gene Assembler Version 1.0 developed by the team was used to decide on the appropriate 2-mer fragments that are required to assemble an 18.5 RVD TALEN construct. The resulting TALEN contains 18.5 TAL effector repeat units and has a target specificity of the sequence 5'-T(N)19-3'

In the first assembly reaction, three 2-mer fragments are assembled into a 6-mer fragment in a kanamycin resistant level 1 backbone plasmid (figure 19A). The first step of the TALE LIC assembly was followed by transformation and selection of kanamycin resistant clones. Validation of the 6-mer assemblies was performed by digestion of positive clones with the *Mva1269I* restriction enzyme. When the ligation was successful, a band of ≈ 650 bp appeared (figure 19B). The lower bands show a slight difference in size which is due to the different ID length used for the ligation-independent cloning, described in section 3.1.4.

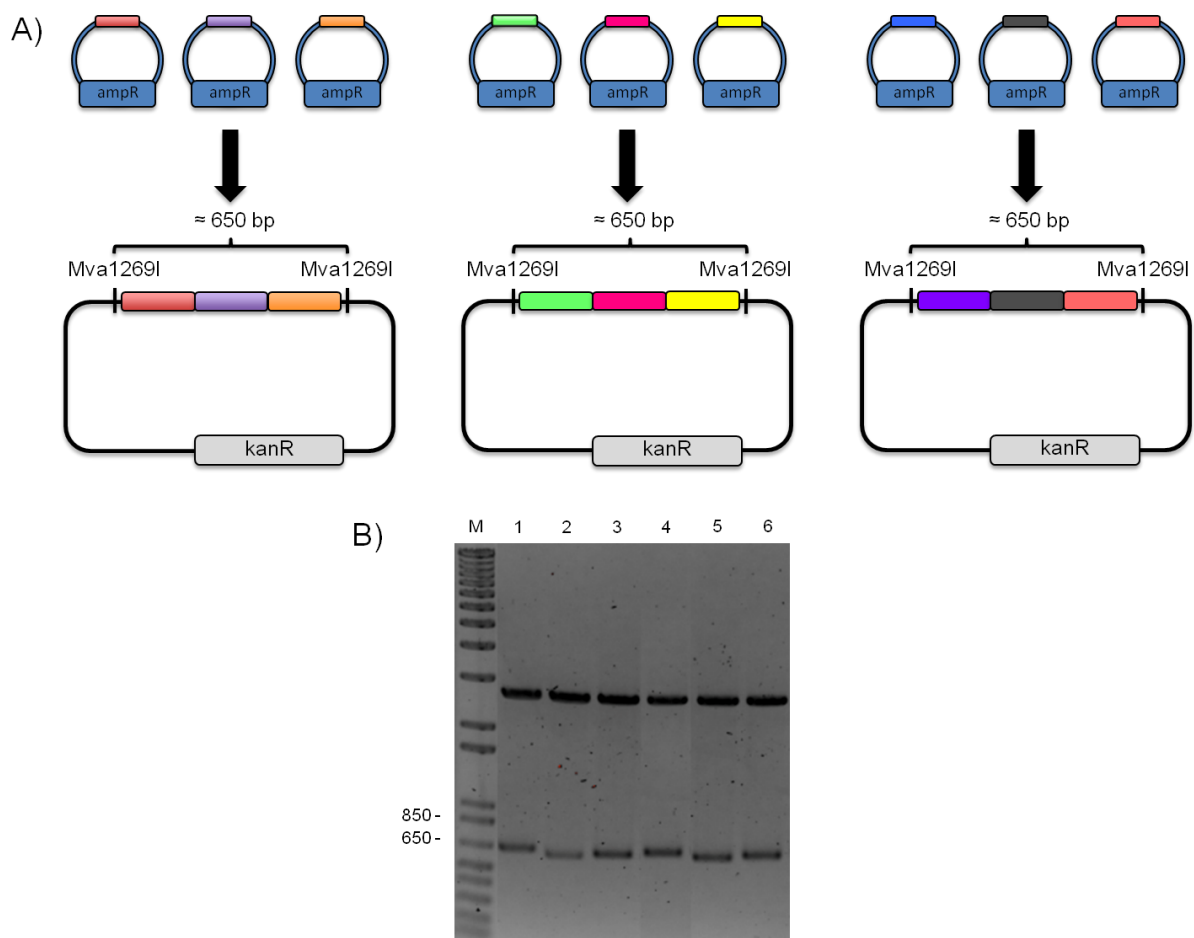


Figure 19: First step of LIC TALE assembly

A) Schematic representation of the first LIC TALE assemblies required for one individual TALEN pair. Each 2-mer required to target 2 nucleobases are represented in the upper part of the figure by coloured boxes. After defining the target sequence, the 2-mer were chosen and digested with *Mva1269I* from

their ampicillin resistant (*ampR*) plasmids in which they were contained. Then they were assembled into 6-mer fragments inside a kanamycin resistant (*kanR*) level 1 backbone using the ligation-independent cloning technique. B) 1 % agarose gel stained with ethidium bromide. Verification of 2-mer fragments assemblies contained in level 1 backbone via *Mva1269I* restriction digestion. M: 1 kb marker. Left TALEN; Lane 1: First 6-mer fragment, lane 2: second 6-mer fragment, lane 3: third 6-mer fragment. Right TALEN; Lane 4: First 6-mer fragment, lane 5: second 6-mer fragment, lane 6: third 6-mer fragment. The size of fragments is around 650 bp.

In a second step, three 6-mer fragments were assembled into an 18-mer fragment contained into an ampicillin resistant level 2 backbone plasmid, giving rise to an 18.5 RVD TALEN construct (figure 20A). After digestion of the 6-mer fragments with *Mva1269I* restriction enzyme, the fragments were assembled and transformed. Ampicillin resistant clones were picked and DNA was prepared. Positive clones were verified with double restriction digestion using *XhoI* and *XbaI* restriction enzymes. Correctly assembled clones show a pattern of 2 bands of 6kb and 3.2 kb as seen in figure 20B and were verified by sequencing (Macrogen Corporation).

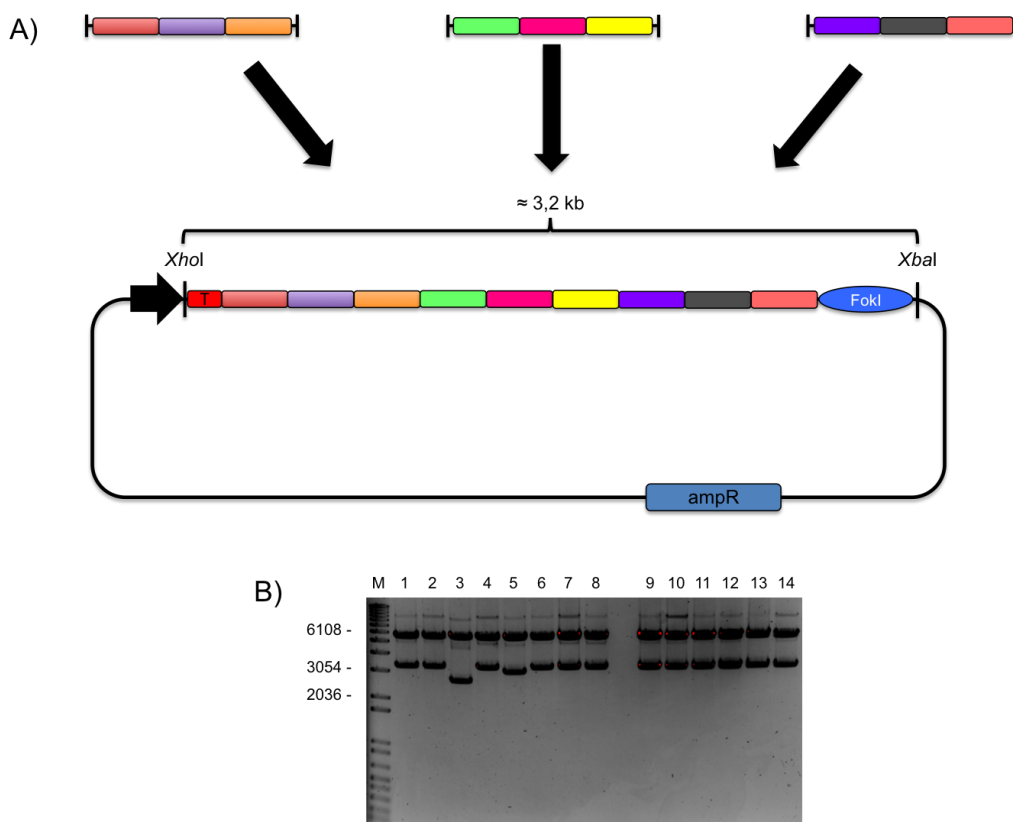


Figure 20: Second step of the LIC TALE assembly

A) Schematic representation of the second LIC TALE assemblies required for one individual 18.5 RVD TALEN construct. After *Mva1269I* restriction digestion of the level 1 plasmids containing the 6-mer fragments, three of the 6-mer (upper part) were assembled into a 18-mer fragment into an ampicillin

resistant level 2 backbone plasmid, giving rise to an 18.5 RVD TALEN construct (lower part). B) 1 % agarose gel stained with ethidium bromide. Verification of 6-mer fragments assemblies contained in level 2 backbone via *XhoI* and *XbaI* restriction digestion. M: 1 kb marker. Left TALEN; Lane 1,2,4,6,7,8: successful assembled 18.5 RVD TALEN left construct, lane 3,5: incorrectly assembled clones. Right TALEN; lane 9,10,11,12,13,14: successfully assembled 18.5 RVD TALEN right construct represented by a pattern of 2 bands of 6kb for the backbone and 3.2 kb for the correct insert.

The generated, 18,5 RVD TALEN constructs targeting the *Cnr2* (called left-mCB2-TALEN and right-mCB2-TALEN) were then lipofected into NIH3T3 cells in order to test its ability as a TALEN pair, to generate targeted DSBs within the *Cnr2* ORF. The surveyor assay was used to assessed this ability.

4.1.3.2 Design and Generation of CRISPR/Cas plasmid

4.1.3.2.1 CRISPR/Cas system design

An important requirement for the CRISPR/Cas system to produce DSBs is a short NGG protospacer-adjacent motif (PAM) located immediately after the guide sequence to be targeted. This NGG motive adjacent to a sequence that was highly divergent between mouse and human was identified using USCS genome browser (Figure 21). Also, the 6 mismatches in 20 base pairs were located at both ends of the sequence, which were reported to be more important for target specificity of gRNAs than the central nucleotides (Cong et al., 2013). This gRNA sequence target therefore appeared to be suitable as a target for a gRNA. The corresponding oligonucleotides (Fwd and Rev CB2 sgRNA) were cloned into the px330 plasmid to obtain the px330-mCB2 construct. This is the only cloning step required to direct the CRISPR/Cas9 system to the *Cnr2* gene locus.

```

hCB2 1 ATGGAGGAATGCTGGGTGACAGAGATAGCCAATGGCTCCAAGGATGGCTTGGATTCCAAC 60
mCB2 1 ATGGAGGGATGCCGGGAGACAGAACTGACCAACGGCTCCAACGGCTGGCTTGGATTCCAAC 60

```

Guide RNA sequence target

Figure 21: Design of a CRISPR/Cas9 system to target the mouse CB2 ORF

Sequence alignment of the human and mouse CNR2-ORF revealed several mismatches, which are highlighted by the dark red background colour. Red letters represent the proto-spacer adjacent motifs (PAM).

4.1.3.2.2 CRISPR/CAS plasmid cloning

Oligonucleotides, Fwd and Rev CB2 sgRNA, were simply annealed and cloned into *BbsI* digested pX330-U6-Chimeric_BB-CBh-hSpCas9 plasmid. After ligation and transformation, bacteria containing ligated clones were selected for ampicillin resistance (figure 22).

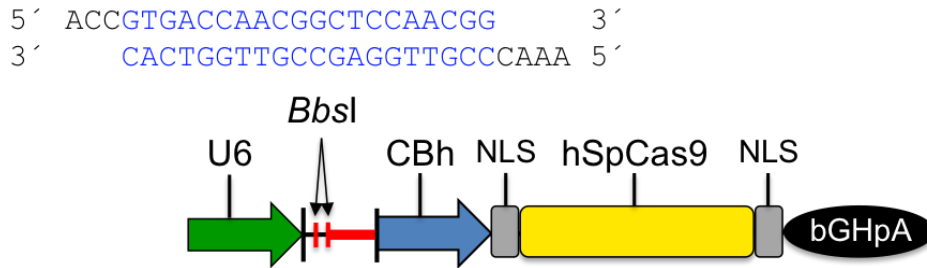


Figure 22: Cloning strategy for CRISPR/Cas9 pX330-U6-Chimeric BB-CBh-hSpCas9 plasmid.

A) The oligonucleotides containing the target sequence with 4 bp *BbsI*-compatible overhangs were cloned into the *BbsI* site of the plasmid px330 represented by the vertical red lines. The horizontal red line represents the sequence encoding the trans-activating crRNA (tracrRNA). U6: polymerase III promoter; CBh: hybrid form of the cytomegalovirus (CMV) and the chicken β -actin (CBA) promoters; NLS: nuclear localization sequence; hSpCas9: humanized *S. pyogenes* Cas9; bGHpA: bovine growth hormone polyadenylation signal.

After transformation and selection for ampicillin resistance, correct clones were identified by PCR. A forward primer, Human U6 seq F Ins, that anneals in the U6 promoter was used in combination with the reverse oligonucleotides (Rev CB2 sgRNA) used for cloning into the pX330-U6-Chimeric_BB-CBh-hSpCas9 plasmid (figure 23A). The forward primer was also used for sequencing to check the correct insertion of the oligonucleotides. A faint band of approximately 200 bp appeared for correct clones whereas no band was seen in *BbsI* digested-religated pX330-U6-Chimeric_BB-CBh-hSpCas9 plasmid (figure 23B). The plasmid obtained was verified by sequence analysis (Macrogen Corporation) and is herein after referred to as px330-mCB2.

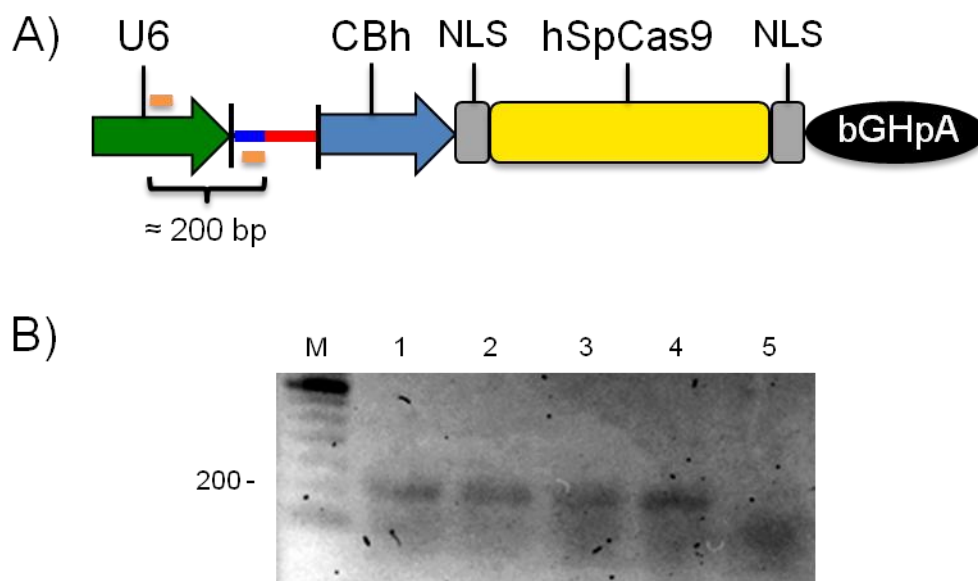


Figure 23: Verification of px330-mCB2 cloning.

A) Schematic representation of the PCR strategy used to check the oligonucleotides ligation. The small salmon lines represent the primers used for the PCR reaction. The blue line depicts the target sequence and the red line the sequence encoding the trans-activating crRNA (tracrRNA) B) 1 % agarose gel stained with ethidium bromide. M: 100 bp marker; lane 1,2,3,4: 4 positive clones ligated correctly represented by a band of approximately 200 bp; lane 5: *BbsI* digested/re-ligated pX330-U6-Chimeric_BB-CBh-hSpCas9 plasmid used as negative control.

The generated, px330-mCB2 construct expressing the two component of the CRISPR/Cas9 system, the gRNA and the Cas9 enzyme, was lipofected into NIH3T3 cells in order to test its ability to generate targeted DSBs within the *Cnr2* ORF. The surveyor assay was used to assessed this ability.

4.1.3.3 Surveyor assay

The surveyor mutation detection kit (Transgenomics, Inc) uses a mismatch-specific DNA endonuclease to detect mutation in heteroduplex DNA. In principle, a DNA mix fragments that contain two different DNA fragments differing by a single point mutation or a huge region deletion, are amplified by PCR, denaturated and then re-annealed. Then, those PCR fragments which are composed of homoduplex and heteroduplex, are submitted to the surveyor endonuclease that recognize the mismatch and produce a cleavage of the fragment. Cleavage which can be easily observed on an agarose gel stained with ethidium bromide.

In order to establish the PCR conditions which were used for every surveyor assays, and moreover to validate that the endonuclease activity would not be disturbed in the PCR mix, the control experiment provided in the kit was performed as follows: the two control plasmids DNAs called C and G, differing at a single base pair, were amplified with provided primers. Amplicons were denaturated, re-annealed and treated with the surveyor nuclease. When denaturated - re-annealed amplicons from C and G were mixed; surveyor nuclease cleaved the heteroduplex and generates two fragments of 217 and 416 bp as seen in figure 24, lane 2 whereas no cleavage was observed for C/C denaturated - re-annealed amplicons treated with Surveyor nuclease (figure 24, lane 3).

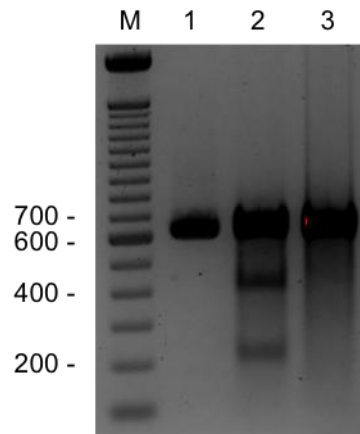


Figure 24: Surveyor control experiment

2 % agarose gel stained with ethidium bromide. M: 100 bp marker. Lane 1: C/C denatured and re-annealed amplicons not treated with the surveyor nuclease as negative control: 633 bp; Lane 2: G/C denatured and re-annealed amplicons treated with Surveyor nuclease. Heteroduplex DNA fragments were efficiently cleaved by the endonuclease at the single base pair point mutation revealing two fragments of 217 bp and 416 bp; Lane 3: C/C denatured and re-annealed amplicons treated with Surveyor nuclease: 633 bp

The control experiment confirmed that the surveyor endonuclease activity is not disturbed by the PCR mix conditions. The efficiency of the designed TALEN pair and CRISPR/Cas9 system, both targeting and inducing double-strand break within the Cnr2 ORF were tested *in vitro* in NIH3T3 cells and validated with the surveyor assay.

DSBs induced by nucleases are repaired and while the reparation process, insertions or deletions occur. This is leading to sequence heterogeneity of a mixed transfected NIH3T3 cell population. The sequence heterogeneity was detected by the surveyor nuclease. A primer pair (Fwd and Rev sgRNA Surveyor) flanking the TALEN pair target region and the px330-mCB2 target sites was selected to generate an amplicon of 688 bp (figure 25A). After denaturation and re-annealing of the amplified DNA fragments, amplicons were treated with the surveyor nuclease. As seen in figure 25A, efficient cleavage of the TALEN pair should reveal a cleavage of the 688 bp wild type fragment into two fragments of 405 bp and 283 bp. Surveyor nuclease treated DNA from NIH3T3 cells transfected with the TALEN pair constructs was not cleaved (figure 25B) supposing no activity of the TALEN pair. Interestingly, surveyor nuclease treated DNA of NIH3T3 cells transfected with the px330-mCB2 construct exhibits the expected wild type band of 688 bp and a faint band around 500 bp. In order to confirm the targeting efficiency of the designed CRISPR/Cas9 system, an additional surveyor assay was performed.

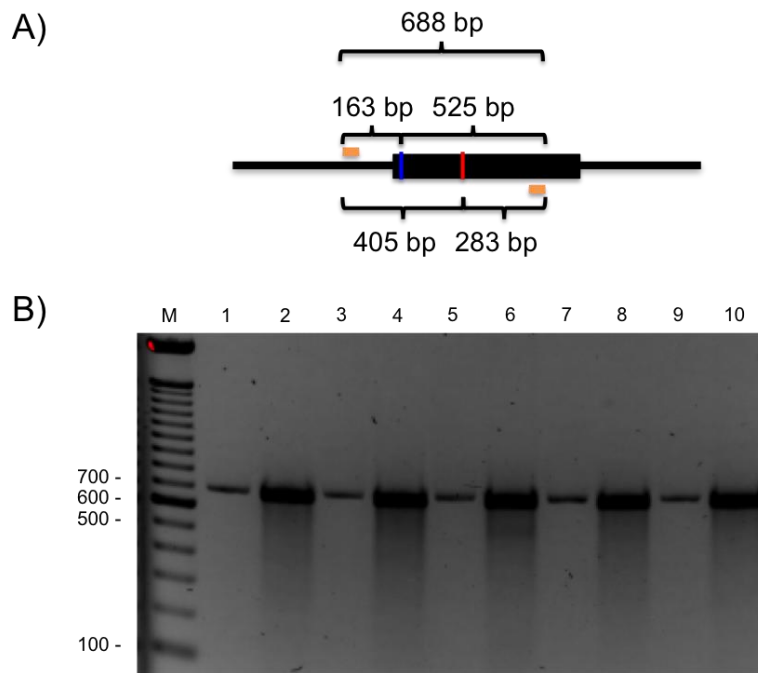


Figure 25: Surveyor assay with DNAs of NIH3T3 cells transfected with TALEN pair or px-330

A) Schematic representation of the PCR strategy used to detect double strand breaks induced by the TALENs or the CRISPR/Cas9 system within the mCB2 ORF. The blue line depicts the px330-mCB2 target sequence and the red line the TALEN pair target sequence. B) 2 % agarose gel stained with ethidium bromide. M: 100 bp marker. Lane 1,3,5,7,9,11: The specificity of the PCR was checked by loading on the gel non surveyor nuclease treated amplicons as negative control. Lane 2: TALEN pair transfected NIH3T3 cells DNA denaturated and re-annealed followed by surveyor nuclease treatment did not revealed additional band, lane 4: Mock TALEN constructs transfected NIH3T3 cells DNA denaturated re-annealed followed by surveyor nuclease treatment, lane 6: px330-mCB2 construct transfected cells DNA denaturated and re-annealed followed by surveyor nuclease treatment revealed a faint band around 500 bp, lane 8: pX330-U6-Chimeric_BB-CBh-hSpCas9 mock plasmid (without guide sequence) transfected cells DNA denaturated and re-annealed followed by surveyor nuclease treatment revealed no additional band, lane: 10: WT NIH3T3 cells DNA denaturated and re-annealed followed by surveyor nuclease treatment.

To validate the capacity of the CRISPR/Cas9 system to induce DSBs within the mCB2 ORF, another surveyor assay was performed using DNA from NIH3T3 cells transfected with the px330-mCB2 plasmid. In order to test whether the amount of genomic DNA used for the PCR could improve the resolution, two volumes (2,5 μ l and 5 μ l) of genomic DNA were used for the PCR amplification. As shown in figure 26B , fragments of 525 bp and of 688 bp were detected after surveyor assay performed with DNA of transfected NIH3T3 cells with the px330-mCB2 construct, thus indicating an efficient generation of DSBs at the target sequence. The signal from the 163 bp cleaved fragment was too faint for visualization.

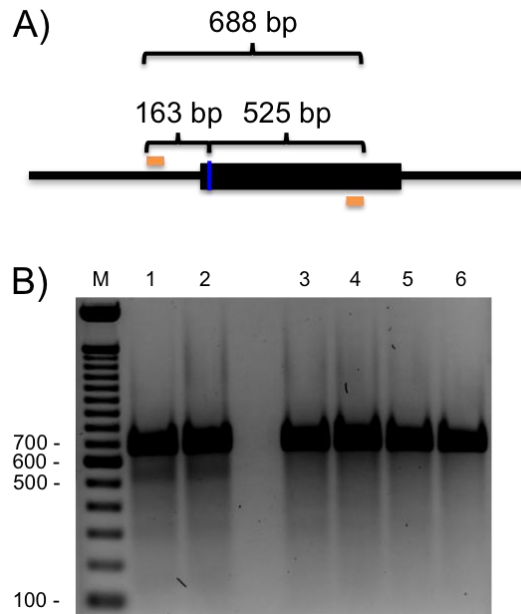


Figure 26: Surveyor assay with NIH3T3 cells transfected with px330-mCB2.

A) Schematic representation of the PCR strategy used to detect double strand breaks induced by the CRISPR/Cas9 system within the mCB2 ORF. The blue line depicts the px330-mCB2 target sequence. B) 2 % agarose gel stained with ethidium bromide. M: 100 bp marker. Lane 1 and 2: Surveyor treated DNA from NIH3T3 cells transfected with the px330-mCB2 construct revealed an additional band of approximately 525 bp. Lane 1: 2.5 μ l of genomic DNA were used for the PCR amplification; lane 2: 5 μ l of genomic DNA were used for the PCR amplification; lanes 3 and 4: 2.5 μ l and 5 μ l genomic DNA from NIH3T3 cells transfected with the pX330-U6-Chimeric_BB-CBh-hSpCas9 mock plasmid (without guide sequence); lanes 5 and 6: 2.5 μ l and 5 μ l genomic DNA from wild type NIH3T3 cells.

The obtained surveyor assay result for the CRISPR/Cas9 system was further confirmed using a functional assay based on the ability of DSBs to enhance HR, when a donor fragment is provided.

4.1.4 Efficiency comparison to humanized the Cnr2 locus

4.1.4.1 Generation of chimeric mice to produce humanized CB2 mice

Homologous recombinant ES cell clones were obtained for both targeting constructs, which were repeatedly injected into blastocysts. A total of seventeen electroporations were performed for the hCB2-Arg targeting construct and eleven for the hCB2-Gln one, using two different ES cell lines: MPI2 (129Sv) and Bruce4 (C57BL/6).

An electroporation for each targeting construct was performed in MP12 ES cells and a total of 465 clones were checked by 3' southern blot strategy. No recombined ES cell clone was detected for neither of the targeting constructs (Supplementary table 3). This ES cells line was excluded from further studies and Bruce4 ES cells were chosen.

Two different batches of Bruce4 ES cells were used for electroporations. Using a first batch of Bruce4 ES cells for electroporations, 624 clones for hCB2-Arg and 564 clones for hCB2-Gln were verified for homologous recombination (summary table 1). One positive clone for each targeting construct was identified. The hCB2-Arg93 and the hCB2-Gln59. Injection of these two positive clones into BALB/c blastocysts led to the generation of chimeric mice. The degree of chimerism was judged by (a mix of black: from C57BL/6 and white: from BALB/c) coat colour. Injection of the positive ES cell clone recombined with hCB2-Arg resulted in four chimeric males with chimerism degrees of 75 %, 75 %, 70 % and 50 %. The positive ES cell clone recombined with hCB2-Gln resulted in two males' chimeras with a chimerism degree of 70 % and 60 %. A photo of one of those chimeras is depicted figure 27A. Germ-line transmission is deduced from the coat colour of the offspring. For C57BL/6 ES cells, germ-line transmission was indicated by black fur. Although the chimeric animals for both targeting construct displayed a relatively high percentage of fur chimerism, the genetic modifications were not transmitted to its progenies.

Table 1: Summary of electroporations performed with Bruce4 ES cells

Bruce4 ES cells	
Targeting construct:	Number of ES cell clones checked:
hCB2-Arg	624
hCB2-Gln	564

In a second round of electroporations a new batch of Bruce4 ES cells was used. 408 clones for hCB2-Arg and 288 clones for hCB2-Gln were verified (summary table 2). Homologous recombined ES cell clones obtained were then injected into (C3H x BALB/c) F1 hybrid blastocysts. These blastocyst were used because (C3H x BALB/c) F1 mice produce more blastocysts than BALB/c mice and moreover, these blastocysts show a higher germ line frequency compared to pure BALB/c blastocysts (Pacholczyk et al., 2008). C3H mouse has an agouti fur colour. Since it was difficult to distinguish between black and agouti fur colour, it was not possible to determine the precise degree of chimerism by coat colour. Thus Chimeras were identified by the presence of black patches of coat (figure 27B). One ES cell clones recombined with hCB2-Arg was identified, called hCB2-Arg31R ES cell clone and injected. The R indicates that the correctly recombined ES cells clones were cultivated into RESGRO medium before being injected into blastocysts. 5 males 'chimeras were obtained. Two correctly recombined ES cell clones for the hCB2-Gln variant (hCB2-Gln7R and hCB2-Gln29R ES cell clones) resulted in two and five chimeric males respectively. However the genetic modifications were not transmitted to its progenies.

Table 2: Summary of electroporations performed in new batch of Bruce4 ES cells

New bench of Bruce4 ES cells	
Targeting construct:	Number of ES cell clones checked:
hCB2-Arg	408
hCB2-Gln	288

Altogether, a total of 26 electroporations into Bruce4 ES cells were performed with the two targeting constructs and 1884 neomycin resistant clones were isolated (supplementary summary table 2). Of those, 5 were identified as homologous recombinants, indicating a targeting frequency of 1:377, or 0.27 %

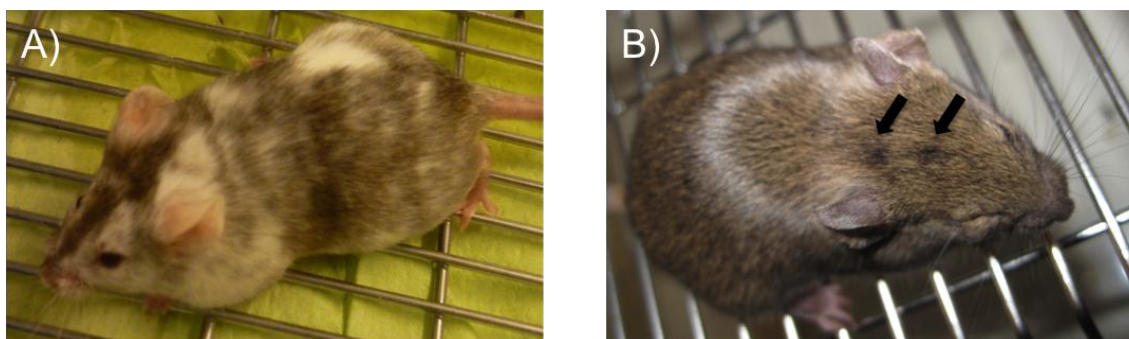


Figure 27: Chimeric animals obtained from blastocyst injection.

A) Chimeric animals obtained from injection of C57BL/6 ES cell clone (hCB2-Arg93) into BALB/c blastocysts displayed black-white mixed fur. B) Injection of C57BL/6 ES cells clone (hCB2-Gln29R) into (C3H x BALB/c) F1 blastocysts resulted in chimeras with brown fur. Chimeras were identified by the presence of black patches of coat (black arrows).

4.1.4.2 Testing the CRIPR/Cas system to enhance the humanization of the Cnr2 locus

As DSBs enhance HR, when a donor fragment is provided, two Bruce4 ES cells electroporations were performed: one with the linearized hCB2-Arg targeting construct alone and another one that also contained the px330-mCB2 construct. From each condition, 94 individual clones were harvested and analysed after G418 antibiotic selection. Figure 28A shows the two different PCR strategies, previously described, were used to confirm that the CRISPR/Cas9 system could enhance the HR frequency. The first PCR strategy was used to confirm the neo gene integration as revealed with a band of 1,9 kb. The second PCR strategy was used to amplify the ORF and was followed by a *SpeI* restriction enzyme digestion in order to confirm the bi-allelic human ORF integration. As shown in Figure 28C, PCR analysis of the neo gene integration identified no positive clones after electroporation of the hCB2Arg63 targeting construct alone, whereas 63 clones contained a targeted Cnr2 locus after co-electroporation with the px330-mCB2 construct and revealed by a specific band of 1,9 kb

(figure28D) This corresponds to a targeting frequency of 1:1.5, or 67 %. The CB2 ORF of the 63 positive identified clones for the neo gene integration were amplified by PCR and the products were digested with the *SpeI* restriction enzyme, because this restriction site is only present in the human sequence. Four of the 63 clones contain the human, but not the mouse sequence, thus indicating that both alleles were targeted. An example of DNA amplified and digested from two clones is depicted figure28B. The clone 46' DNA contains only the double bands of 605 bp and 646 bp reflecting a bi-allelic recombination of the murine CB2 ORF by the human one whereas the clone number 48 contains both, the murine and the human CB2 ORF. As explained previously, only one band of approximately 650 bp is visible due to the impossibility to separate the two bands of 605 and 646 bp using a 1 % agarose gel.

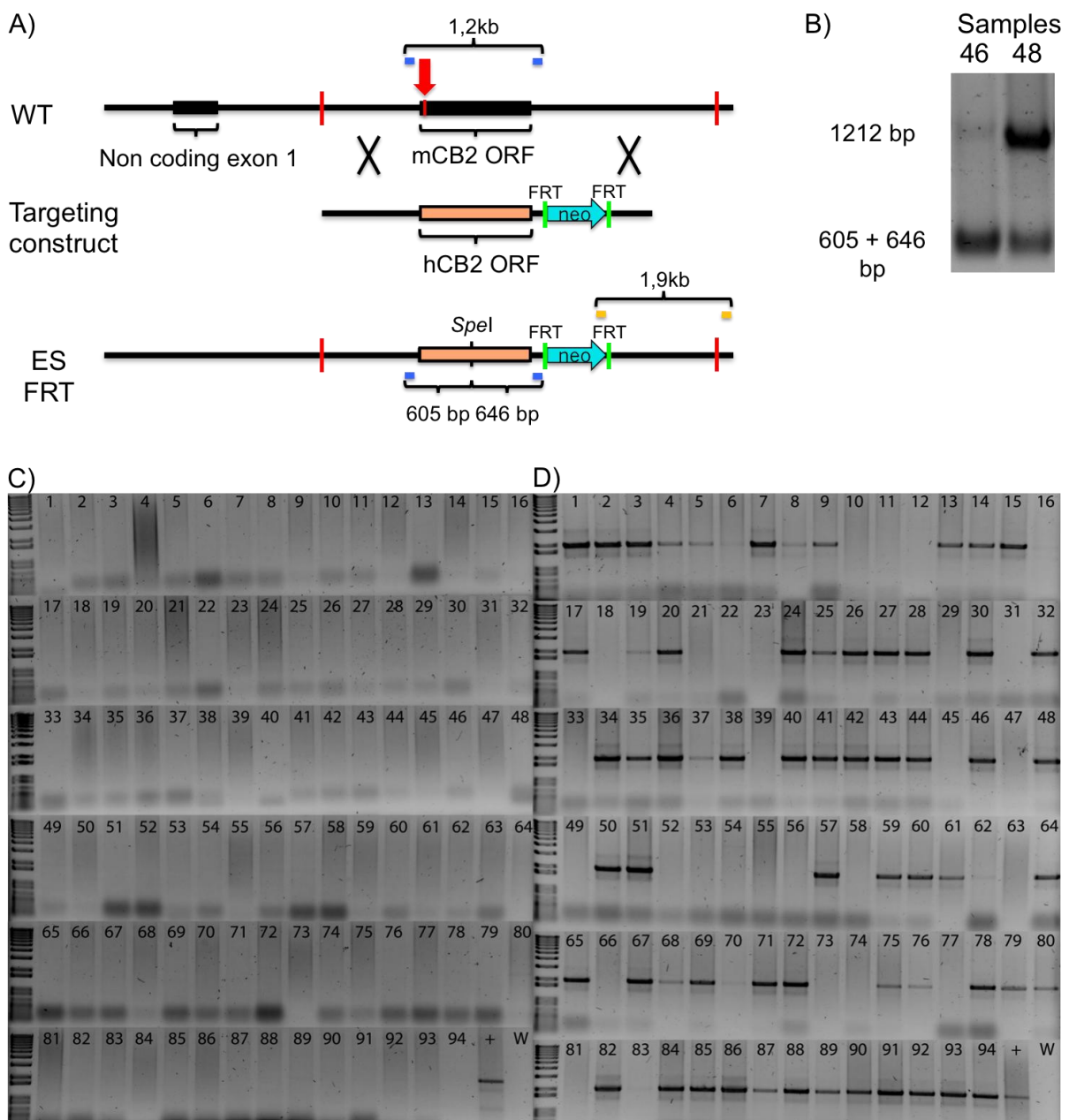


Figure 28: Detection of homologous recombination.

A) Schematic representation of the PCR strategy used to check the homologous FRT-neo-FRT integration in ES cells and bi-allelic recombination. WT represents the mouse wild type allele with a non-coding exon 1 and the open reading frame of exon 2. The small red bar and the red arrow at the beginning of the mouse CB2 open reading frame represent the guide sequence target. The targeting construct, hCB2-neo, is depicted with the human CB2 ORF in salmon colour and the neomycin/kanamycin cassette in blue flanked by FRT sites represented by green bars. Crosses indicate the regions of homologous recombination. ES FRT indicated the “humanized” allele after homologous recombination with the targeting construct. Primers used for the analysis of the bi-allelic recombination are indicated as blue lines, while the yellow line indicate primers used for the analysis of the neo integration. B) PCR amplification of the CB2 ORF followed by SpeI digestion results in a 1212 bp fragment indicative of the mouse ORF, or two similar size fragments (605 and 646 bp) indicative of the humanized ORF. Please note that sample 46 contained only the humanized ORF, suggesting a bi-allelic homologous recombination. C) Electroporation with the linearized hCB2-neo did not produce a PCR product of 1953 bp, indicative of no homologous recombination, in any of the 94 selected ES cell clones. D) After electroporation of the linearized hCB2-neo with the circular px330-mCB2 vector, numerous ES cell clones show the expected 1953 bp fragment indicating homologous recombination. + denotes a recombined ES cell clone identified previously as a positive control and W indicates a negative water control.

The CRISPR/Cas9 system designed to target the murine CB2 showed a really high efficiency to target the desired region and more importantly improved significantly homologous recombination frequency when a donor fragment was provided.

4.2 Generation of human CB2 recombinant lentiviral vectors

The functional difference existing between the human CB2 variants could be assessed *in vivo* with the generation of humanized transgenic animals but also *in vitro*, using different strategies. One strategy consists in the delivery of the human CB2 variants into CB2 deficient murine cells using lentiviruses. In order to achieve this, viral vectors expressing the human CB2 variants alone or the human CB2 variants and eGFP on one transcript were generated in order to be used for bone marrow-derived macrophages transduction. This part described the cloning of the different lentiviral vectors.

4.2.1 rrl-CMV-hCB2 vector construct generation

rrl-CMV-eGFP self inactivated vector construct provided by Dr. Katrin Zimmermann from the Institute for Pharmacology and Toxicology was first digested with *Bam*HI and *Sal*I restriction enzymes in order to exchange the eGFP ORF with the human CB2 ORF variants (figure 29A). The vector represented by the upper band of 6682 bp (figure 29B) was isolated by gel purification. The inserts consist of the two ORFs of the human variants. They were amplified by PCR using oligonucleotides named Fwd hCB2 ORF *Bam*HI and Rev hCB2 ORF *Sal*I,

containing the two restriction sites: *Bam*HI on the forward one and *Sal*I on the reverse one, as depicted in figure 29C. First, PCR amplified fragments were checked for their size of 1.1 kb on agarose gel as showed on figure 29D, followed by a digestion with *Bam*HI and *Sal*I restriction enzymes. Finally, insert and vectors were ligated and electoporated into bacteria which were selected for ampicillin resistance.

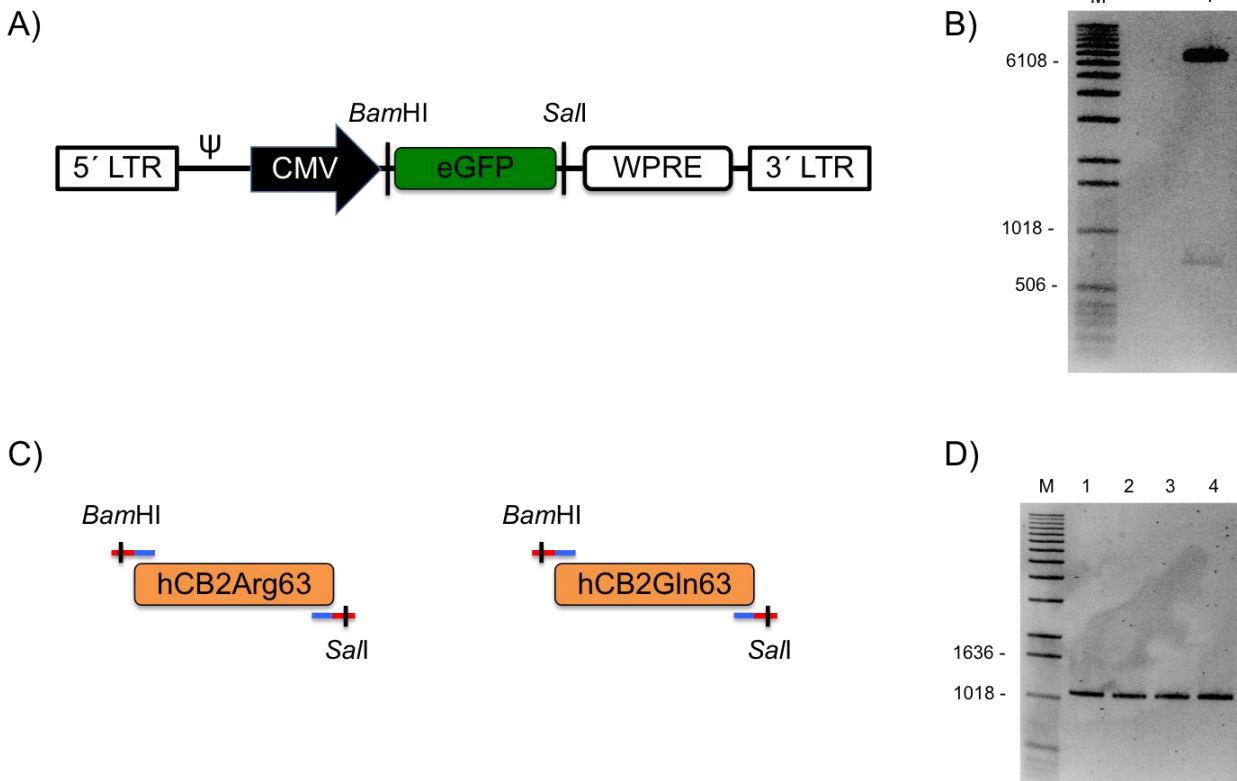


Figure 29: rrl-CMV-hCB2 vector constructs generation.

A) Schematic representation of the rrl-CMV-eGFP vector construct. B) 0.8 % agarose gel stained with ethidium bromide. M: 1 kb marker; lane 1: rrl-CMV-eGFP digested with *Bam*HI and *Sal*I; restriction pattern: two bands of 6682 bp and 748 bp. C) Schematic representation of the PCR strategy used to amplify the ORFs of the human variants. The two restriction sites sequences were added on the 5' sides of the oligonucleotides used to amplify the fragment. D) 1 % agarose gel stained with ethidium bromide. M: 1 kb marker; lane 1 and 2: human CB2-Arg63 ORF flanked by *Bam*HI and *Sal*I restriction sites; lane 3 and 4: human CB2-Gln63 ORF flanked by *Bam*HI and *Sal*I restriction sites. PCR product size: 1.1 kb. CMV: Cytomegalovirus promoter, Ψ : Viral vector packaging signal, LTR: Long terminal repeat, WPRE: Woodchuck hepatitis virus posttranscriptional regulatory element.

Ampicillin resistant clones were picked from agar plates and correctly ligated DNA was verified by digesting the plasmid DNA with *Stu*I restriction enzyme. As seen in the lower parts of figure 30A and B, one positive clone was identified for the rrl-CMV-hCB2-Arg63 and two for the rrl-CMV-hCB2-Gln63 represented by the expected patterns of two bands of 6272 bp and 1505 bp. The positive clones were verified by sequence analysis (Macrogen Corporation).

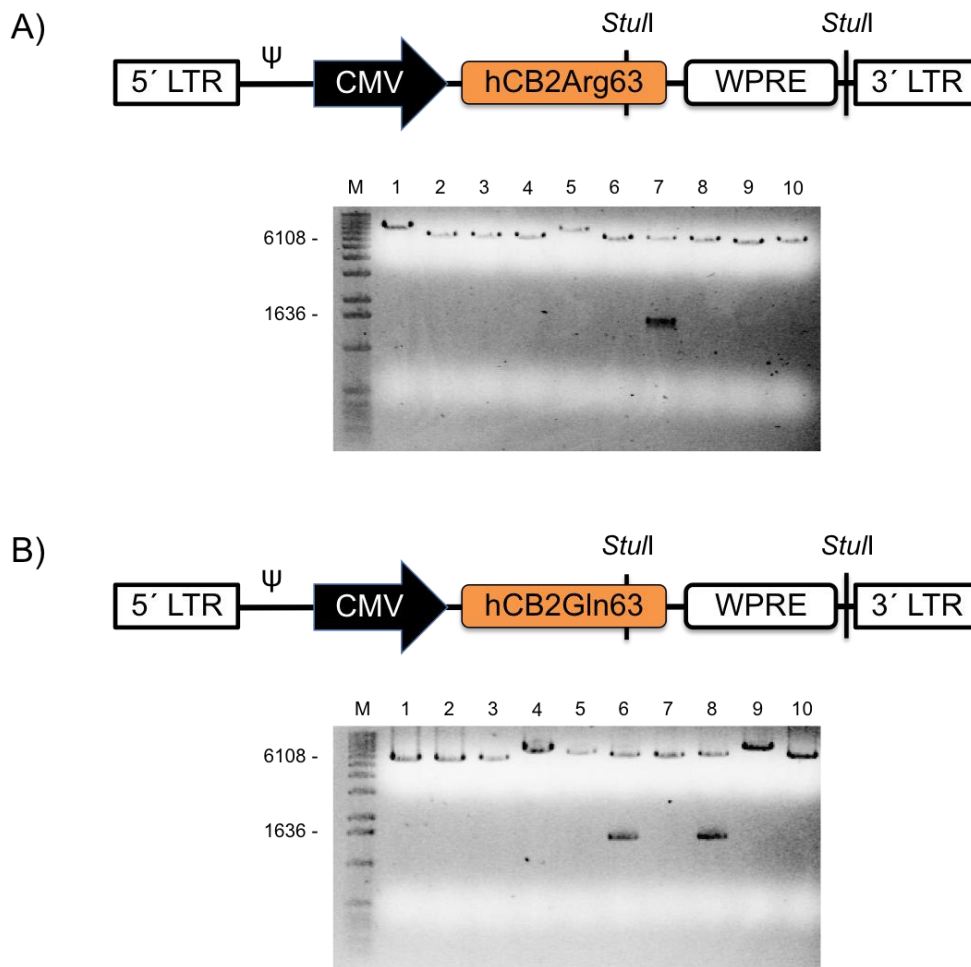


Figure 30: rrl-CMV-hCB2 vector constructs validation using *Stul* restriction analysis

A) Upper part: schematic representation of the rrl-CMV-hCB2-Arg63 vector construct and *Stul* restriction sites localisations. Lower part: 1 % agarose gel stained with ethidium bromide. M: 1 kb marker. Lane 1,2,3,4,5,6,8,9,10: re-ligated clones which do not contain the insert; restriction pattern: one single band of 6272 bp or more. Lane 7: positive ligated clone; restriction pattern: one band of 6272 bp and one of 1505 bp. B) Upper part: schematic representation of the rrl-CMV-hCB2-Gln63 vector construct and *Stul* restriction sites localisations. Lower part: 1 % agarose gel stained with ethidium bromide. M: 1 kb marker. Lane 1,2,3,4,5,7,9,10: re-ligated clones which do not contain the insert; restriction pattern: one single band of 6272 bp or more. Lane 6 and 8: positive ligated clone; restriction pattern: one band of 6272 bp and one of 1505 bp. CMV: Cytomegalovirus promoter, Ψ : Viral vector packaging signal, LTR: Long terminal repeat, WPRE: Woodchuck hepatitis virus posttranscriptional regulatory element.

4.2.2 rrl-CMV-hCB2-IRES2-eGFP vector constructs generation

Additional vector constructs were generated to express the human CB2 variants and eGFP bicistronically. To achieve this, a fragment containing the second version of an internal ribosome entry site (IRES2) coupled to an enhanced green fluorescent protein (eGFP) ORF was cloned into the previously generated rrl-CMV-hCB2 vector constructs. The IRES2 is the a nucleotide sequence that allows the translation of the two proteins, hCB2 and eGFP, within one mRNA transcript. The vector constructs rrl-CMV-hCB2 were linearized with *Sall* restriction

enzymes and used as vector (figure 31A). The insert sequence consisting of the IRES2 followed by the eGFP ORF was amplified by PCR using oligonucleotides named Fwd and Rev IRES2-eGFP *SalI*, containing the restriction sites: *SalI* on the forward and reverse one, as depicted in figure 31B. PCR fragment size of 1334 bp was verified on an agarose gel (figure 31C) and purified after gel extraction. The IRES2 nucleotide sequence is a GC rich sequence leading to unpredictable secondary structures during the PCR procedure. The gel purification of the fragment was necessary due to the unspecific additional band appearing below the 500 bp. *SalI* digested vector and inserts were ligated and electroporated into bacteria followed by ampicillin selection.

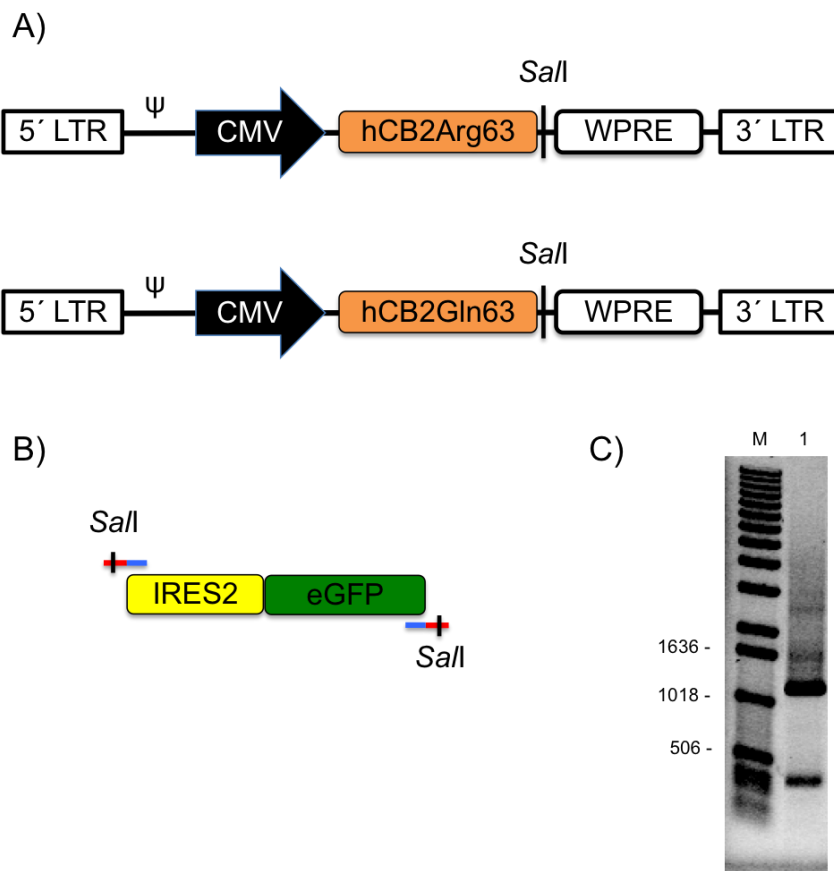


Figure 31: rrl-CMV-hCB2-IRES2-eGFP vector constructs generation

A) Schematic representation of the rrl-CMV-hCB2 vector constructs and *SalI* restriction site localisation. B) Schematic representation of the PCR strategy used to amplify the IRES2-eGFP fragment. The two *SalI* restriction sites sequences were added at the 5' sides of the oligonucleotides used to amplify the fragment. C) 1 % agarose gel stained with ethidium bromide. M: 1 kb marker; lane 1: the band of 1334 represent the IRES2-eGFP PCR fragment flanked by *SalI* restriction sites and the band of less than 500 bp represent an unspecific amplified fragment. CMV: Cytomegalovirus promoter, Ψ : Viral vector packaging signal, LTR: Long terminal repeat, WPRE: Woodchuck hepatitis virus posttranscriptional regulatory element, IRES2: Internal ribosome entry site version 2, eGFP: Enhanced green fluorescent protein.

Ampicillin resistant clones were picked from agar plates and ligation was verified by digesting the plasmid DNA contained into ampicillin resistant bacteria with *StuI* restriction enzyme. As seen in the lower parts of figure 32A and B, eight positive clones were identified for the rrl-CMV-hCB2-Arg63-IRES2-eGFP and six for the rrl-CMV-hCB2-Gln63-IRES2-eGFP represented by the expected patterns of two bands of 6272 bp and 2813 bp.. The sequence of the inserts in positive clones was verified by sequence analysis (Macrogen Corporation).

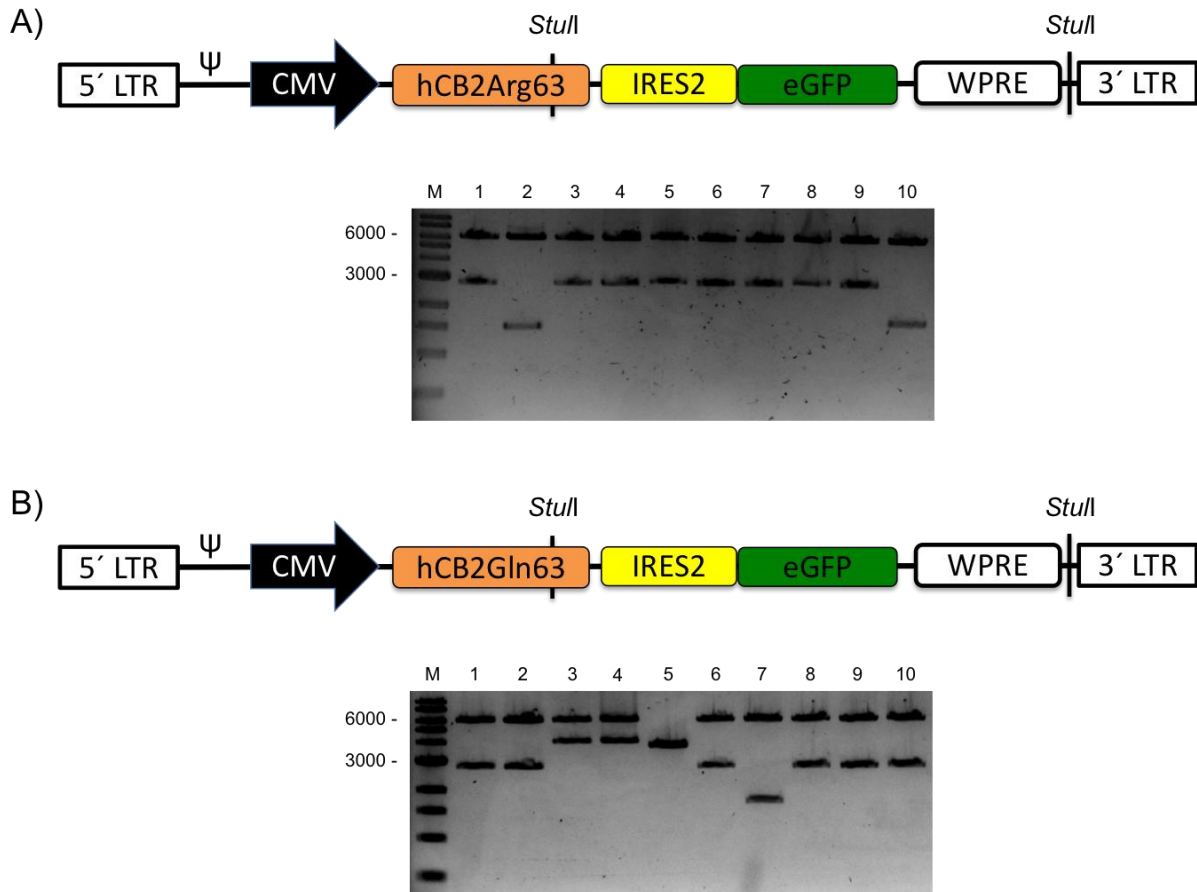


Figure 32: rrl-CMV-hCB2-IRES2-eGFP vector constructs validation using *StuI* restriction analysis

A) Upper part: schematic representation of the rrl-CMV-hCB2-Arg63-IRES2-eGFP lentiviral vector and localisation of *StuI* restriction sites. Lower part: 1 % agarose gel stained with ethidium bromide. M: 1 kb marker. Lane 1,3,4,5,6,7,8,9: ligated clones identified with a restriction pattern of one band of 6272 bp and one of 2813 bp. Lane 2,10: clones which contain the insert in the wrong orientation. B) Upper part: schematic representation of the rrl-CMV-hCB2-Gln63-IRES2-eGFP lentiviral vector and localisation of *StuI* restriction sites. Lower part: 1 % agarose gel stained with ethidium bromide. M: 1 kb marker. Lane 1,2,6,8,9,10: ligated clones identified with a restriction pattern of one band of 6272 bp and one of 2813 bp. Lane 3,4,5,7: clones which contain the insert in the wrong orientation or more than one insert. CMV: Cytomegalovirus promoter, Ψ : Viral vector packaging signal, LTR: Long terminal repeat, WPRE: Woodchuck hepatitis virus posttranscriptional regulatory element, IRES2: Internal ribosome entry site version 2, eGFP: Enhanced green fluorescent protein.

Vector construct DNA from each construct was provided to the Institute for Pharmacology and Toxicology where recombinant lentiviral vectors were produced and further used for the transduction of bone marrow derived macrophages.

4.2.3 Mouse bone marrow-derived macrophages expressing the human CB2 receptors variants

The transduction efficiency of cells with lentiviral particles is commonly assessed by fluorescence-activated cell sorting (FACS), using a fluorescent reporter gene as for example eGFP or a specific antibody directly linked or not to a fluorochrome and directed against the protein of interest. The first lentiviral vectors that were generated with the human CB2 variants alone did not contain any reporter gene. For this purpose, different CB2 antibodies were tested for their specificity using BMMs from CB2 knockout mice. At the end of this part, recombinant viral vectors expressing both CB2 and eGFP were used to assess the transduction efficiency of the recombinant lentiviral vectors in BMMs without sorting the use of antibodies.

4.2.3.1 Specificity control of CB2 polyclonal N-Terminal antibody

The specificity of the CB2 polyclonal N-Terminal antibody (1-32 amino acids, Abcam 3561) was analyzed by flow cytometry using wild type and CB2 knockout BMMs. First auto fluorescence of BMMs was controlled by sorting the cells without submitting them to any antibody staining (unstained control). As seen in the figure.33, in the two dot plot of the first row, the cells are depicted in the bottom left quadrant which indicates less auto fluorescence of BMMs. Then BMMs were stained with an antibody coupled to an eFluor® 450 fluorochrome and directed against CD11b, and with the primary N-terminal CB2 antibody revealed by an Alexa Fluor® 488 secondary antibody. CD11b or cluster of differentiation molecule 11b (integrin α_M) forms with the cluster of differentiation molecule 18 (CD18 or integrin β_2) the macrophage-1 antigen (or integrin $\alpha_M \beta_2$). CD11b is expressed on the surface of many leukocytes including monocytes, neutrophils, natural killer cells, granulocytes and macrophages. The CD11b marker is commonly used to assess macrophage colony stimulating factor (M-CSF) induced differentiation of hematopoietic stem cells contained in bone marrow into macrophages using FACS. As depicted in the middle column of figure 33, the representation of BMMs stained with CD11b antibody and N-terminal CB2 antibody revealed with a secondary antibody was exactly the same in wild type BMMs and CB2 knockout BMMs indicating unspecificity of the tested CB2 antibody. The cells are depicted in the upper right quadrant of the dot plot with the equivalent distribution of 75-77%. To verify that the unspecificity observed for the CB2 antibody was not due to unspecificity of the secondary antibody, BMMs from wild type and CB2 knockout animals were labelled only with the CD11b antibody and the secondary antibody (secondary antibody control). As depicted in

the last row of figure 33, only approximately 1 % of the cells were not specifically labelled by the secondary antibody confirming that the N-terminal CB2 receptor antibody tested was not specific.

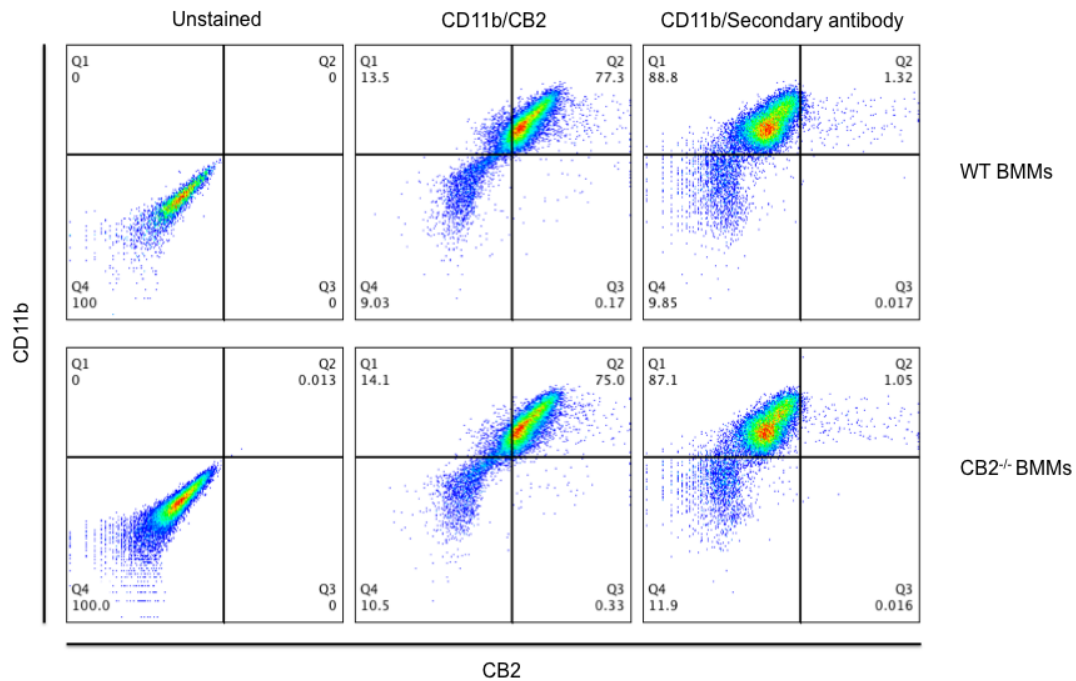


Figure 33: Specificity control of the CB2 receptor polyclonal antibody (1-32 amino acids, N-terminus) in BMMs

Representative flow cytometry dot plots of CD11b vs. CB2 expression in WT and CB2^{-/-} BMMs. First row: unstained BMMs. Second row: BMMs stained with CD11b eFluor® 450, CB2 N-terminal antibody and secondary Alexa Fluor® 488 secondary antibody. Third row: BMMs stained with CD11b eFluor® 450 and Alexa Fluor® 488 secondary antibody. CD11b: cluster of differentiation molecule 11b, WT: wild type, CB2^{-/-}: CB2 knockout animal, BMMs: bone marrow-derived macrophages.

As the first N-terminal antibody tested was not specific for the CB2 receptor in FACS experiment, another CB2 polyclonal N-terminal antibody (1-33 amino acids, Thermo Scientific PA1-744), reported to be specific for the human CB2 receptor, was tested for its specificity in FACS. The first and last rows of figure 34 depict unstained and secondary antibody controls, respectively. In this experiment, the secondary antibody shows a non-specific binding in approximately 30 % of the cells as depicted in the last row of the figure 34. This particular N-terminal CB2 antibody was never tested in FACS experiment, that is why different dilutions of 1/10, 1/25 and 1/50 of the antibody were tested. Despite the non-specificity of the secondary antibody and the different dilutions tested for the CB2 polyclonal N-Terminal antibody, BMMs from wild type and CB2 knockout animals exhibit the same pattern in the different dot blots. Approximately 90 % of the cells were positive for CD11b and CB2 in wild type and in CB2

knockout BMMs indicating that the antibody is not specific for the human CB2 receptor in a relative pure macrophages population.

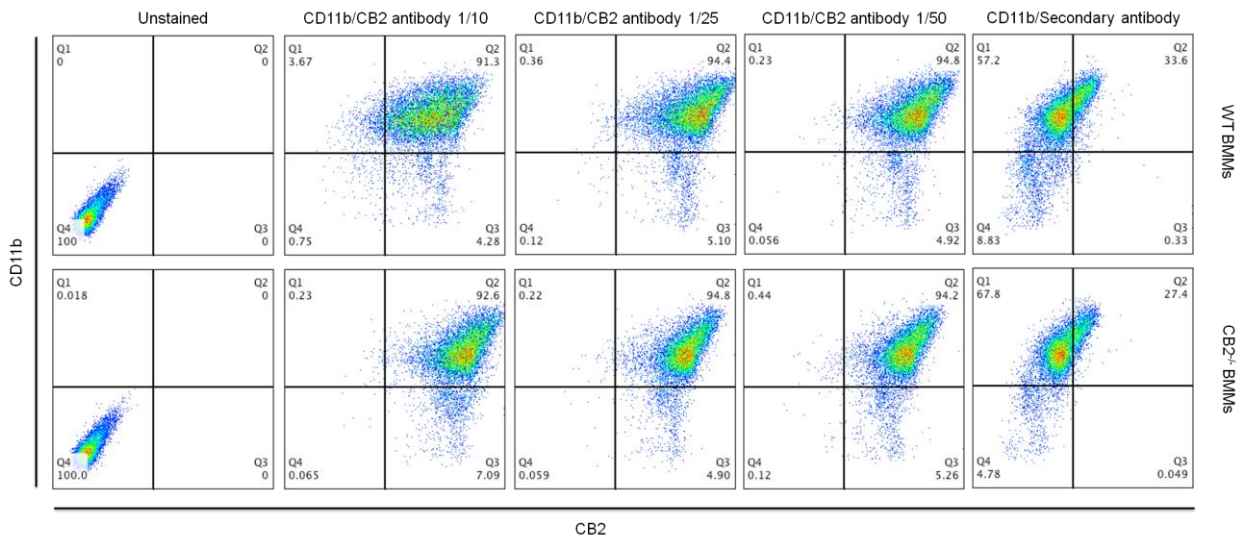


Figure 34: Specificity control of cannabinoid the CB2 receptor antibody (1-33 amino acids, N-terminus) in BMMs

Representative flow cytometry dot plots of CD11b vs. CB2 expression in WT and CB2^{-/-} BMMs. First row: unstained BMMs. Second, third and fourth rows: BMMs stained with CD11b eFluor® 450, different dilutions of the CB2 N-terminal antibody (1/10, 1/25 and 1/50) and the secondary Alexa Fluor® 488 antibody. Fifth row: BMMs stained with the CD11b eFluor® 450 antibody and the Alexa Fluor® 488 secondary antibody. CD11b: cluster of differentiation molecule 11b, WT: wild type, CB2^{-/-}: CB2 knockout animal, BMMs: bone marrow-derived macrophages.

Both CB2 polyclonal N-terminal antibodies previously tested showed no specificity for the CB2 receptor protein by FACS. Finally a C-terminal antibody was tested for its specificity toward the CB2 receptor protein.

4.2.3.2 Specificity control of CB2 polyclonal C-Terminal antibody

A last polyclonal antibody directed against the C-terminal part of the mouse CB2 receptor protein was tested for its specificity (200-300 amino acids, Abcam 45942). To allow access of the antibody to the intracellular C-terminus of the CB2 protein, cells were fixed and permeabilized in an additional step, leading to an important cell loss as observed in the different dot plots of figure 35 compared with the dot plots of figure 33 or 34. The secondary antibody control depicted in the last row did not show unspecific binding as less than 3 % of the cells were labelled (last row of the figure 35). As depicted in the middle row, BMMs from wild type and CB2 knockout animals were labelled for the CB2 and CD11b in the same proportion of approximately 90 % indicating a relatively pure macrophages population but no specificity for the C-terminal antibody tested by FACS.

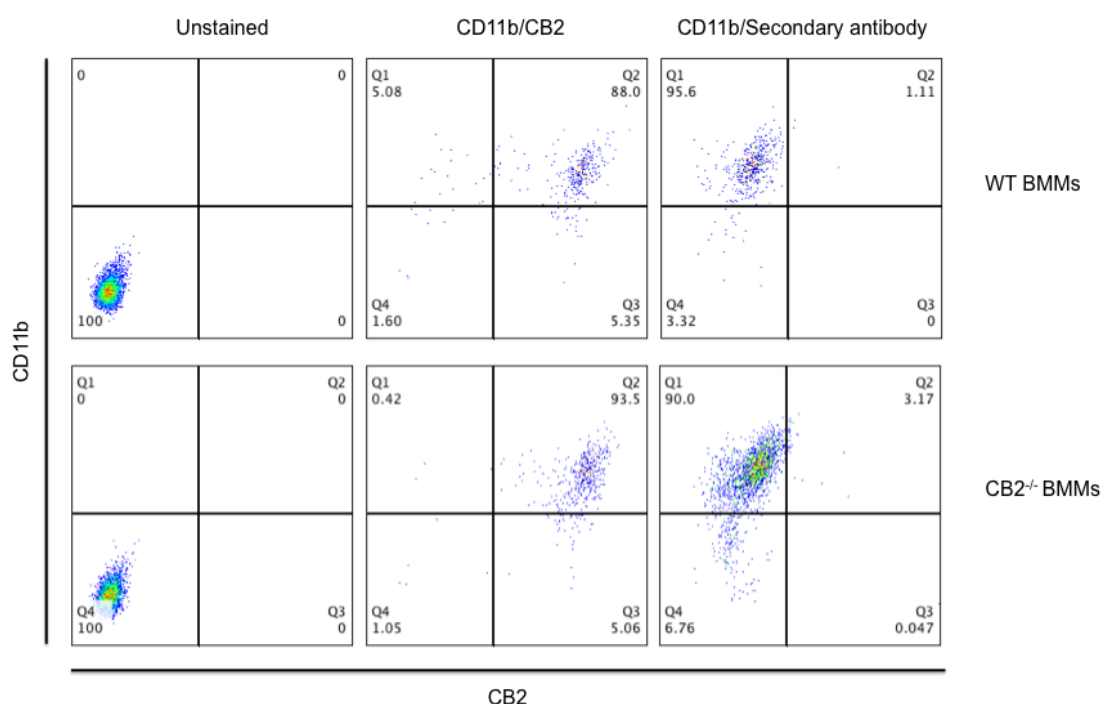


Figure 35: Specificity control of the CB2 receptor antibody (200-300 amino acids, C-terminus) in BMMs

Representative flow cytometry dot plot of CD11b vs. CB2 expression in WT and CB2^{-/-} BMMs. First row: unstained BMMs. Second row: BMMs stained with CD11b eFluor® 450, CB2 N-terminal antibody and secondary Alexa Fluor® 488 secondary antibody. Third row: BMMs stained with CD11b eFluor® 450 and Alexa Fluor® 488 secondary antibody. CD11b: Cluster of differentiation molecule 11B, WT: wild type, CB2^{-/-}: CB2 knockout animal, BMMs: bone marrow-derived macrophages.

Unfortunately CB2 polyclonal N-terminal and C-terminal antibodies tested showed non-specific binding in CB2 knockout BMMs measured by FACS. The fact that no real specific CB2 antibody exists was published two years later after the experiment was performed and confirmed the negative results obtained by flow cytometry (Baek et al., 2013).

4.2.3.3 Measurement of transduction efficiency independent of CB2 antibody use

Due to the lack of specificity of all CB2 antibody tested, recombinant lentiviral vectors containing human CB2 variants coupled to an IRES2 and eGFP were used. This allowed to circumvent the use of CB2 antibody and allowed the physical titer measurement of the transduction efficiency of BMMs by the recombinant lentiviral vectors using FACS. First, recombinant lentiviral vectors generated from rrl-CMV-eGFP vector construct was used to control the transduction efficiency of BMMs from CB2 knockout mice. To calculate the physical titer, numbers from data between 1-10 % infection rates were used (second row of the figure 36). Physical titer for BMMs transduced with recombinant lentiviral vector generated from the rrl-CMV-eGFP vector construct was calculated using the formula: ((# cells at starting

time)*(percent infection)) / vol virus solution added expressed in ml , $(100000*0,055)/0.0001= 5.5*10^7$ TU/ml.

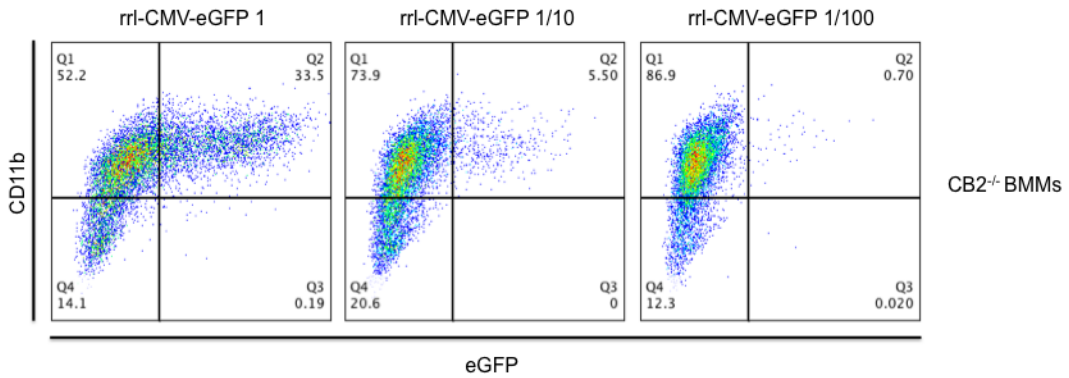


Figure 36: Figure : eGFP lentiviral vector infection rate in CB2^{-/-} transduced BMMs

Representative flow cytometry dot plot of CD11b vs. eGFP expression in CB2^{-/-} BMMs transduced with rrl-CMV-eGFP. CD11b: Cluster of differentiation molecule 11B, WT: wild type, CB2^{-/-}: CB2 knockout animal, BMMs: bone marrow-derived macrophages.

Physical titers were determined for BMMs from CB2 knockout animals transduced with recombinant lentiviral vectors generated from rrl-CMV-hCB2-Arg-IRES2-eGFP and rrl-CMV-hCB2-Gln-IRES2-eGFP vectors constructs using the same formula. Infection rate between 1 and 10 % were observed for BMMs transduced with 10 μl lentiviral vectors (first row figure 37) giving a titer of:

- rrl-CMV-hCB2-Arg-IRES2-eGFP titer: $(100000*0.043)/0.01= 4.3*10^5$ TU/ml.
- rrl-CMV-hCB2-Gln-IRES2-eGFP titer: $(100000*0.0145)/0.01=1.45*10^5$ TU/ml.

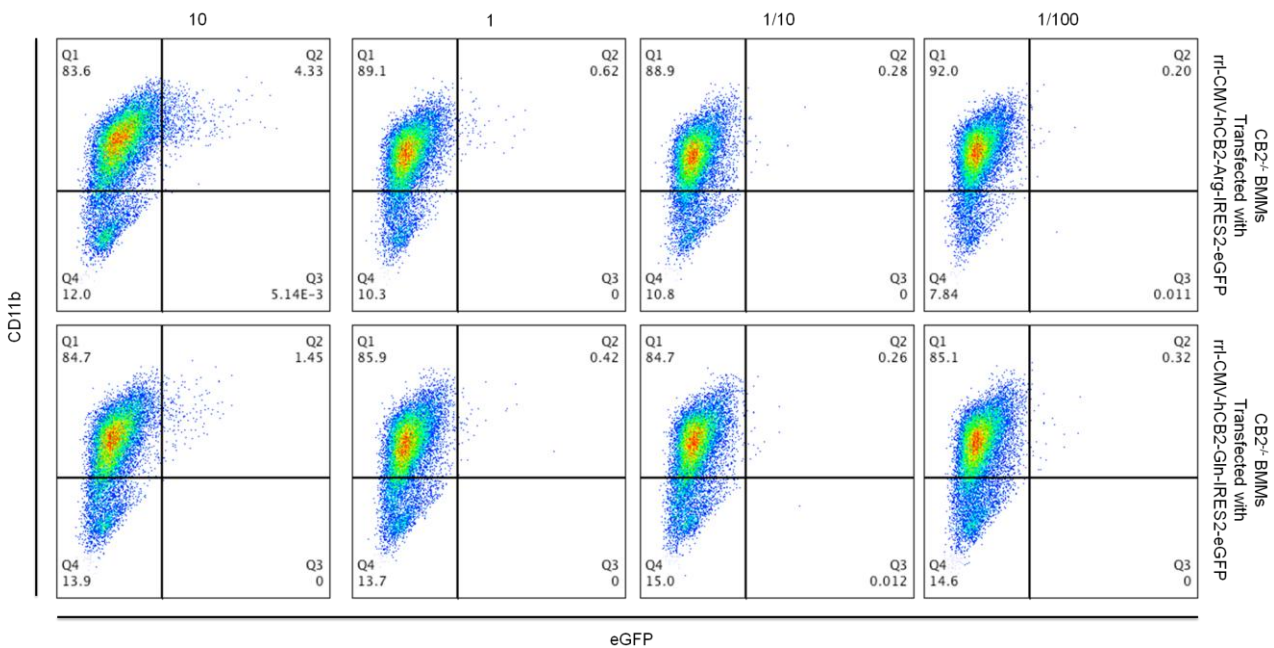


Figure 37: Human CB2-IRES2-eGFP lentiviral vectors infection rates in CB2^{-/-} transduced BMMs

Representative flow cytometry dot plot of CD11b vs. eGFP expression in CB2^{-/-} BMMs transduced with rrl-CMV-hCB2-Arg-IRES2-eGFP and rrl-CMV-hCB2-Gln-IRES2-eGFP. CD11b: Cluster of differentiation molecule 11B, WT: wild type, CB2^{-/-}: CB2 knockout animal, BMMs: bone marrow-derived macrophages.

The titers measured for BMMs transduced with recombinant lentiviral vectors generated from the vector constructs rrl-CMV-hCB2-Arg63-IRES2-eGFP and rrl-CMV-hCB2-Gln63-IRES2-eGFP were 1000 times lower than the titer measured from BMMs transduced with recombinant lentiviral vector generated from rrl-CMV-eGFP vector construct.

4.3 Functional analysis of CB2 receptor activation in mouse bone marrow derived-macrophages

This result part is divided into two parts. BMMs were characterized for their two main properties, which are the ability to be driven into different activation states in response to pro- or anti-inflammatory substances in a first part and the ability to engulf zymosan particles by phagocytosis in second part.

4.3.1 Activation state analysis of mouse bone marrow-derived-macrophages

4.3.1.1 Markers expression analysis

To ensure that BMMs undergo M1 or M2 activation states, they were stimulated with different concentrations of IFN γ (5, 10 and 20 ng/ml), LPS/IFN γ (10/5, 50/10, 100/20 ng/ml) and IL-4 (10, 50 and 100 ng/ml). Three markers: CD86, the major histocompatibility complex class II molecule (MHCII) and MMR expression, respectively were analysed by flow cytometry. CD86 expression was found to be upregulated after stimulation with IFN γ and even greater with a combination of LPS/ IFN γ , whereas IL-4 showed no effect on CD86 expression (figure 38, left graphic). The expression of major histocompatibility complex (MHC) class II molecules by BMMs was upregulated by interferon IFN γ . LPS in combination with IFN γ showed a lower upregulation of MHC class II expression induced by IFN γ . And IL-4 stimulation had no effect on MHCII expression (figure 38, middle graphic). When BMMs were overnight stimulated with IL-4, MMR was upregulated whereas stimulation with IFN γ or LPS/IFN γ at the highest concentrations showed a slight downregulation (figure 38, right graphic).

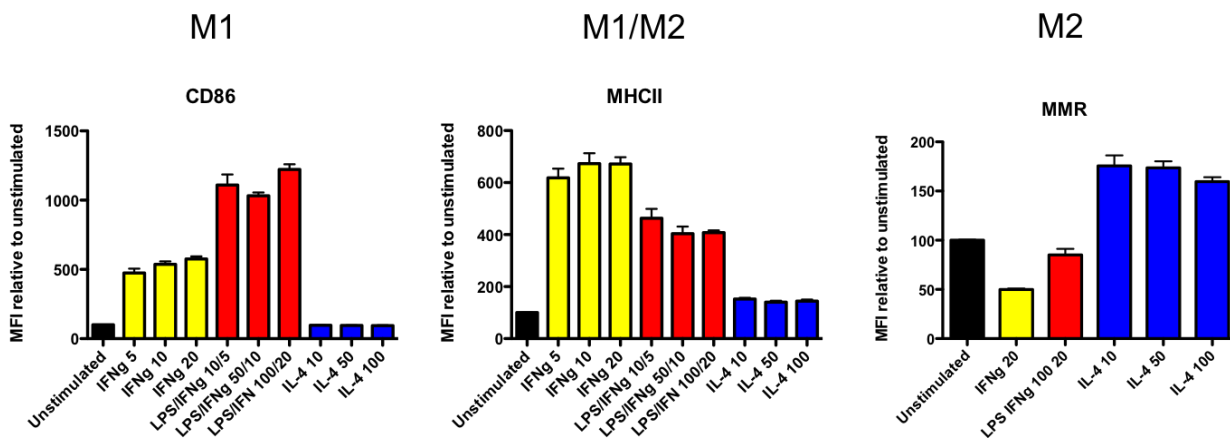


Figure 38: Cell surface marker molecules associated with activation of BMMs tested by flow cytometry.

CD86, MHCII, and MMR mean fluorescence intensity (MFI) relative to unstimulated controls. CD86: cluster of Differentiation 86 detected with PE labelled antibody, MHCII: major histocompatibility complex class II molecules detected with APC labelled antibody, MMR: mannose receptor detected with a biotin preliminary antibody revealed by a PerCP-Cy5.5 labelled secondary antibody. IFN γ : Interferon-gamma (IFN γ), LPS: lipopolysaccharide, IL-4: Interleukin 4, MFI: mean fluorescent intensity. Concentration are expressed in ng/ml.

BMMs underwent into M1 phenotypes after IFN γ or combination of LPS/IFN γ overnight stimulation or in M2 phenotype after IL-4 overnight stimulation. The M1 phenotypes was clearly observable by the upregulation of CD86 and MHCII markers expression whereas the effect of IL-4 stimulation on MMR expression was a moderate effect observed by the slight upregulation.

4.3.1.2 Effect of CB2 agonists on pro-inflammatory cytokine release

Cannabinoid receptor 2 specific agonists such as beta-caryophyllene (BCP) and the compound JWH-133 were tested for their abilities to modulate the pro-inflammatory cytokine TNF α release by BMMs polarized into M1 state. BMMs were stimulated overnight with LPS/IFN γ and different CB2 specific agonists and the pro-inflammatory cytokine TNF α released was measured by ELISA. High TNF α amounts were released upon LPS/IFN γ and LPS/IFN γ tocrisolve as observed in figure 39. Tocrisolve (1:4 ratio of soya oil/water) was the vehicle used to solubilise the two CB2 specific agonists.

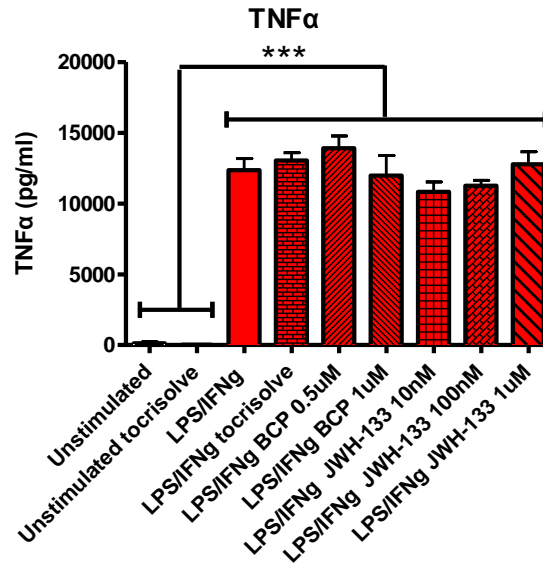


Figure 39: Effect of CB2 agonist on TNF α pro-inflammatory cytokine release by a LPS/IFN γ overnight stimulated BMMs

Measurement of TNF α release in the supernatant by Elisa. IFN γ : Interferon-gamma (IFN γ), LPS: lipopolysaccharide, BCP: Beta-Caryophyllene. Statistical analysis: one-way ANOVA followed by post-hoc Bonferroni test: $F_{8,9}=52.00$; $p<0.001$.

CB2 specific agonists, BCP and JWH-133, had no statistical effect on the pro-inflammatory cytokine TNF α release.

4.3.1.3 Cannabinoid receptors real time expression

M1 polarizing stimulus effects on cannabinoid receptor 1, cannabinoid receptor 2 and GRP18 receptor expressions were analysed by real time PCR using TaqMan assays. As depicted in the left part of the figure 40, the CB1 receptor expression was downregulated upon IFN γ , LPS and combination of LPS/IFN γ stimulations. CB2 receptor expression was slightly downregulated when BMMs were stimulated with IFN γ . This effect was more pronounced when LPS/IFN γ and LPS were used (middle part of figure 40). In contrast to CB1 and CB2, GPR18 was slightly upregulated when BMMs were stimulated with IFN γ and more than 10 times upregulated when LPS/IFN γ and LPS were used (right part of figure 40).

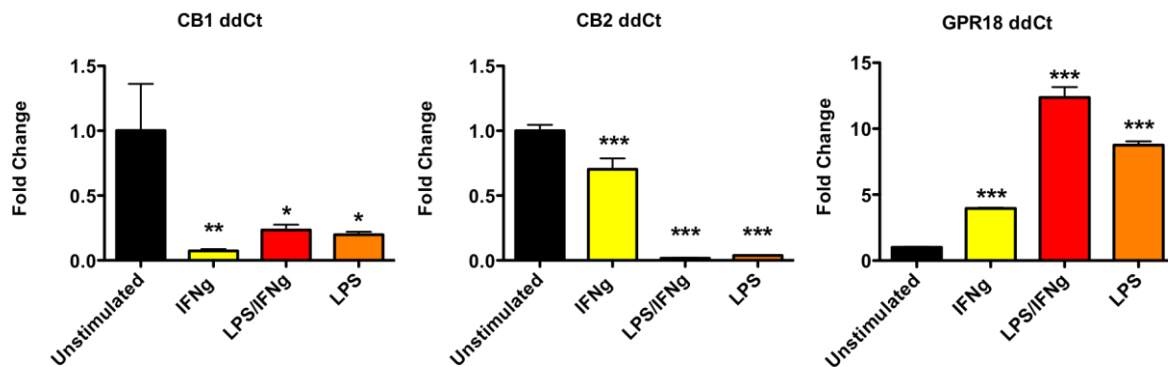


Figure 40: Quantitative cannabinoid receptor expression analysis by real-time PCR (RT-PCR).

Stimulated BMMS were tested for altered gene expression of CB1, CB2, and GPR18, Statistical analysis: one-way ANOVA followed by post-hoc Bonferroni test. CB1: $F_{3,32}=5.188$; $p<0.01$. CB2: $F_{3,32}=107.8$; $p<0.001$. GPR18: $F_{3,32}=145.4$; $p<0.001$. Values represent mean \pm SEM, * $p < 0.05$ vs. unstimulated control, ** $p < 0.01$ vs. unstimulated control, *** $p < 0.001$ vs. unstimulated control. ddCt: delta-delta-Ct, IFN: Interferon gamma (IFN γ), LPS: lipopolysaccharide.

BMMS stimulated with IFN γ , combination of LPS/IFN γ or LPS undergone into M1 phenotype (pro-inflammatory) show a change in cannabinoid receptors expressions. The CB1 and CB2 receptors are downregulated whereas GPR18 is upregulated in M1 macrophages.

4.3.2 Analysis of zymosan phagocytosis by BMMS

As an antigen-presenting cell, macrophage has the ability to phagocyte (Wang et al., 2013a; Weischenfeldt and Porse, 2008). The effect of cannabinoid receptor 2 agonists on phagocytosis of fluorescein isothiocyanate (FITC)-labelled zymosan by BMMS was measured by FACS and by fluorescence microscopy.

4.3.2.1 Zymosan phagocytosis by BMMS upon CB2 agonists stimulation measured by FACS

The effect of cannabinoid receptor 2 agonists was tested on BMMS phagocytosis of zymosan particles at three time points of incubation (30, 60 and 90 minutes). Tocrisolve was used to solubilize JWH-133 and BCP and showed no effect on zymosan phagocytosis in all the assays performed. Two selective CB2 agonists were tested: beta-caryophyllene (BCP) and JWH-133. Giving JWH-133 and zymosan particles at the same time (figure 41A) or JWH-133 one hour before zymosan particles (figure 41B) had no statistical treatment effect on phagocytosis after 30, 60 or 90 minutes of incubation but a statistical time effect was observed.

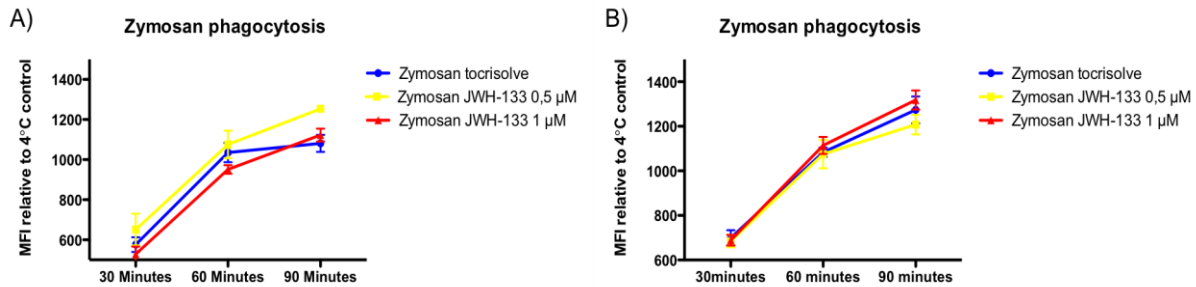


Figure 41: Flow cytometry measurement of JWH-133 effects on zymosan particles phagocytosis by BMMs.

A) Zymosan particles and agonist were given at the same time. B) Agonist was given one hour before providing the zymosan particles. Fluorescein isothiocyanate (FITC)-labelled zymosan particles were used. MFI: mean fluorescence intensity. Statistical analysis: Two-way ANOVA followed by post-hoc Bonferroni test. A) Treatment $F_{2,12}=4.427$; $p>0.05$, Treatment x time $F_{4,12}=0.8184$; $p>0.05$, Time $F_{2,12}=145.9$; $p<0.001$. B) Treatment $F_{2,12}=1.312$; $p>0.05$, Treatment x time $F_{4,12}=0.4167$; $p>0.05$, Time $F_{2,12}=138.3$; $p<0.001$.

Giving BCP and zymosan particles at the same time (figure 42A) or BCP one hour before zymosan particles (figure 42B) showed also no statistical treatment effect on phagocytosis after 30, 60 or 90 minutes of incubation but a statistical time effect was observed.

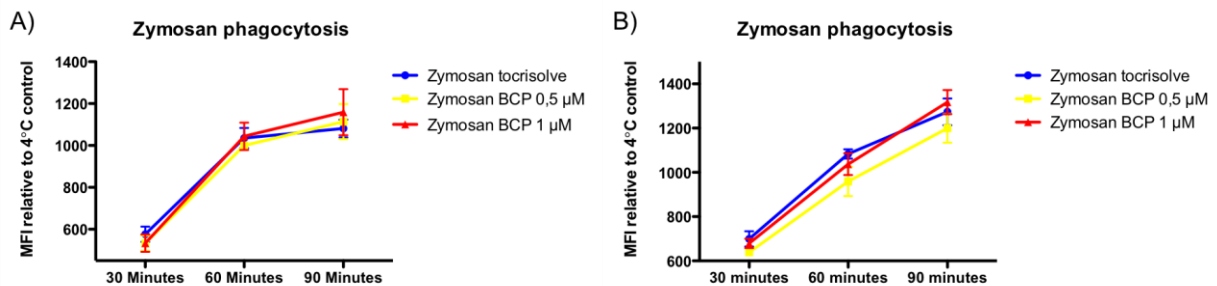


Figure 42: Flow cytometry measurement of beta-caryophyllene effects on zymosan particles phagocytosis by BMMs.

Fluorescein isothiocyanate (FITC)-labelled zymosan particles were used. BCP: beta-caryophyllene, MFI: mean fluorescence intensity. Statistical analysis: Two-way ANOVA followed by post-hoc Bonferroni test. A) Treatment $F_{2,12}=0.2678$; $p>0.05$, Treatment x time $F_{4,12}=0.2452$; $p>0.05$, Time $F_{2,12}=68.52$; $p<0.001$. B) Treatment $F_{2,12}=4.091$; $p>0.05$, Treatment x time $F_{4,12}=0.3184$; $p>0.05$, Time $F_{2,12}=106.6$; $p<0.001$.

As specific CB2 agonists had no effect on zymosan phagocytosis, the endocannabinoid 2-AG, ligand for the cannabinoid receptors (CB1 and CB2) was diluted in 100 % ethanol (vehicle) and tested for its effect on zymosan phagocytosis by BMMs. The vehicle showed no effect on phagocytosis in all the assays performed. 2-AG had no statistical

effect on phagocytosis of zymosan particles by BMMs figure 43 and didn't show any statistical treatment effect after 60 and 90 minutes incubation. A statistical time effect was observed

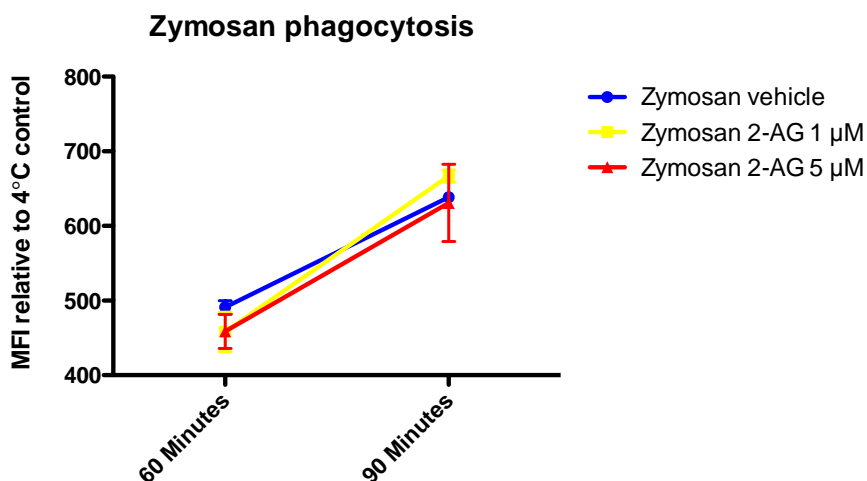


Figure 43: Flow cytometry measurement of 2-arachidonylglycerol (2-AG) effects on zymosan particles phagocytosis by BMMs.

Fluorescein isothiocyanate (FITC)-labelled zymosan particles were used. The vehicle control used was 100 % ethanol. 2-AG: 2-arachidonylglycerol, MFI: mean fluorescence intensity. Statistical analysis: Two-way ANOVA followed by post-hoc Bonferroni test. Treatment $F_{2,6}=0.3065$; $p>0.05$, Treatment x time $F_{2,6}=0.8254$; $p>0.05$, Time $F_{1,6}=80.84$; $p<0.001$.

BMMs were starved 24hours before performing the phagocytosis assay for the macrophage colony-stimulating factor (M-CSF) used to differentiate myeloid progenitors into cells of the macrophage/monocyte lineage like BMMs. Starving BMMs for this differentiating factor was thought to be responsible for the non observable effect of cannabinoid agonists on zymosan phagocytosis by BMMs. As seen in figure 44 starving the cells leads to an global statistical increase of zymosan phagocytosis by BMMs. This effect was observed after 60 minutes incubation in the presence, or not, of the vehicle (100 % ethanol) in which 2-AG was initially dissolved.

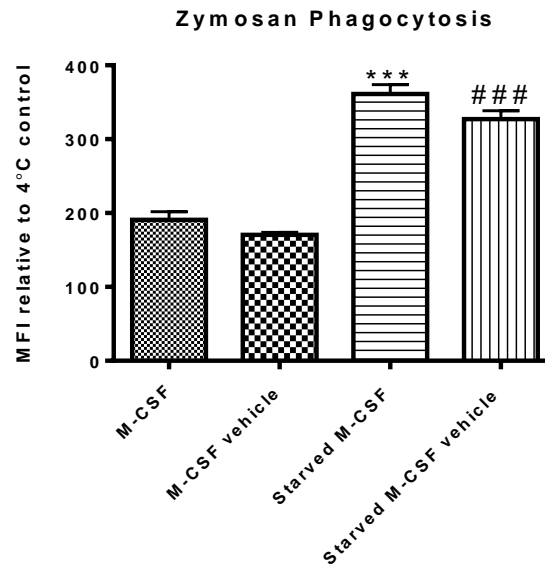


Figure 44: Flow cytometry comparison of BMMs starved or not for M-CSF 24h before phagocytosis assay

Fluorescein isothiocyanate (FITC)-labelled zymosan particles were used. The vehicle control: 100 % ethanol. MFI: mean fluorescence intensity. Statistical analysis: One-way ANOVA followed by post-hoc Bonferroni test: $F_{3,10}=75.37$; $p < 0.001$. Values represent mean \pm SEM, *** $p < 0.001$ vs. M-CSF treated BMMs, ### $p < 0.001$ vs. M-CSF vehicle treated BMMs.

After finding a modulation of zymosan phagocytosis activity due to the starvation of BMM for M-CSF, 2-AG was tested for its ability to modulate the zymosan phagocytosis activity of BMMs after they starved for M-CSF 24 hours before performing the phagocytosis assay. As depicted in figure 45 no statistical treatment effect was observed, as the statistical time effect was still present.

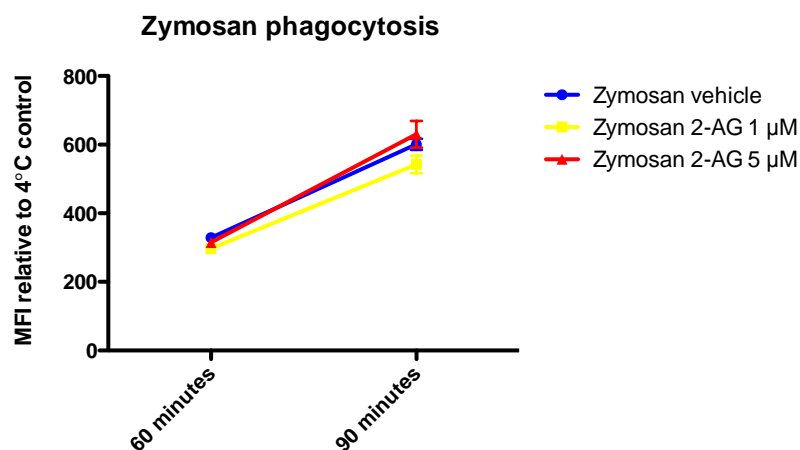


Figure 45: Flow cytometry measurement of 2-arachidonylglycerol (2-AG) effects on zymosan particles phagocytosis by BMMs.

Fluorescein isothiocyanate (FITC)-labelled zymosan particles were used. The vehicle control: 100 % ethanol. 2-AG: 2-arachidonylglycerol, MFI: mean fluorescence intensity. Statistical analysis: Two-way

ANOVA followed by post-hoc Bonferroni test. Treatment $F_{2,6}=3.378$; $p>0.05$, Treatment x time $F_{2,6}=1.151$; $p>0.05$, Time $F_{1,6}=214.7$; $p<0.001$.

As no effect was observed with usually used 2-AG concentrations in cell culture experiments, the effect of a high concentration (10 μM) was tested on zymosan phagocytosis of M-CSF starved BMMs. As seen in Figure 46 no statistical difference in zymosan phagocytosis by BMMs was observed between vehicle and 2-AG treatment after 60 minutes incubation.

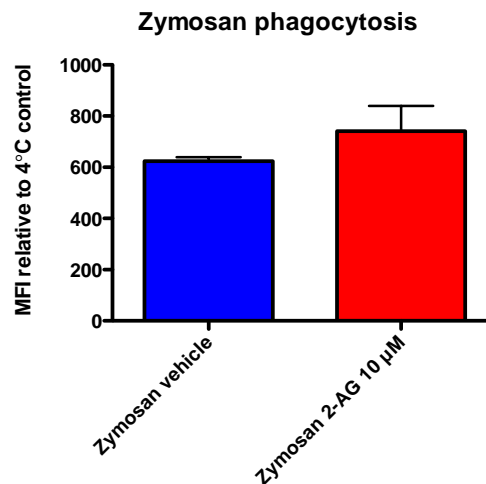


Figure 46: Flow cytometry measurement of 2-arachidonylglycérol (2-AG) effects on zymosan particles phagocytosis by BMMs.

Fluorescein isothiocyanate (FITC)-labelled zymosan particles were used. The vehicle control used was 100 % ethanol. 2-AG: 2-arachidonylglycerol, MFI: mean fluorescence intensity. Statistical analysis: Mann Whitney test $p>0.05$

Finally a commercial available M-CSF was used instead of our “self made” M-CSF to differentiate myeloid stem cells from bone marrow into macrophages as a possible reason for the non response of BMM on phagocytosis after cannabinoid agonists treatment. Cells were starved 24 hour before starting the phagocytosis assay, which was performed during 60 minutes. No statistical difference was observed while comparing 2-AG treated BMMs vehicle reference treated BMMs (figure 47).

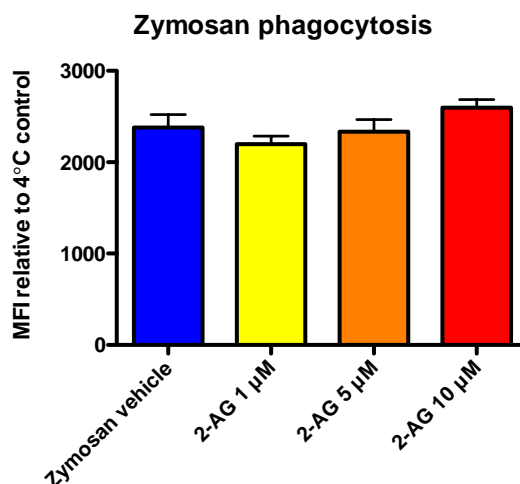


Figure 47: Flow cytometry measurement of 2-arachidonylglycérol (2-AG) effects on zymosan particles phagocytosis by BMMs.

Fluorescein isothiocyanate (FITC)-labelled zymosan particles were used. The vehicle control used was 100 % ethanol. 2-AG: 2-arachidonylglycerol, MFI: mean fluorescence intensity. Statistical analysis: One-way ANOVA followed by Bonferroni's post-hoc comparison to Zymosan vehicle: $F_{3,12}=2.017$; $p>0.05$.

To confirm the results obtain previously by flow cytometry, a phagocytosis assay was performed using fluorescence microscopy.

4.3.2.2 Zymosan phagocytosis by BMMS upon CB2 agonists stimulation measured by fluorescence microscopy

BMM were treated in the same way than for flow cytometry experiments, but instead using the fluorescence-activated cell sorting to measure phagocytosis activity, fluorescence microscopy was used. As seen in the two pictures figure 48A, B, DAPI labelling (blue) of nucleus allowed the identification of the cells and the FITC zymosan particles (green) engulfed by BMMS were counted on six different areas of a cover slip and three cover slips per treatment condition were analyzed. BMMs engulfed the same relative number of zymosan particles under vehicle or 2-AG treatments (figure 49A). The two-way ANOVA followed by post-hoc Bonferroni test revealed a statistical difference in the number of particles, and a treatment x particles interaction. Furthermore the post-hoc Bonferroni test showed a significance difference between the number of macrophages engulfing more than 5 zymosan particles after vehicle or 2-AG (5 µM) treatments (figure 49B).

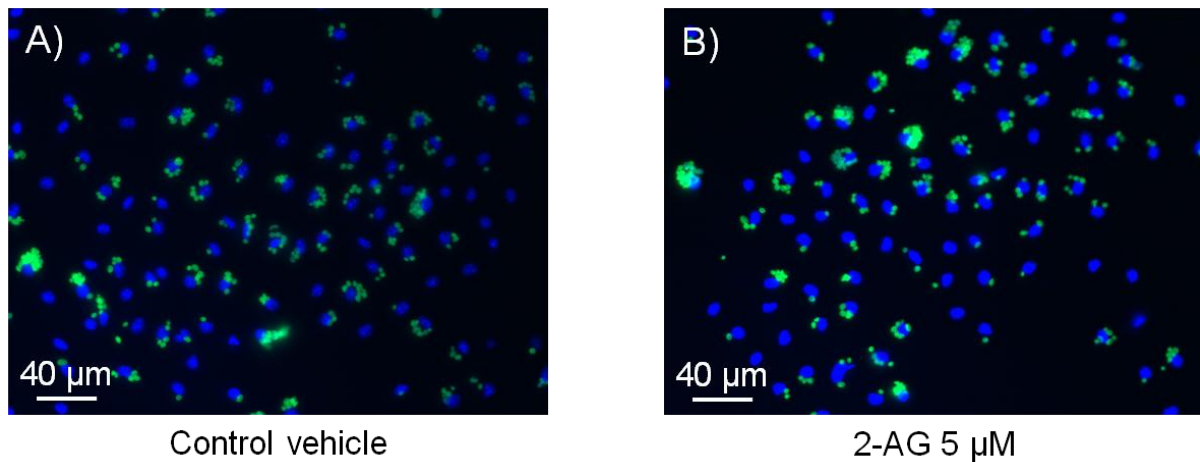


Figure 48: Example of pictures used to count engulfed zymosan particles by BMMs
40X magnification of zymosan particles engulfed by BMMs under vehicle (A) and 2-AG 5 µM (B) after 60 minutes of incubation. Nucleus of macrophages: DAPI (blue); Zymosan particles: FITC (green).

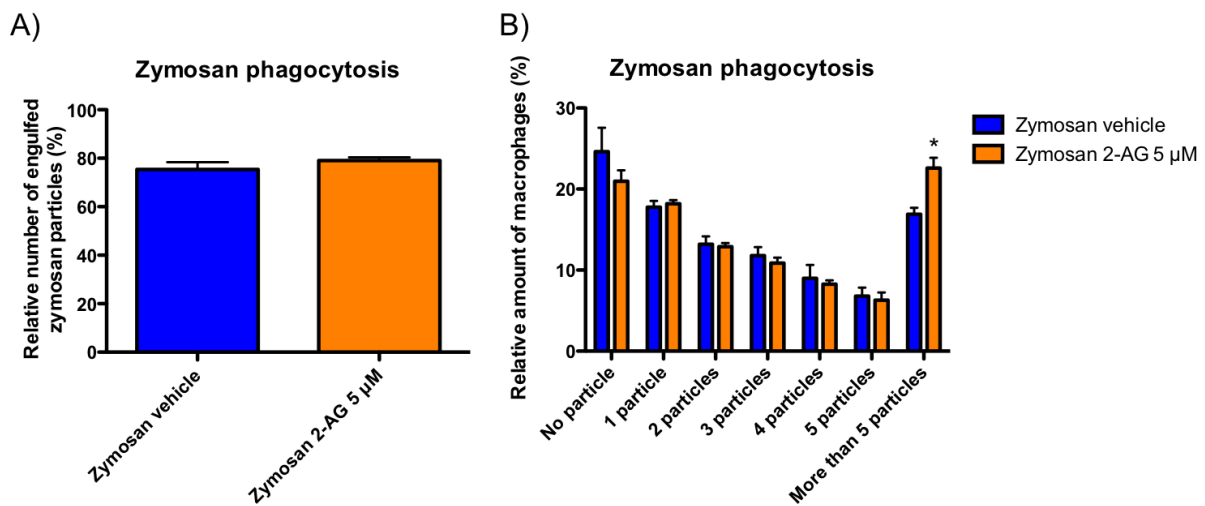


Figure 49: Fluorescence microscopy analysis of zymosan particles engulfed by BMMs
A) Comparison of relative number of engulfed zymosan particles by BMMs after vehicle or 2-AG 5 µM treatments. Statistical analysis: Mann Whitney test $p > 0.05$ B) Relative amount of macrophages which after treatments, engulfed no particles, 1,2,3,4,5 or more than 5 zymosan particles. Statistical analysis: Two-way ANOVA followed by post-hoc Bonferroni test. Treatment $F_{1,28}=0.0$; $p > 0.05$, Treatment x particles $F_{6,28}=2.612$; $p < 0.05$, Particles $F_{6,28}=47.59$; $p < 0.001$. * $p < 0.05$.

The cannabinoid agonist 2-AG had no effect on zymosan phagocytosis by BMMs measured by flow cytometry, but a statistical effect was observed for the phagocytosis of more than five zymosan particles by BMMs using fluorescence microscopy.

5 DISCUSSION

The first aim of this thesis work was to generate humanized CB2 receptor mouse lines. Therefore, humanized targeting vectors were generated and subsequently used for the generation of chimeric mice by injecting targeted ES cells into blastocysts. Due to the lack of germ-line transmission, new engineering technologies (CRISPR/Cas9 system and TALENs) were designed and tested for their ability to target the *Cnr2* locus and improve HR efficiency in ES cells.

The second aim was the establishment of an *in vitro* model to characterize the functional difference between the two human CB2 receptor variants. In a first step, recombinant lentiviral vectors were generated to express the human CB2 receptor variants and used to transduce BMMs. In a second step BMMs were characterized for their two main properties, which are the ability to be driven into different activation states in response to pro- or anti-inflammatory substances and the ability to engulf zymosan particles by phagocytosis. To determine the CB2 receptor's role in macrophages, different CB2 agonists were tested for their capacity to modulate the characterized functions of BMMs.

5.1 Humanizing the mouse CB2 locus

For the generation of the humanized cannabinoid receptor 2 mice, targeting constructs were generated. The design of both targeting construct was identical and based on several considerations. First the length of DNA homology arms required for HR to occur was chosen on minimum size recommendations of 4 kb and 1kb for the long and shorts arms, respectively, as recommended in the literature (Hasty et al., 1991). This was achieved using a BAC and the Red/ET recombineering method to subclone the fragment of interest. On the 5' side of the mouse ORF, a long arm of 4.3 kb was chosen. This long arm consists of the region located between the *EcoRV* restriction site used to linearize the targeting constructs and the last base before the starting codon of the ORF. On the 3' side of the ORF, the short arm was designed such as the homology arm located directly after the insertion point of the selection cassette to the end of the targeting constructs measure 1.7 kb. The mouse CB2 ORF was replaced by the human ones keeping intact the 5' and 3' untranslated regions surrounding the mouse CB2 ORF, in order to not disturb the expression. Finally a selection cassette flanked by FRT sites was inserted 933 bp after the ORF's stop codon in order to select for homologously recombined ES cells clones.

In a first step, both targeting constructs were electroporated into MPI12 ES cells (129sv background), as well as into Bruce4 ES cells (C57Bl/6 background). First electroporations

were performed into MPI12 ES cells. No homologous recombined ES cells were obtained using this ES cell line, which can be due to the fact that the targeting constructs were generated from C57BL/6 DNA and the different genetic background of the two strains could account for the absence of HR. 129sv-derived ES cells are the most widely used ES cells for generation of genetically modified mice, mainly for their ability to generate chimeras and for their good germ line transmission rates. But these ES cell lines due to their 129sv background have a major inconvenient. In fact the peripheral CB2 receptor was characterized to be involved in immune response, and immunologists mainly rely on the extensively characterized C57BL/6 immune response (Bauler et al., 2007; Rolink et al., 2004; Schwarz et al., 2003). If germ line transmitted mice would have been obtained using MPI12 ES cells, they would have to be breed and subsequent backcross to C57BL/6 background to generate congenic strains. The breeding and backcrossing steps can take a long time: 30-36 month. In order to reduce the breeding time to 15-18 months, a marker-assisted breeding strategy (speed congenic) based on a microsatellite marker panel polymorphic between C57BL/6 and 129sv has been developed. The major inconvenient of the speed congenic is the extreme cost that it represent.

MPI12 ES cells were no further used and targeting constructs were then electroporated into Bruce4 ES cells, to avoid extensive backcrossing steps and costs. Moreover, C57BL/6-derived ES cell lines represent a valuable tool for the generation of mouse models due to the fact that the genome of C57BL/6 mouse is available as the RPCI-23 (RP23) BAC library and completely sequenced (Osoegawa et al., 2000), making the design and the development of sequence-specific targeting constructs more convenient. A total of 26 electroporations were performed for both targeting constructs and 1884 neomycin resistant clones were isolated. Of those, 5 were identified as completely homologously recombined clones, indicating a targeting frequency of 1:377, or 0,27 %, which is lower than HR rates reported in the literature (Seong et al., 2004). The absolute frequencies of recombination are locus-dependent, as differences in chromatin structure can influence the accessibility of the required enzymatic machinery (Muller, 1999; te Riele et al., 1992). The low recombination frequency observed can also be explained by the difficulty to obtain recombination of the human ORF and the FRT-neo-FRT sequence in one recombination event. In fact many positive clones identified with the neo integration strategy were negative for the human PCR/digestion, which indicates that the FRT floxed neo cassette was recombined, but not the human ORF. This is the reason why positive clones were first identified using the neo integration PCR strategy and confirmed for the human CB2 ORF recombination using the PCR/digestion strategy. PCR reactions were pipetted using a liquid handling system to automate the process and simplify handling of numerous clones to check. The positive identified clones were further confirmed using the 5' and 3' southern blot strategies before being injected into blastocysts. At last, improvement

could have been done to diminish the number of ES cell clones to check by inserting a negative selection marker (e.g. thymidine kinase, TK) into the targeting construct. This negative selection marker would have probably diminished tremendously the number of ES cells clones to verified but probably not improve the recombination in the same time of the human CB2 ORF and the FRT-neo-FRT sequence.

Repeated blastocyst injections were performed with the identified positive clones and various chimeric animals were born. 9 chimeras from two recombined clones were obtained for the human CB2-Arg variant as well as 9 chimeras out of three recombined clones for the human CB2-Gln variant. It is generally recommended to breed chimera males and wait for them to produce 6 or more litters in order to observe germ line transmission. After the 18 chimera males produced 100 pups, and the genetic modifications were not passed to its progeny, they were not likely to go germline and were discarded. C57BL/6 ES cell lines are known to be less efficient in producing genetically modified mice compared to ES cells on a 129Sv background (Nagy et al. 1993). They are reputed for their susceptibility to become aneuploid and this genetic instability decreases their germ line transmission potency (Hughes et al., 2007; Longo et al., 1997). In addition, maintaining Bruce4 ES cells into culture is quite demanding. The RESGRO medium was used in order to improve chimera generation and germ line transmission potency of our identified Bruce4 ES cells clones. This culture medium is described as able to rescue established ES cell lines that have started drifting, generate low percentage chimeras or have lost germ line transmission capability. It allows separation of differentiated and undifferentiated clones into culture, and sub-clone specifically undifferentiated ES cells to further use them for blastocyst injections. RESGRO medium rescuing of our positive identified ES cell clones did not improved germ line transmission. Mouse ES cell lines have the main disadvantage to be demanding for culture conditions and even if these ES cell lines are used for the generation of transgenic mice since the late eighties (Robertson et al., 1986; Thompson et al., 1989), for other species like for example rats, the story just begin with the establishment in 2008 of the first ES cell line for transgenic models generation (Li et al., 2008).

While the efforts to generate transgenic mice using ES cells, new DNA engineering technologies were developed and interest among the scientific community for these new tools emerged. Moreover, these technologies exhibit a great potential for the generation of transgenic animals without resorting to ES cells. These technologies known as ZFNs, TALENs and CRISPR/Cas9 system are based on two main components: a designed sequence-specific DNA-binding module(s) linked to a non-specific DNA cleavage domain. Thus when a small double-stranded or single stranded template of DNA are supplied consecutively to these DNA

engineering tools, HR is stimulated by DSBs and lead to precise genetic engineering (Hockemeyer et al., 2011; Wang et al., 2013b). HR initiates with extensive 5' to 3' end-processing at broken end, which in eukaryotic cells is regulated by the MRE11/RAD50/NBS1 (MRN) complex, histone H2AX, Breast cancer 1 (BRCA1), Breast cancer 2 (BRCA2), DNA-dependent protein kinase catalytic subunit (DNA-PKcs), and ataxia telangiectasia-mutated (ATM) kinase. The resulting 3' single strand DNA (ssDNA) tails are bound by the replication protein A (RPA), which is replaced with Rad51 in a reaction mediated by Rad52. The resulting Rad51 nucleoprotein filament searches for and invades a homologous sequence. The Srs2 helicase is thought to dissociate Rad51 from ssDNA, allowing normal base pairing of the invading and complementary donor strands and subsequent strand extension by DNA polymerase. Both ends may invade producing a double-Holliday junction that is resolved to yield crossover or non-crossover recombinants. Once intermediates are resolved, the remaining ssDNA gaps and nicks are repaired by DNA polymerase and ligase (Shrivastav et al., 2008).

As ZFNs were reported to have a potential cytotoxic activity, presumably due to cleavage at non-targeted sites (Cornu et al., 2008; Pruett-Miller et al., 2008; Radecke et al., 2010), efforts were only concentrated on the generation and testing of one TALEN pair and a CRISPR/Cas9 system, both targeting the *Cnr2* locus. An important factor for the generation of TALENs is the spacer region, which is defined as the region separating the two TALENs after binding on the genomic sequence. As reported by Schmid-Burgk et al, a spacer region of 14-15 bp showed the highest TALENs efficiency (Schmid-Burgk et al., 2013). Due to this consideration one TALENs pair was designed to target the murine CB2 ORF 300 bp after the start codon with a spacer region of 14 bp. The TALEN pair was also designed to avoid targeting of the human CB2 ORF and activity of the TALENs in the targeting construct. Unfortunately the TALEN pair designed did not show any activity in the mouse locus using the surveyor assay. It would have increase the chance to target the *Cnr2* locus by designing more than one TALENs pair. Due to the sequence requirements (spacer and sequence heterogeneity) this was not possible. Moreover, the LIC assembly of TALENs, which is supposed to simplify the construction of TALEN pairs in a really short time, is certainly more convenient than the PCR/Golden gate cloning method (Sanjana et al., 2012) but is still time consuming. The ligation independent cloning assembly of TALEN remains a valuable high throughput technique that enables the semi-automated generation of TALE genes using liquid handling systems for the establishment of TALE gene library.

Since 2012 the CRISPR/Cas9 system offered a faster and more efficient way to edit the genome. This system is based on two distinct components: a synthetic guide RNA (gRNA)

and the bacterial CRISPR associated (Cas) nuclease, Cas9. The gRNA consists in the fusion of the CRISPR RNA (crRNA), responsible for the targeting specificity and the trans-activating crRNA (tracrRNA) that is involved in the recruitment of the Cas9. The system has only one requirement that is necessary for nuclease activity. The target site needs to be flanked on the 3' end by a 3 bp NGG called protospacer-adjacent motif (PAM). A well-suited 20 bp sequence located 25 bp after the start codon of the murine CB2 ORF was found and this sequence differs in 6 bp between mouse and human ORFs. These mismatches are located at both ends of the targeted sequence, which were reported to be important for targeting specificity of gRNA than the central nucleotides (Cong et al., 2013). It can be speculated that the designed CRISPR/Cas9 system will have activity only in the murine ORF and not in the human ORF present in the targeting constructs. The only required cloning step to build this system is the ligation of a double stranded oligonucleotide containing sticky ends compatible with the restriction site used to linearize the CRISPR/Cas9 plasmid. The plasmid successfully cloned was called px330-mCB2. This plasmid expresses the gRNA targeting the murine ORF and the Cas9 when lipofected or electroporated into cells. The ability to mediate double strand breaks of our designed CRISPR/Cas9 system was first assessed and confirmed by surveyor assay. But to further confirm that this system is relevant for the generation of transgenic mice, HDR process was tested in the Bruce4 ES cells previously used for Cnr2 locus targeting by homologous recombination. The results suggest that CRISPR/Cas-mediated double strand breaks at the Cnr2 locus dramatically increased the frequency of homologous recombination in neomycin resistant ES clones from 0.27 % to 67 % meaning an increase of more than 200 fold. Furthermore, 4 % of all clones showed a bi-allelic recombination. It is thus possible to generate completely humanized cell lines with a single electroporation and normal selection conditions. Moreover, with this super-efficient system, modifications can be introduced by directly injecting RNAs encoding the Cas9 protein, the gRNA targeting the mCB2 ORF and the targeting constructs into developing mouse embryos. This eliminates the long and laborious processes of transfecting and selecting mouse ES cells that are required to create targeted mutant mice using classical homologous recombination techniques. Finally It has to be taken into consideration that the CRISPR/Cas9 system, as well as TALENs, induce also mutations at non-specific loci also called off-site effects. For the moment these mutations can be difficult to identify and require to scan the genome for mutations at sites with sequence similarities to the gRNA or the TALEN pair. In the optic of transgenic animal generation, the experimenter could get rid of these non-specific mutations after some subsequent breeding steps with wild type animals.

Previous studies showed the utility of CRISPR/Cas9 system or TALENs technologies to enhance the frequency of HDR with short single-stranded DNA sequences in mice (Wang et

al.). In addition, CRISPR/Cas-mediated double strand breaks also enhanced the frequency of homologous recombination in plants and *C. elegans* (Chen et al., 2013; Dickinson et al., 2013; Li et al., 2013b) with double-stranded DNA. Here it was demonstrated that this technology also boost gene replacements with large DNA constructs in the mouse genome. This new and simple technology thus holds a great promise to improve genetic engineering of the mouse, apes and even human genome. It remains to be determined if the CRISPR/Cas9 technology is more efficient than TALENs (Cong et al., 2013; Yu et al., 2014) to stimulate homologous recombination. Anyhow, considering the easiness to clone guide sequences in comparison to the rather cumbersome task of engineering TALENs, it will be much easier to experiment different gRNAs, if necessary. It should be taken into consideration that it might be required to design the guide sequence such that it does not direct double strand breaks within the targeting construct. In practice, this should also not impose any problems, because it should always be possible to utilize sequences where the targeting construct diverges from the target locus for example when humanizing a mouse gene or using the loxP site of a floxed gene.

5.2 Functional analysis

In this section, in vitro assays were developed to assess the functional difference between the two human variants. Carrasquer et al did not find any difference in binding of cannabinoid ligands and signal transduction between the two human CB2 variants but revealed a difference in ligand-induced cyclic AMP accumulation (Carrasquer et al., 2010). Based on this observation and the fact that CB2 receptor is well accepted among the scientific community to play a role in immune functions, two components necessary for the assay were developed and tested. First, recombinant lentiviral vectors expressing each of the human variants were designed and cloned in order to transduce CB2^{-/-} BMMs. In a second step murine BMMs were checked for their ability to turn into pro or anti-inflammatory phenotypes called M1 and M2, and also to check, as it was previously reported (Shiratsuchi et al., 2008), the influence of cannabinoid ligands on zymosan phagocytosis.

5.2.1 Recombinant lentiviral vectors expressing the human CB2 variants

After cloning the hCB2 ORF variants into distinct vector constructs, recombinant lentiviral vectors were produced in collaboration with Dr. Katrin Zimmermann from the Institute of Pharmacology and Toxicology, Bonn. Our collaborators also determined the titer of these newly produced lentiviral particles by measuring the reverse transcriptase (RT) activity using a cell free colorimetric assay (ELISA). Measuring the activity of reverse transcriptase present in the virions is a valuable technique to estimates or predicts a functional titer. But since the functional titer is dependent on the vector construct and the cell type used for transduction, the transgene expression levels in transduced cells had to be determined by FACS. As the first vector constructs designed did not contained fluorescent gene, establishment of CB2

antibodies had to be performed. Different antibodies binding either at the N or C-terminal of the protein were established and tested for FACS measurement. As recommended by Ashton et al., the specificity of these antibodies were tested in CB2 knockout BMMS (Ashton, 2011) . The non-specificity of commercially available CB2 antibodies is often debated in the literature (Baek et al., 2013) and remain today one of the biggest issue in the endocannabinoid field. This is mainly due to the fact that the detection or quantification of the CB2 protein is for the moment not reliable. Our data confirmed that the CB2 protein detection by FACS using the most used CB2 antibodies is not possible due to a lack of specificity. To overcome the use of CB2 antibodies, recombinant lentiviral vectors were generated with an IRES version2 and an eGFP gene. It was then possible to assess the transduction efficiencies of the generated recombinant lentiviral vectors into BMMS. The functional titer of $5.5 \cdot 10^7$ TU/ml measured for the eGFP recombinant lentiviral vector indicates a good transduction efficiency of BMMS. However, titration measured for the hCB2-IRES2-eGFP recombinant lentiviral vectors were one hundred times lower which indicate a low transduction efficiency. The recombinant lentiviral vectors eGFP and the hCB2-IRES2-eGFP were produced in the same manner by our collaborators of the Institute of Pharmacology and Toxicology, Bonn. Production of recombinant lentiviral vectors using the hCB2-IRES2-eGFP vector constructs were repeated and gave always rise to a low transduction efficiency. This low titer could be explained by either the nature of the constructs which is interfering with the transduction ability or by the fact that the CB2 receptor expression into 293T cells may affect the HIV-1 replication machinery as reported previously (Ramirez et al., 2013) during the recombinant lentiviral vector production in these cells. Considering the considerable amount of viruses that had to be used to obtain transduction of BMMS, lentiviruses expressing in parallel the human CB2 variants and eGFP were not further used.

Now that a functional CRISPR/Cas9 system was developed and tested to target the *Cnr2* locus, it could be reasonable to imagine transfecting BMMS with the px330-mCB2 in combination with targeting constructs expressing eGFP paralleling the human CB2 variants to study the functional difference between the two human variants. Even if BMMS are known to be hard-to-transfect cells, some protocols exist (Weischenfeldt and Porse, 2008). Avoiding the use of lentiviruses in favour of transfection with DNA plasmids, also decrease the time of BMMS in culture, which is a point of importance when testing these macrophages with a functional assay such as phagocytosis for example.

5.2.2 Functional analysis of CB2 receptor activation in mouse bone marrow derived-macrophages

The cannabinoid receptor 2 is expressed in many macrophage-derived cells. These include microglia, many circulating macrophages, osteocytes and osteoclasts, dendritic cells, and hepatic Kupffer cells (Atwood et al., 2012). Macrophages play a key role in the polarized innate and adaptive immune response. As an antigen presenting cells and in order to initiate the adaptive response, they are able to phagocyte (Murray and Wynn, 2011). Moreover they can be stimulated with different substances to drive them into different activation states characterized by different cell surface markers expression and cytokine release (Mantovani et al., 2004). These functional abilities with regards to a possible modulation by the CB2 receptor were investigated in BMMs.

5.2.2.1 Bone marrow macrophages phenotypes

BMMs were driven into M1 activation state due to high expression of CD86 cell surface marker observed after overnight stimulation with IFN γ or a combination of LPS/IFN γ . The MHCII cell surface marker normally expressed by both M1 and M2 macrophages was only observed after IFN γ or combination of LPS/IFN γ stimulations. Only a slight upregulation of this cell surface marker was observed after IL-4 overnight stimulation. Expression of MMR was also significantly increased after overnight stimulation with IL-4. The effects of IL-4 could maybe be improved by a longer exposure of 48 hours instead of 16 hours, as reported in the literature (Guzman-Morales et al., 2011; Ruffell et al., 2011). Furthermore, once the BMMs were activated into M1 phenotype, they release high amount of the pro-inflammatory cytokine TNF α after overnight stimulation with a combination of LPS/IFN γ and no effect of CB2 agonists such as BCP or JWH-133 was observed on the TNF α release. As reported in the literature (Ehrhart et al., 2005; Romero-Sandoval et al., 2009), the stimulation of the CB2 receptor suppresses microglial activation *in vitro*. It was shown that incubation with the CB2 agonist JWH-015 is able to suppress microglial TNF α production induced by IFN γ (Ehrhart et al., 2005). In the present study, it was found that the expression of the CB2 receptor was down regulated after overnight incubation of BMMS with LPS or combination of LPS/ IFN γ . Which indicates that LPS stimulation is maybe the factor responsible for the no effect of CB2 agonists on TNF α release. As the CB2 receptor expression in BMMs was only slightly down regulated after overnight stimulation with IFN γ , it is reasonable to imagine an effect of CB2 agonists on TNF α release by BMMs after IFN γ overnight stimulation. While CB2 expression was down regulated in BMMs after pro-inflammatory stimulations, GPR18 expression was highly up regulated. As reported in an immortalized microglia cell line (BV-2), GPR18 plays a role in the migration of this cells (McHugh et al., 2012). The increased expression in BMMs under pro-inflammatory conditions could indicate a role for this GPCR in the migration ability of macrophages during

inflammation. Even if CB1 receptor expression is reported as low in immune cells (Kaplan, 2013; Nong et al., 2001), the down regulation in its expression after overnight pro-inflammatory stimulations indicate that this receptor could also play a role in immune cells. Finally, efforts should be concentrated maybe on expression patterns of the different cannabinoid receptors in pro and anti-inflammatory situations more than concentrated only on single receptor expression and its possible effect.

5.2.2.2 Zymosan phagocytosis

Shiratsuchi and colleagues investigated phagocytosis of zymosan by murine elicited peritoneal macrophages (Shiratsuchi et al., 2008). They found that 2-AG or CP55 940, agonists for both CB1 and CB2 receptors, increase phagocytosis of zymosan. Moreover they showed that both, the number of zymosan particles engulfed by macrophages and the ratio of macrophages that had engulfed zymosan, increased in the presence of 2-AG. Based on the observed result that cannabinoid receptors stimulation increases the phagocytosis ability of macrophages, the same functionality was tested in BMMs. The time points of 30, 60 and 90 minutes were chosen to not miss any effect on an increase or a decrease in phagocytosis activity. Generally, the phagocytosis assay is performed after 60 minutes incubation (Weischenfeldt and Porse, 2008). Furthermore, starving the differentiated BMMs for M-CSF, 24 hours before performing the phagocytosis assay induces an increase in the phagocytosis ability of BMMs, which indicates that the phagocytosis activity of BMMs can be modulated. To confirm the results obtain by Shiratsuchi et al., different CB2 specific agonists such as beta caryophyllene and JWH-133, and agonist for both CB1 and CB2 such as 2-AG were used at different concentrations. Unfortunately cannabinoid agonists did not show any modulation of the phagocytosis activity analyzed by flow cytometry or fluorescence microscopy. The only significant result found was an increase in the relative amount of macrophages that had engulfed more than five zymosan particles after 2-AG treatment by fluorescence microscopy. But the relative number of engulfed zymosan remained the same with our without 2-AG. This effect could be due to a loss of control of BMMs in engulfing more than five zymosan particles after 2-AG treatment. Flow cytometry result did not indicate such of loss of control, which may indicates that this result is an artefact.

As our result did not confirm those observed by Shiratsuchi and colleagues, it is reasonable to wonder if there are any differences between bone marrow-derived macrophages and thioglycolate-elicited peritoneal macrophages. It was recently showed that peritoneal macrophages and BMMs differ even if they are used in same functional assays such as phagocytosis assay. Peritoneal macrophages appear to be more mature than bone marrow derived macrophages based on their morphology and surface molecular characteristics (Wang et al., 2013a). Furthermore BMMs showed a stronger capacity in both

proliferation and phagocytosis than peritoneal macrophages (Wang et al., 2013a) which could encounter for the difficulties to observe any modulation by the CB2 receptor stimulation in BMMs. As 2-AG has an effect on zymosan phagocytosis by peritoneal macrophages but not by BMMs, it could be that BMMs are too naïve or that they have to be previously stimulated in order to activate their potential to respond to cannabinoid stimulation.

6 BIBLIOGRAPHY

Alger, B.E. (2012). Endocannabinoids at the synapse a decade after the dies mirabilis (29 March 2001): what we still do not know. *The Journal of physiology* 590, 2203-2212.

Anand, P., Whiteside, G., Fowler, C.J., and Hohmann, A.G. (2009). Targeting CB2 receptors and the endocannabinoid system for the treatment of pain. *Brain research reviews* 60, 255-266.

Ashton, J.C. (2011). Knockout controls and the specificity of cannabinoid CB2 receptor antibodies. *British journal of pharmacology* 163, 1113; author reply 1114.

Atwood, B.K., and Mackie, K. (2010). CB2: a cannabinoid receptor with an identity crisis. *British journal of pharmacology* 160, 467-479.

Atwood, B.K., Straiker, A., and Mackie, K. (2012). CB(2): therapeutic target-in-waiting. *Progress in neuro-psychopharmacology & biological psychiatry* 38, 16-20.

Babinet, C. (2000). Transgenic mice: an irreplaceable tool for the study of mammalian development and biology. *Journal of the American Society of Nephrology : JASN* 11 Suppl 16, S88-94.

Baek, J.H., Darlington, C.L., Smith, P.F., and Ashton, J.C. (2013). Antibody testing for brain immunohistochemistry: brain immunolabeling for the cannabinoid CB(2) receptor. *Journal of neuroscience methods* 216, 87-95.

Baldassarre, M., Giannone, F.A., Napoli, L., Tovoli, A., Ricci, C.S., Tufoni, M., and Caraceni, P. (2013). The endocannabinoid system in advanced liver cirrhosis: pathophysiological implication and future perspectives. *Liver international : official journal of the International Association for the Study of the Liver* 33, 1298-1308.

Basu, S., and Dittel, B.N. (2011). Unraveling the complexities of cannabinoid receptor 2 (CB2) immune regulation in health and disease. *Immunologic research* 51, 26-38.

Bauler, T.J., Hughes, E.D., Arimura, Y., Mustelin, T., Saunders, T.L., and King, P.D. (2007). Normal TCR signal transduction in mice that lack catalytically active PTPN3 protein tyrosine phosphatase. *J Immunol* 178, 3680-3687.

Bifulco, M., Malfitano, A.M., Pisanti, S., and Laezza, C. (2008). Endocannabinoids in endocrine and related tumours. *Endocrine-related cancer* 15, 391-408.

Bilkei-Gorzo, A. (2012). The endocannabinoid system in normal and pathological brain ageing. *Philosophical transactions of the Royal Society of London Series B, Biological sciences* 367, 3326-3341.

Bingham, B., Jones, P.G., Uveges, A.J., Kotnis, S., Lu, P., Smith, V.A., Sun, S.C., Resnick, L., Chlenov, M., He, Y., *et al.* (2007). Species-specific in vitro pharmacological effects of the cannabinoid receptor 2 (CB2) selective ligand AM1241 and its resolved enantiomers. *British journal of pharmacology* 151, 1061-1070.

Bouabe, H., Fassler, R., and Heesemann, J. (2008). Improvement of reporter activity by IRES-mediated polycistronic reporter system. *Nucleic acids research* 36, e28.

Buckley, N.E., McCoy, K.L., Mezey, E., Bonner, T., Zimmer, A., Felder, C.C., Glass, M., and Zimmer, A. (2000). Immunomodulation by cannabinoids is absent in mice deficient for the cannabinoid CB(2) receptor. *Eur J Pharmacol* 396, 141-149.

- Burke, B., Sumner, S., Maitland, N., and Lewis, C.E. (2002). Macrophages in gene therapy: cellular delivery vehicles and in vivo targets. *Journal of leukocyte biology* 72, 417-428.
- Cabral, G.A., and Griffin-Thomas, L. (2009). Emerging role of the cannabinoid receptor CB2 in immune regulation: therapeutic prospects for neuroinflammation. *Expert reviews in molecular medicine* 11, e3.
- Carrasquer, A., Nebane, N.M., Williams, W.M., and Song, Z.H. (2010). Functional consequences of nonsynonymous single nucleotide polymorphisms in the CB2 cannabinoid receptor. *Pharmacogenetics and genomics* 20, 157-166.
- Castillo, P.E., Younts, T.J., Chavez, A.E., and Hashimoto, Y. (2012). Endocannabinoid signaling and synaptic function. *Neuron* 76, 70-81.
- Cermak, T., Doyle, E.L., Christian, M., Wang, L., Zhang, Y., Schmidt, C., Baller, J.A., Somia, N.V., Bogdanove, A.J., and Voytas, D.F. (2011). Efficient design and assembly of custom TALEN and other TAL effector-based constructs for DNA targeting. *Nucleic acids research* 39, e82.
- Chen, C., Fenk, L.A., and de Bono, M. (2013). Efficient genome editing in *Caenorhabditis elegans* by CRISPR-targeted homologous recombination. *Nucleic acids research* 41, e193.
- Chylinski, K., Le Rhun, A., and Charpentier, E. (2013). The tracrRNA and Cas9 families of type II CRISPR-Cas immunity systems. *RNA biology* 10, 726-737.
- Cong, L., Ran, F.A., Cox, D., Lin, S., Barretto, R., Habib, N., Hsu, P.D., Wu, X., Jiang, W., Marraffini, L.A., *et al.* (2013). Multiplex genome engineering using CRISPR/Cas systems. *Science* 339, 819-823.
- Console-Bram, L., Brailoiu, E., Brailoiu, G.C., Sharir, H., and Abood, M.E. (2014). Activation of GPR18 by Cannabinoid compounds: A tale of biased agonism. *British journal of pharmacology*.
- Coppola, N., Zampino, R., Bellini, G., Macera, M., Marrone, A., Pisaturo, M., Boemio, A., Nobili, B., Pasquale, G., Maione, S., *et al.* (2014). Association between a polymorphism in cannabinoid receptor 2 and severe necroinflammation in patients with chronic hepatitis C. *Clinical gastroenterology and hepatology : the official clinical practice journal of the American Gastroenterological Association* 12, 334-340.
- Cornu, T.I., Thibodeau-Beganny, S., Guhl, E., Alwin, S., Eichinger, M., Joung, J.K., and Cathomen, T. (2008). DNA-binding specificity is a major determinant of the activity and toxicity of zinc-finger nucleases. *Molecular therapy : the journal of the American Society of Gene Therapy* 16, 352-358.
- Devane, W.A., Dysarz, F.A., 3rd, Johnson, M.R., Melvin, L.S., and Howlett, A.C. (1988). Determination and characterization of a cannabinoid receptor in rat brain. *Molecular pharmacology* 34, 605-613.
- Devane, W.A., Hanus, L., Breuer, A., Pertwee, R.G., Stevenson, L.A., Griffin, G., Gibson, D., Mandelbaum, A., Etinger, A., and Mechoulam, R. (1992). Isolation and structure of a brain constituent that binds to the cannabinoid receptor. *Science* 258, 1946-1949.
- Dickinson, D.J., Ward, J.D., Reiner, D.J., and Goldstein, B. (2013). Engineering the *Caenorhabditis elegans* genome using Cas9-triggered homologous recombination. *Nature methods* 10, 1028-1034.

Ehrhart, J., Obregon, D., Mori, T., Hou, H., Sun, N., Bai, Y., Klein, T., Fernandez, F., Tan, J., and Shytle, R.D. (2005). Stimulation of cannabinoid receptor 2 (CB2) suppresses microglial activation. *Journal of neuroinflammation* 2, 29.

Evans, M.J., and Kaufman, M.H. (1981). Establishment in culture of pluripotential cells from mouse embryos. *Nature* 292, 154-156.

Fernandez-Lopez, D., Lizasoain, I., Moro, M.A., and Martinez-Orgado, J. (2013). Cannabinoids: well-suited candidates for the treatment of perinatal brain injury. *Brain sciences* 3, 1043-1059.

Gaj, T., Gersbach, C.A., and Barbas, C.F., 3rd (2013). ZFN, TALEN, and CRISPR/Cas-based methods for genome engineering. *Trends in biotechnology* 31, 397-405.

Gasperi, V., Dainese, E., Oddi, S., Sabatucci, A., and Maccarrone, M. (2013). GPR55 and its interaction with membrane lipids: comparison with other endocannabinoid-binding receptors. *Current medicinal chemistry* 20, 64-78.

Guindon, J., and Hohmann, A.G. (2009). The endocannabinoid system and pain. *CNS & neurological disorders drug targets* 8, 403-421.

Guzman-Morales, J., Ariganello, M.B., Hammami, I., Thibault, M., Jolicoeur, M., and Hoemann, C.D. (2011). Biodegradable chitosan particles induce chemokine release and negligible arginase-1 activity compared to IL-4 in murine bone marrow-derived macrophages. *Biochemical and biophysical research communications* 405, 538-544.

Hasty, P., Rivera-Perez, J., and Bradley, A. (1991). The length of homology required for gene targeting in embryonic stem cells. *Molecular and cellular biology* 11, 5586-5591.

Hockemeyer, D., Soldner, F., Beard, C., Gao, Q., Mitalipova, M., DeKolver, R.C., Katibah, G.E., Amora, R., Boydston, E.A., Zeitler, B., *et al.* (2009). Efficient targeting of expressed and silent genes in human ESCs and iPSCs using zinc-finger nucleases. *Nat Biotechnol* 27, 851-857.

Hockemeyer, D., Wang, H., Kiani, S., Lai, C.S., Gao, Q., Cassady, J.P., Cost, G.J., Zhang, L., Santiago, Y., Miller, J.C., *et al.* (2011). Genetic engineering of human pluripotent cells using TALE nucleases. *Nat Biotechnol* 29, 731-734.

Hughes, E.D., Qu, Y.Y., Genik, S.J., Lyons, R.H., Pacheco, C.D., Lieberman, A.P., Samuelson, L.C., Nasonkin, I.O., Camper, S.A., Van Keuren, M.L., *et al.* (2007). Genetic variation in C57BL/6 ES cell lines and genetic instability in the Bruce4 C57BL/6 ES cell line. *Mammalian genome : official journal of the International Mammalian Genome Society* 18, 549-558.

Idris, A.I. (2010). Cannabinoid receptors as target for treatment of osteoporosis: a tale of two therapies. *Current neuropharmacology* 8, 243-253.

Ishiguro, H., Carpio, O., Horiuchi, Y., Shu, A., Higuchi, S., Schanz, N., Benno, R., Arinami, T., and Onaivi, E.S. (2010a). A nonsynonymous polymorphism in cannabinoid CB2 receptor gene is associated with eating disorders in humans and food intake is modified in mice by its ligands. *Synapse* 64, 92-96.

Ishiguro, H., Horiuchi, Y., Ishikawa, M., Koga, M., Imai, K., Suzuki, Y., Morikawa, M., Inada, T., Watanabe, Y., Takahashi, M., *et al.* (2010b). Brain cannabinoid CB2 receptor in schizophrenia. *Biological psychiatry* 67, 974-982.

Ishiguro, H., Iwasaki, S., Teasenfitz, L., Higuchi, S., Horiuchi, Y., Saito, T., Arinami, T., and Onaivi, E.S. (2007). Involvement of cannabinoid CB2 receptor in alcohol preference in mice and alcoholism in humans. *The pharmacogenomics journal* 7, 380-385.

Kaplan, B.L. (2013). The role of CB1 in immune modulation by cannabinoids. *Pharmacology & therapeutics* 137, 365-374.

Karsak, M., Cohen-Solal, M., Freudenberg, J., Ostertag, A., Morieux, C., Kornak, U., Essig, J., Erxlebe, E., Bab, I., Kubisch, C., *et al.* (2005). Cannabinoid receptor type 2 gene is associated with human osteoporosis. *Human molecular genetics* 14, 3389-3396.

Katona, I., and Freund, T.F. (2012). Multiple functions of endocannabinoid signaling in the brain. *Annual review of neuroscience* 35, 529-558.

Li, D., Qiu, Z., Shao, Y., Chen, Y., Guan, Y., Liu, M., Li, Y., Gao, N., Wang, L., Lu, X., *et al.* (2013a). Heritable gene targeting in the mouse and rat using a CRISPR-Cas system. *Nat Biotechnol* 31, 681-683.

Li, J.F., Norville, J.E., Aach, J., McCormack, M., Zhang, D., Bush, J., Church, G.M., and Sheen, J. (2013b). Multiplex and homologous recombination-mediated genome editing in *Arabidopsis* and *Nicotiana benthamiana* using guide RNA and Cas9. *Nat Biotechnol* 31, 688-691.

Li, P., Tong, C., Mehrian-Shai, R., Jia, L., Wu, N., Yan, Y., Maxson, R.E., Schulze, E.N., Song, H., Hsieh, C.L., *et al.* (2008). Germline competent embryonic stem cells derived from rat blastocysts. *Cell* 135, 1299-1310.

Li, T., Huang, S., Zhao, X., Wright, D.A., Carpenter, S., Spalding, M.H., Weeks, D.P., and Yang, B. (2011). Modularly assembled designer TAL effector nucleases for targeted gene knockout and gene replacement in eukaryotes. *Nucleic acids research* 39, 6315-6325.

Longo, L., Bygrave, A., Grosveld, F.G., and Pandolfi, P.P. (1997). The chromosome make-up of mouse embryonic stem cells is predictive of somatic and germ cell chimaerism. *Transgenic research* 6, 321-328.

Mahmoud Gouda, H., and Mohamed Kamel, N.R. (2013). Cannabinoid CB2 receptor gene (CNR2) polymorphism is associated with chronic childhood immune thrombocytopenia in Egypt. *Blood coagulation & fibrinolysis : an international journal in haemostasis and thrombosis* 24, 247-251.

Mantovani, A., Sica, A., Sozzani, S., Allavena, P., Vecchi, A., and Locati, M. (2004). The chemokine system in diverse forms of macrophage activation and polarization. *Trends in immunology* 25, 677-686.

Martin, G.R. (1981). Isolation of a pluripotent cell line from early mouse embryos cultured in medium conditioned by teratocarcinoma stem cells. *Proceedings of the National Academy of Sciences of the United States of America* 78, 7634-7638.

Matsuda, L.A., Lolait, S.J., Brownstein, M.J., Young, A.C., and Bonner, T.I. (1990). Structure of a cannabinoid receptor and functional expression of the cloned cDNA. *Nature* 346, 561-564.

McHugh, D., Roskowski, D., Xie, S., and Bradshaw, H.B. (2014). Delta(9)-THC and N-arachidonoyl glycine regulate BV-2 microglial morphology and cytokine release plasticity: implications for signaling at GPR18. *Frontiers in pharmacology* 4, 162.

- McHugh, D., Wager-Miller, J., Page, J., and Bradshaw, H.B. (2012). siRNA knockdown of GPR18 receptors in BV-2 microglia attenuates N-arachidonoyl glycine-induced cell migration. *Journal of molecular signaling* 7, 10.
- Mechoulam, R., Ben-Shabat, S., Hanus, L., Ligumsky, M., Kaminski, N.E., Schatz, A.R., Gopher, A., Almog, S., Martin, B.R., Compton, D.R., *et al.* (1995). Identification of an endogenous 2-monoglyceride, present in canine gut, that binds to cannabinoid receptors. *Biochemical pharmacology* 50, 83-90.
- Mechoulam, R., and Gaoni, Y. (1965). A Total Synthesis of DI-Delta-1-Tetrahydrocannabinol, the Active Constituent of Hashish. *Journal of the American Chemical Society* 87, 3273-3275.
- Menke, D.B. (2013). Engineering subtle targeted mutations into the mouse genome. *Genesis* 51, 605-618.
- Mukherjee, S., Adams, M., Whiteaker, K., Daza, A., Kage, K., Cassar, S., Meyer, M., and Yao, B.B. (2004). Species comparison and pharmacological characterization of rat and human CB2 cannabinoid receptors. *Eur J Pharmacol* 505, 1-9.
- Muller, U. (1999). Ten years of gene targeting: targeted mouse mutants, from vector design to phenotype analysis. *Mechanisms of development* 82, 3-21.
- Munro, S., Thomas, K.L., and Abu-Shaar, M. (1993). Molecular characterization of a peripheral receptor for cannabinoids. *Nature* 365, 61-65.
- Murray, P.J., and Wynn, T.A. (2011). Protective and pathogenic functions of macrophage subsets. *Nature reviews Immunology* 11, 723-737.
- Murray, R.M., Morrison, P.D., Henquet, C., and Di Forti, M. (2007). Cannabis, the mind and society: the hash realities. *Nature reviews Neuroscience* 8, 885-895.
- Nong, L., Newton, C., Friedman, H., and Klein, T.W. (2001). CB1 and CB2 receptor mRNA expression in human peripheral blood mononuclear cells (PBMC) from various donor types. *Advances in experimental medicine and biology* 493, 229-233.
- Oliere, S., Joliette-Riopel, A., Potvin, S., and Jutras-Aswad, D. (2013). Modulation of the Endocannabinoid System: Vulnerability Factor and New Treatment Target for Stimulant Addiction. *Frontiers in psychiatry* 4, 109.
- Onaivi, E.S., Ishiguro, H., Gong, J.P., Patel, S., Meozzi, P.A., Myers, L., Perchuk, A., Mora, Z., Tagliaferro, P.A., Gardner, E., *et al.* (2008). Brain neuronal CB2 cannabinoid receptors in drug abuse and depression: from mice to human subjects. *PLoS one* 3, e1640.
- Osoegawa, K., Tateno, M., Woon, P.Y., Frengen, E., Mammoser, A.G., Catanese, J.J., Hayashizaki, Y., and de Jong, P.J. (2000). Bacterial artificial chromosome libraries for mouse sequencing and functional analysis. *Genome research* 10, 116-128.
- Pacholczyk, G., Suhag, R., Mazurek, M., Dederscheck, S.M., and Koni, P.A. (2008). Generation of C57BL/6 knockout mice using C3H x BALB/c blastocysts. *BioTechniques* 44, 413-416.
- Porteus, M.H., and Carroll, D. (2005). Gene targeting using zinc finger nucleases. *Nat Biotechnol* 23, 967-973.
- Pruett-Miller, S.M., Connelly, J.P., Maeder, M.L., Joung, J.K., and Porteus, M.H. (2008). Comparison of zinc finger nucleases for use in gene targeting in mammalian cells. *Molecular therapy : the journal of the American Society of Gene Therapy* 16, 707-717.

- Radecke, S., Radecke, F., Cathomen, T., and Schwarz, K. (2010). Zinc-finger nuclease-induced gene repair with oligodeoxynucleotides: wanted and unwanted target locus modifications. *Molecular therapy : the journal of the American Society of Gene Therapy* 18, 743-753.
- Ramirez, S.H., Reichenbach, N.L., Fan, S., Rom, S., Merkel, S.F., Wang, X., Ho, W.Z., and Persidsky, Y. (2013). Attenuation of HIV-1 replication in macrophages by cannabinoid receptor 2 agonists. *Journal of leukocyte biology* 93, 801-810.
- Robertson, E., Bradley, A., Kuehn, M., and Evans, M. (1986). Germ-line transmission of genes introduced into cultured pluripotential cells by retroviral vector. *Nature* 323, 445-448.
- Rolink, A.G., Andersson, J., and Melchers, F. (2004). Molecular mechanisms guiding late stages of B-cell development. *Immunological reviews* 197, 41-50.
- Rom, S., and Persidsky, Y. (2013). Cannabinoid receptor 2: potential role in immunomodulation and neuroinflammation. *Journal of neuroimmune pharmacology : the official journal of the Society on NeuroImmune Pharmacology* 8, 608-620.
- Romero-Sandoval, E.A., Horvath, R., Landry, R.P., and DeLeo, J.A. (2009). Cannabinoid receptor type 2 activation induces a microglial anti-inflammatory phenotype and reduces migration via MKP induction and ERK dephosphorylation. *Molecular pain* 5, 25.
- Rossi, F., Bellini, G., Alisi, A., Alterio, A., Maione, S., Perrone, L., Locatelli, F., Miraglia del Giudice, E., and Nobili, V. (2012a). Cannabinoid receptor type 2 functional variant influences liver damage in children with non-alcoholic fatty liver disease. *PLoS one* 7, e42259.
- Rossi, F., Bellini, G., Nobili, B., Maione, S., Perrone, L., and del Giudice, E.M. (2011a). Association of the cannabinoid receptor 2 (CB2) Gln63Arg polymorphism with indices of liver damage in obese children: an alternative way to highlight the CB2 hepatoprotective properties. *Hepatology* 54, 1102; author reply 1102-1103.
- Rossi, F., Bellini, G., Tolone, C., Luongo, L., Mancusi, S., Papparella, A., Sturgeon, C., Fasano, A., Nobili, B., Perrone, L., *et al.* (2012b). The cannabinoid receptor type 2 Q63R variant increases the risk of celiac disease: implication for a novel molecular biomarker and future therapeutic intervention. *Pharmacological research : the official journal of the Italian Pharmacological Society* 66, 88-94.
- Rossi, F., Mancusi, S., Bellini, G., Roberti, D., Punzo, F., Vetrella, S., Matarese, S.M., Nobili, B., Maione, S., and Perrotta, S. (2011b). CNR2 functional variant (Q63R) influences childhood immune thrombocytopenic purpura. *Haematologica* 96, 1883-1885.
- Ruffell, B., Poon, G.F., Lee, S.S., Brown, K.L., Tjew, S.L., Cooper, J., and Johnson, P. (2011). Differential use of chondroitin sulfate to regulate hyaluronan binding by receptor CD44 in Inflammatory and Interleukin 4-activated Macrophages. *The Journal of biological chemistry* 286, 19179-19190.
- Russo, E.B., Jiang, H.E., Li, X., Sutton, A., Carboni, A., del Bianco, F., Mandolino, G., Potter, D.J., Zhao, Y.X., Bera, S., *et al.* (2008). Phytochemical and genetic analyses of ancient cannabis from Central Asia. *Journal of experimental botany* 59, 4171-4182.
- Sanjana, N.E., Cong, L., Zhou, Y., Cunniff, M.M., Feng, G., and Zhang, F. (2012). A transcription activator-like effector toolbox for genome engineering. *Nature protocols* 7, 171-192.
- Scheer, N., Snaith, M., Wolf, C.R., and Seibler, J. (2013). Generation and utility of genetically humanized mouse models. *Drug discovery today* 18, 1200-1211.

Schmid-Burgk, J.L., Schmidt, T., Kaiser, V., Honing, K., and Hornung, V. (2013). A ligation-independent cloning technique for high-throughput assembly of transcription activator-like effector genes. *Nat Biotechnol* 31, 76-81.

Schwarz, K., Storni, T., Manolova, V., Didierlaurent, A., Sirard, J.C., Rothlisberger, P., and Bachmann, M.F. (2003). Role of Toll-like receptors in costimulating cytotoxic T cell responses. *European journal of immunology* 33, 1465-1470.

Seong, E., Saunders, T.L., Stewart, C.L., and Burmeister, M. (2004). To knockout in 129 or in C57BL/6: that is the question. *Trends in genetics : TIG* 20, 59-62.

Shiratsuchi, A., Watanabe, I., Yoshida, H., and Nakanishi, Y. (2008). Involvement of cannabinoid receptor CB2 in dectin-1-mediated macrophage phagocytosis. *Immunology and cell biology* 86, 179-184.

Shrivastav, M., De Haro, L.P., and Nickoloff, J.A. (2008). Regulation of DNA double-strand break repair pathway choice. *Cell research* 18, 134-147.

Silvestri, C., and Di Marzo, V. (2013). The endocannabinoid system in energy homeostasis and the etiopathology of metabolic disorders. *Cell metabolism* 17, 475-490.

Sipe, J.C., Arbour, N., Gerber, A., and Beutler, E. (2005). Reduced endocannabinoid immune modulation by a common cannabinoid 2 (CB2) receptor gene polymorphism: possible risk for autoimmune disorders. *Journal of leukocyte biology* 78, 231-238.

Stephens, A.S., Stephens, S.R., and Morrison, N.A. (2011). Internal control genes for quantitative RT-PCR expression analysis in mouse osteoblasts, osteoclasts and macrophages. *BMC research notes* 4, 410.

Sugiura, T., Kondo, S., Sukagawa, A., Nakane, S., Shinoda, A., Itoh, K., Yamashita, A., and Waku, K. (1995). 2-Arachidonoylglycerol: a possible endogenous cannabinoid receptor ligand in brain. *Biochemical and biophysical research communications* 215, 89-97.

Tanasescu, R., and Constantinescu, C.S. (2010). Cannabinoids and the immune system: an overview. *Immunobiology* 215, 588-597.

te Riele, H., Maandag, E.R., and Berns, A. (1992). Highly efficient gene targeting in embryonic stem cells through homologous recombination with isogenic DNA constructs. *Proceedings of the National Academy of Sciences of the United States of America* 89, 5128-5132.

Thompson, S., Clarke, A.R., Pow, A.M., Hooper, M.L., and Melton, D.W. (1989). Germ line transmission and expression of a corrected HPRT gene produced by gene targeting in embryonic stem cells. *Cell* 56, 313-321.

Tong, D., He, S., Wang, L., Jin, L., Si, P., and Cheng, X. (2013). Association of single-nucleotide polymorphisms in the cannabinoid receptor 2 gene with schizophrenia in the Han Chinese population. *Journal of molecular neuroscience : MN* 51, 454-460.

Urnov, F.D., Miller, J.C., Lee, Y.L., Beausejour, C.M., Rock, J.M., Augustus, S., Jamieson, A.C., Porteus, M.H., Gregory, P.D., and Holmes, M.C. (2005). Highly efficient endogenous human gene correction using designed zinc-finger nucleases. *Nature* 435, 646-651.

Verma, I.M., and Weitzman, M.D. (2005). Gene therapy: twenty-first century medicine. *Annual review of biochemistry* 74, 711-738.

- Wang, C., Yu, X., Cao, Q., Wang, Y., Zheng, G., Tan, T.K., Zhao, H., Zhao, Y., Wang, Y., and Harris, D. (2013a). Characterization of murine macrophages from bone marrow, spleen and peritoneum. *BMC immunology* 14, 6.
- Wang, H., Yang, H., Shivalila, C.S., Dawlaty, M.M., Cheng, A.W., Zhang, F., and Jaenisch, R. One-step generation of mice carrying mutations in multiple genes by CRISPR/Cas-mediated genome engineering. *Cell* 153, 910-918.
- Wang, H., Yang, H., Shivalila, C.S., Dawlaty, M.M., Cheng, A.W., Zhang, F., and Jaenisch, R. (2013b). One-step generation of mice carrying mutations in multiple genes by CRISPR/Cas-mediated genome engineering. *Cell* 153, 910-918.
- Wang, J.P., and Zhang, Y.M. (2005). [The application of Red/ET recombination to high efficient gene-targeting vector construction]. *Yi chuan = Hereditas / Zhongguo yi chuan xue hui bian ji* 27, 953-958.
- Weischenfeldt, J., and Porse, B. (2008). Bone Marrow-Derived Macrophages (BMM): Isolation and Applications. *CSH protocols* 2008, pdb prot5080.
- Yao, B.B., Mukherjee, S., Fan, Y., Garrison, T.R., Daza, A.V., Grayson, G.K., Hooker, B.A., Dart, M.J., Sullivan, J.P., and Meyer, M.D. (2006). In vitro pharmacological characterization of AM1241: a protean agonist at the cannabinoid CB2 receptor? *British journal of pharmacology* 149, 145-154.
- Yu, Z., Chen, H., Liu, J., Zhang, H., Yan, Y., Zhu, N., Guo, Y., Yang, B., Chang, Y., Dai, F., *et al.* (2014). Various applications of TALEN- and CRISPR/Cas9-mediated homologous recombination to modify the *Drosophila* genome. *Biology open* 3, 271-280.
- Zimmer, A., Zimmer, A.M., Hohmann, A.G., Herkenham, M., and Bonner, T.I. (1999). Increased mortality, hypoactivity, and hypoalgesia in cannabinoid CB1 receptor knockout mice. *Proceedings of the National Academy of Sciences of the United States of America* 96, 5780-5785.

7 APPENDIX

7.1 Supplemental material

Supplementary table 1: Summary of electroporations performed in MPI ES cells

MPI ES cells	Electroporation number	Number of checked clones
Targeting construct: hCB2-Arg	1	232
Targeting construct: hCB2-Gln	2	233

Supplementary table 2: Summary of all electroporations performed in Bruce4ES cells

Bruce 4 ES cells	Electroporation number	Number of checked clones
Targeting construct: hCB2-Arg	3	214
	5	16
	6	2
	9	153
	14	27
	15	17
	16	52
	17	34
	18	40
	19	36
	20	33
	TOTAL	624

Bruce 4 ES cells	Electroporation number	Number of checked clones
Targeting construct: hCB2-Gln	4	157
	7	26
	8	34
	10	171
	11	87
	12	42
	13	47
	TOTAL	564

New Bruce 4 ES cells	Electroporation number	Number of checked clones
Targeting construct: hCB2-Arg	21	96
	23	96
	25	24
	27	96
	28	96
TOTAL		408

New Bruce 4 ES cells	Electroporation number	Number of checked clones
Targeting construct: hCB2-Gln	22	96
	24	96
	26	96
TOTAL		288

Oligonucleotides used during the study:

Targeting construct cloning:

Fwd mCB2 subcloning	GTGCCTTCTAGAAGACCTATTTCTAGGGCAAGGATGTGT TTGATGTATAACAATTGACAGCTTGTCTGTAAGCGGATG
Rev mCB2 subcloning	GTTTAAGTTCCTCGGAGTTCTTGTTAAGTTCAACGGACA AAAGATAGACTCAATTGGCTCTCCTGAGTAGGACAAATC
Fwd hCB2 flanked HA first	ACAGCCCAGTCTTCTGGGACAGCTCCAGTAGAAGAAGC CAAAGCCCATCCATGGAGGAATGCTGGGTGACAGAG
Rev hCB2 flanked HA first	GACAGGTGGTGTGTCAGCAGTTGGAGCAGCCTGGAGTTCT GGATCCTGGCTCTCAGCAATCAGAGAGGTCTAGATC
Fwd hCB2 flanked HA second	GCTCTCAGTTGACGTCATCACCTGTTAACATTCAAGGAT TGTTTTCTCCTTGCCACAGCCAGTCTTCTGGGACAGC T
Rev hCB2 flanked HA second	CTCTTCGAGGGAGTGAACGACTTCTGACTCGG GCTGTTTCCAGTAGAAAGACAGGTGGTGTGTCAGCAGTTG GAG

Fwd FRT-neo-FRT	CACTATCCCAGTCTTGCCTAGCTTCAGTACAAAGCAAGA TATTCACACAGAATTAACCCTCACTAAAGGGCG
Rev FRT-neo-FRT	CAGTGGGGCTGAGTCAAGCATCACTGGGAACAGCCTAG GACCCAAAGAATTAATACGACTCACTATAGGGCTC

Targeting strategies:

Fwd ES cell check	TTTCATGATCTGTGTGTTGG
Rev ES cell check	GAGTTGCCGAAGAGATTGA

Fwd seq hCB2	CTTGATTGGTGTGTCAGCTCTC
Rev seq hCB2	ACAGGTGGTGTGTCAGCAGTT

Fwd 3' CB2 probe	TCTCCCAGTTTTCCCCACAC
Rev 3' CB2 probe	GAGTAACGATTGGCTTGGAAGG

Fwd 5' hCB2 probe	TTCCATCCCCAGTACACACA
Rev 5' hCB2 probe	GAAAAGGTGTGGCAGGTTGT

CRISPR/Cas9 cloning and checking:

Fwd CB2 sgRNA	CACCGTGACCAACGGCTCCAACGG
Rev CB2 sgRNA	AAACCCGTTGGAGCCGTTGGTCAC

Human U6 seq F Ins	ACTATCATATGCTTACCGTAAC
Rev CB2 sgRNA	AAACCCGTTGGAGCCGTTGGTCAC

Fwd sgRNA Surveyor	CTTGATTGGTGTGTCAGCTCTC
Rev sgRNA Surveyor	TAGTCGTTAGGGATCAGTGG

Viral vector construct generation:

Fwd hCB2 ORF <i>Bam</i> HI	TCTAGAGGATCCGCCACCATGGAGGAATGCTGGGTGA CAGAG
Rev hCB2 ORF <i>Sa</i> II	TTGATTGTCGACTCAGCAATCAGAGAGGTCTAGATC
Fwd IRES2-eGFP <i>Sa</i> II	TCTAGAGTCGACGCCCTCTCCCTCCCCCCCCCTAAC
Rev IRES2-eGFP <i>Sa</i> II	TTGATTGTCGACTTACTTGTACAGCTCGTCCATGCC

7.2 Declaration

I hereby solely declare that I prepared this thesis entitled “The cannabinoid receptor 2: from mouse to human” entirely by myself except otherwise stated. All text passages that are literally or correspondingly taken from published or unpublished papers/writings are indicated as such. All materials or services provided by other persons are equally indicated.

Bonn, January 2015

(Benjamin Gennequin)

7.3 Curriculum Vitae

Benjamin Gennequin

Publications

Nader J, Rapino C, **Gennequin B**, Chavant F, Francheteau M, Makriyannis A, Duranti A, Maccarrone M, Solinas M, Thiriet N. Prior stimulation of the endocannabinoid system prevents methamphetamine-induced dopaminergic neurotoxicity in the striatum through activation of CB₂ receptors. *Neuropharmacology*. 2014 Apr 5.

Gennequin B, Otte DM, Zimmer A. CRISPR/Cas-induced double-strand breaks boost the frequency of gene replacements for humanizing the mouse *Cnr2* gene. *Biochem Biophys Res Commun*. 2013 Nov 6.

Thiriet N, **Gennequin B**, Lardeux V, Chauvet C, Decressac M, Janet T, Jaber M, Solinas M. Environmental Enrichment does not Reduce the Rewarding and Neurotoxic Effects of Methamphetamine. *Neurotox Res*. 2010 Feb 9.

8 ACKNOWLEDGMENTS

I would like to express my special appreciation and thanks to my advisor Professor Dr. Andreas Zimmer. I would like to thank you for encouraging my research and for allowing me to grow as a research scientist.

To Professor Dr. Jörg Höhfeld, I thank you very much for accepting to be the second supervisor of my PhD work.

To Dr. David-M Otte, I would like to thank you for the last five years we have shared in the laboratory. I will miss our scientific discussions, our crazy cloning ideas and your ability to put pressure... I wish you the best for the rest of your career and personal life.

A special thanks to my collaboration partners Dr Katrin Zimmermann and Jonathan L Schmid-Burgk (PhD) who always accept to take time to answer my questions. It was a great pleasure to work with you.

Words cannot express how grateful I am to Dr. Britta Schürmann, Dr. Eva Drews , Dr Alexandra Krämer and Dr Svenja Ternes for being who they are. I would like to thank you for everything: your welcome, your help, the energy you spent to push me finishing this PhD, the time spent together in and outside the lab... And even if today I lose colleagues, I made new friends on whom I can count. Many thanks also to Benni and Stephan on whom I count too!

Many thanks to all my other colleagues Anna-Lena, Bruno, Imke, Irene, Ramona, Anne, Dr. Ildikò Racz and Dr. Andras Bilkei-Gorzo for the great atmosphere in the lab, during our yearly retreats and after work.

Je tiens tout d'abord à remercier mes parents et mes frères pour leurs soutiens. Je leur serais toujours redevable pour leur inconditionnel soutien tout au long de ma vie dans mes bons choix comme dans les mauvais. C'est ce qui m'a permis d'en être là où j'en suis aujourd'hui. Je remercie aussi mes beaux parents pour leur soutien tout au long de cette thèse.

Un grand merci à mon autre famille, les copains. Que ce soit les copains proches (Caroline et François, Xavier, Julien) ainsi que les copains rencontrés tout a long de ma vie, (Antoine et Marie, Romain et Marie, Julien, Anne Sophie, Gaëlle et Laurent, Hélène et Will) je tiens à vous remercier énormément pour toutes vos visites. Elles m'ont permis de tenir jusqu'au

bout. Et maintenant que cette thèse est finie, je vais vous rendre la pareille en venant vous rendre visite dès que possible!!!

Enfin, je tiens à remercier un nombre incalculable de fois ma moitié, Virginie. Sans elle, je ne pense pas que j'aurais terminé cette thèse... Elle m'a apporté un incommensurable soutien et a su me remotiver dans les moments les plus dures. Mille merci Virginie, je t'aime